From Pluripotency to Definitive Endoderm:

Delineating the Signalling Events of Endoderm Specification in Human Pluripotent Stem Cells

Max Lycke

Master Thesis in Molecular Bioscience

Department of Biosciences

Faculty of Mathematics and Natural Sciences

UNIVERSITY of OSLO

November 2016

2016

From Pluripotency to Definitive Endoderm: *Delineating the Signalling Events of Endoderm Specification in Human Pluripotent Stem Cells*

Max Lycke

http://www.duo.uio.no

Trykk: Reprosentralen, Universitetet i Oslo

Acknowledgements

It takes a village to raise a thesis, and there are many people whose guidance and help have been integral to the development of this one.

First I would like to thank my supervisor Gareth J. Sullivan whose encouragement, incisive guidance, and curiosity have been central to shaping this exciting period of research. Participating in the Sullivan lab has been inspiring and a great learning experience. I am very happy to have had the opportunity to do so. I am also grateful for the all the help I have received from my colleagues Richard Siller, Santosh Mathapati, and Agata Impellizzeri who have come to my assistance in the lab innumerable times, and given me successions of feedback on my thesis and presentations, as well as laughs, and cake. I would also like to thank my internal supervisor Ragnhild Eskeland for her assistance and interest.

I am much obliged to our collaborators: Stefan Krauss, for encouraging me to do all the guest work I have done in his lab, while also providing important feedback and discussions. For their mentorship in western blotting, I want to thank Jo Waaler, Kaja Lund, and Arkady Rutkovskiy. I must also thank Kulbhushan Sharma for his enthusiastic collaboration, interest and helpful comments. Many friends have helped me along the way, and I must express my gratitude to Sigrid Aslaksen, Shoshy Mahmuda, Vera Blankson, and Ananya Chakravorty for their proofreading, helpful comments, and lab-assistance.

I would also like to thank Wedel Jarlsbergs fond for the funding they provided to this project.

Finally I would like to thank my family for their encouragement and support. I would be remiss not to thank them for the love they've given me throughout my entire life, but they should also be thanked for their support in regard to my education, particularly during my academic life. My parents and brothers have always been a source of comfort and support, as have my extended family, to whom I am also thankful.

Abstract

In order to faithfully reproduce human tissues and cell types using pluripotent stem cells, it is essential to have an accurate understanding of the developmental pathways controlling cell fate from early development to mature, specialized cell types.

Definitive Endoderm (DE) is an early embryonic cell layer that gives rise to multiple organs such as the gut, liver, pancreas, bladder, thyroid gland, thymus, and lungs. Our group has developed a protocol that efficiently generates hepatocyte like cells (HLCs) from human pluripotent stem cells (hPSCs). This protocol uses the small molecule CHIR99021, a potent activator of canonical WNT signalling to direct hPSCs towards endodermal differentiation. During the differentiation process the predicted sequence of developmental markers was observed, demonstrating a transition through primitive streak to DE using gene expression analysis. This platform allows us to study the cell signalling events that initiate the shift from hPSCs to DE. A detailed understanding of these events will provide the tools to develop more accurate models of human tissues, such as the liver. The signalling events leading to endodermal development involve a myriad of signalling proteins belonging to families such as WNTs, TGFβs, FGFs, BMPs, and the PI3K/Akt pathway.

Our results demonstrate new facets of a Wnt-driven interplay between these pathways, uncovering novel relationships between the signalling proteins that drive endodermal differentiation. We demonstrate that the Wnt-mimicking process of GSK3 inhibition, drives DE differentiation, mediating crosstalk between pathways previously established to be important for DE development but not known to be regulated or initiated by canonical Wnt-signalling specifically, such as the PI3K/Akt and Nodal signalling pathways. Furthermore we highlight an interesting pattern of Axin2 and TNKS signalling in DE differentiation. We also show that these events are conserved across different hPSC lines. We therefore conclude that canonical Wnt/GSK3 signalling acts as a master-regulator and initiator of mesendodermal differentiation.

Abbreviations

ACTB: β-actin
ACVR: Activin Receptor
ADE: Anterior Definitive Endoderm
AKT: aka Protein Kinase B
ALK: Activin Receptor Like Kinases
AMPK: AMP-Activated Protein Kinase
AMP: Adenosine Monophosphate
APC: Adenomatous Polyposis Coli
ARTD: ADP-ribosyltransferases
ATCC: American Type Culture Collection
ATP: Adenosine Triphosphate
AXIN: Axis Inhibition Protein
BIO: 6-Bromoindirubin-3'-oxime
BMP: Bone Morphogenic Protein
BSA: Bovine Serum Albumin
CDH1: Cadherin 1 aka Epithelial Cadherin (E-cadherin)
CDH2: Cadherin 1 aka Neural Cadherin (N-cadherin)
cDNA: Complementary DNA
CER1: Cereberus 1
CHIR99021: 6-[[2-[[4-(2,4-Dichlorophenyl)-5-(5-methyl-1H-imidazol-2-yl)-2-pyrimidinyl]amino]ethyl]amino]-3-pyridinecarbonitrile
CK1 and CK2: Casein Kinase 1 and Casein Kinase 2
c-MYC: Avian Myelocytomatosis Virus Oncogene Cellular Homolog
CXCR4: C-X-C Chemokine Receptor Type 4
DAPI: 4',6-diamidino-2-phenylindole
DE: Definitive Endoderm
DMEM/F12: Dulbecco's Modified Eagle Medium/Ham's F-12
DMSO: Dimethyl Sulphoxide
DNA: Deoxyribonucleic Acid
DPBS: Dulbecco's Phosphate-buffered Saline
DVL: Dishevelled
ECM: Extracellular Matrix
EDTA: Ethylenediaminetetraacetic Acid
EGF: Epidermal Growth Factor
EMT: Epithelial to Mesenchymal Transition
EOMES: Eomesodermin
ERK: Extracellular Signal-Regulated Kinases
FGF: Fibroblast Growth Factors
FOXA2: Forkhead Box A2
FOXG1: Forkhead Box G1
FZD: Frizzled
GAPDH: Glyceraldehyde 3-Phosphate Dehydrogenase
GATA4/6: GATA-Binding Protein 4/6
GDF: Growth Differentiation Factor
GREM1: Gremlin 1, DAN Family BMP Antagonist

GS: Glycogen Synthase
GSC: Goosecoid
GSK3: Glycogen Synthase Kinase 3
hESCs: Human Embryonic Stem Cells
HHEX: Hematopoietically Expressed Homeobox
HLCs: Hepatocyte-Like Cells
hiPSCs: Human Induced Pluripotent Stem Cells
hPSCs: Human Pluripotent Stem Cells
HRP: Horseradish Peroxidase
H3k18ac: Histone H3 acetyl Lysine 18
H3k9me3: Histone H3 tri-methyl Lysine 9.
ICM: Inner Cell Mass
IGF1: insulin-like Growth Factor 1
IVF: *In Vitro* Fertilization
KLF4: Krüppel-Like Factor 4
LKB1: Liver Kinase B1
LRP5/6: Low Density Lipoprotein Receptor-Related Protein 5/6
MAPK: Mitogen-Activated Protein Kinases
ME: Mesendoderm
mEpiSC: Mouse Epiblast Stem Cells
mESCs: Mouse Embryonic Stem Cells
MIXL1: Mix Paired-Like Homeobox Protein 1
mRNA: Messenger Ribonucleic Acid
mTOR: Mechanistic Target of Rapamycin
mTORC: Mechanistic Target of Rapamycin Complex
NAD^+/NADH: Nicotinamide Adenine Dinucleotide
NE: Neuroectoderm
NGS: Normal Goat Serum
NP-40: Tergitol-type NP-40, (Nonyl Phenoxypolyethoxylethanol-40)
OCT4: Octamer-binding Transcription Factor 4
OXPHOS: Oxidative Phosphorylation
PAGE: Polyacrylamide Gel Electrophoresis
PARP: Poly (ADP-ribose) Polymerase
PARsylation: Poly (ADP)-Ribosylation
PAX6: Paired Box Protein 6
PBS: Phosphate Buffered Saline
PDK1: Phosphoinositide-Dependent Kinase 1
PIP2: Phosphatidylinositol (4,5)-bisphosphate
PIP3: Phosphatidylinositol (3,4,5)-trisphosphate
PI3K: Phosphoinositide 3-Kinase
PS: Primitive Streak
PTEN: Phosphatase and Tensin Homolog
PVDF: Polyvinylidene Difluoride
p70S6K: p70 Ribosomal Protein S6 Kinase
qRT-PCR or RT-qPCR: Real-Time Quantitative Reverse Transcription Polymerase Chain Reaction
RIPA: Radio-immunoprecipitation Assay Buffer
RNA: Ribonucleic Acid

RNF146: E3 Ubiquitin Protein Ligase RNF146
RPMI: Roswell Park Memorial Institute
RQ: Relative Quantification
RSK: 90 kDa Ribosomal S6 Kinase
SDS: Sodium dodecyl sulfate
siRNA: Small Interfering Ribonucleic Acid
SMAD: Mothers Against Decapentaplegic Homolog
SOX2: SRY (Sex Determining Region Y)-Box 2
SOX17: SRY (sex determining region Y)-Box 17
S6RP or RPS6: Ribosomal Protein S6
T: T Brachyury Transcription Factor
TBS: Tris Buffered Saline
TCF/LEF: T Cell Factor/Lymphoid Enhancer Factor
TGF-β: Transforming Growth Factor Beta
TNKS: Telomeric Repeat Factor TRF1-interacting Ankyrin-Related Adenosine Diphosphate ADP-rRbose Polymerases or Tankyrase
TSC: Tuberous Sclerosis Protein
VEGF: Vascular Endothelial Growth Factor
WNT: Wingless-Type MMTV Integration Site
Wnt3a: Wnt Family Member 3A
β-TrCP: Beta-Transducin Repeat Containing E3 Ubiquitin Protein Ligase
4E-BP1: Eukaryotic Translation Initiation Factor 4E-Binding Protein 1

1 Table of Contents

1 Introduction

1.1 General Overview of Human Pluripotent Stem Cell Research

Human pluripotent stem cells (hPSCs) have recieved interest for their ability to potentially produce any cell type in the human body. Stem cell-derived tissue holds great promise for overcoming practical obstacles in biomedical research and the development of therapies for disease. This thesis will focus on the differentiation of hPSCs toward definitive endoderm (DE); an embryonic cell layer that gives rise to hepatic, pancreatic, gut and lung tissue among other endodermal tissues. To illustrate one such example we can consider the use of stem cells to derive human liver tissue, namely hepatocytes, for biomedical research. Hepatocytes are essential for the testing of xenobiotics and understanding how the human liver metabolizes new drugs, a pre-requisite for drug development[1,2]. The need for human liver tissue is highlighted by the large number of promising drug candidates and medical therapies that have been shown to work without deleterious effects in animal models but ultimately fail in human clinical trials[3,4,5,6]**.** Despite many similarities in the effects of drugs and the conserved physiology of hepatic structures across animal models, there are idiosyncrasies to human genetics and liver physiology that cause drug failure in clinical trials[7,8]. Stem cell-derived liver tissue could be used to improve drug trials by enabling the creation of a diverse biobank of hPSC lines that reflect the genetic diversity found in human populations, and uncover population-specific differences in drug response[9,10]**.** *In vitro* models could thus be used as a supplementary, and perhaps, eventually a more accurate model for high throughput screening of drugs than animal models. One caveat to *in vitro* models however is that they have a limited capacity to uncover systemic effects that would be found *in vivo*, additionally *in vitro* derived hepatocytes, or liver tissue would not function as efficiently as a fully formed liver[11]. Working to address these issues, another area of stem cell research that has gained momentum is the

construction of functional human organs in the lab[12], as well as organoids[13,14] and organs on-a-chip[15,16,17,18]. All the aforementioned methodologies rely heavily on a comprehensive understanding of the developmental pathways and signalling events that specify the formation of the germ layers, cells and ultimately organs. Currently there are large gaps in our understanding of cell signalling events regulating pluripotency, and the transition from pluripotency to the differentiation pathways that specify and engender the three germ layers. Ultimately the utility of stem cells depends on the ability to faithfully produce specific cell types. This necessitates a basic understanding of the pathways involved and their subsequent manipulation at precise time points to generate the desired cell type. Below is an overview of the current landscape of development in pluripotent stem cell models, and a review of the signalling events that accompany the transition from pluripotency to lineage commitment.

1.2 A Brief Overview of Human Development: Early Stages of Human Embryonic Development

The process of embryonic development differs between different phyla of animals[19,20]. Humans and most other bilaterians are triploblastic (forming three germ layers)[21]. In humans a series of intermittent rounds of cleavage occur within 24 hours after fertilization[22]. The zygote cytoplasm is divided into smaller cells by rapid mitotic division, eventually forming the blastocyst which consists of smaller cells called blastomeres that organize into the outer epithelial layer called the trophoblast (which eventually forms part of the placenta) and a centrally placed, pluripotent inner cell mass (ICM) which generates the embryo[22,23,24]. After exiting the zona pellucida the blastocyst initiates the process of implantation into the uterine endometrium. By week two post-fertilization, the ICM has differentiated into two layers: the upper epiblast and lower hypoblast[22]. Implantation initiates the process of gastrulation, when a thickening with a midline groove starts to form in the epiblast, the epiblast cells undergo an epithelial-to-mesenchymal transition (EMT)[25] and subgroups of epiblast cells migrate toward, enter, and then migrate away from the primitive streak (PS). This movement of cells through the PS into the interior of the embryo is known as ingression[22]. The PS

defines all major body axes, such as the body's left-right axis and dorsal-ventral axis.[22] The PS is subdivided into distinct regions; the anterior, middle, and posterior regions based on cell lineage development and gene-expression patterns[26]. The first epiblast cells to ingress through the PS invade the hypoblast region, producing a new endodermal layer of cells (DE), derived from the anterior region of the PS (Figure 1)[22]. The endoderm layer is classically defined as the inner germ layer of the embryo, ultimately giving rise to the epithelial lining of the digestive tract and contributing to many other organs mentioned previously. In addition, some epiblast cells migrate into the space between the epiblast and endoderm, to form the mesoderm layer, derived from the posterior region of PS[27,28]. After formation of the endodermal and mesodermal layers the remaining epiblast cells do not ingress through the PS but remain in the epiblast layer and develop into ectoderm[22]. These carefully choreographed events lead to the organization of the three germ layers, ectoderm, endoderm and mesoderm, and ultimately all resident cells of the body.

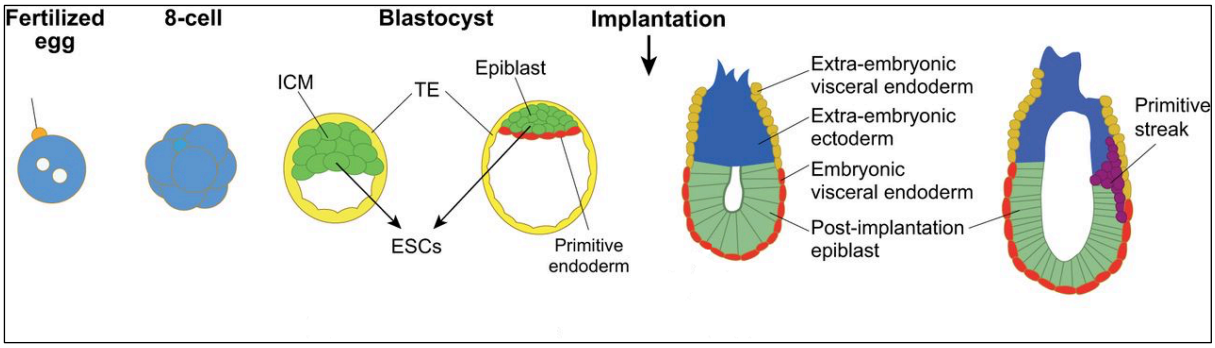

Figure 1. Embryonic development from fertilization to gastrulation: The diagram shows the process of embryonic development from the point of fertilization until the formation of PS, including the formation of the morula, and blastocyst followed by implantation and PS formation. (TE: trophoectoderm). The figure is based on embryonic development in mice and adapted from Davidson et al. Development, 2015[53].

1.3 Varieties of Pluripotent Stem Cells

Human embryonic stem cells (hESCs) are derived from the inner cell mass (ICM) of a blastocyst prior to implantation[29]. The ICM is manually isolated from blastocysts deemed of not high enough quality for implantation after *in vitro* fertilization (IVF). These cells are then cultured under defined conditions that allow them to proliferate and replicate indefinitely while maintaining pluripotency[24,30]**.** However, there are ethical and legal considerations associated with the derivation and use of hESCs, due to the destruction of human embryos[31,32]. This has resulted in concerted efforts to find an alternative source[33]. One alternative is human induced pluripotent stem cells (hiPSCs) that are derived from somatic, differentiated cells such as fibroblasts, blood, or kidney epithelial cells isolated from urine[34,35]. These somatic cells can be reprogrammed to a pluripotent, stem cell-like state, by the expression of a combination of transcription factors, which have been demonstrated to be central agents of pluripotency, such as octamer-binding transcription factor 4 (OCT4), Krüppel-like factor 4 (KLF4), SRY (sex determining region Y)-box 2 (SOX2), and Avian myelocytomatosis virus oncogene cellular homolog (c-MYC)[36]. The field of hiPSC reprogramming has since demonstrated somatic cell reprogramming with alternative combinations of transcription factors[37]. For an in depth review of reprogramming methods see review by *Kazutoshi Takahashi and Shinya Yamanaka: A decade of transcription factor-mediated reprogramming to pluripotency, Nature Reviews Molecular Cell Biology, 2016*[33]*.* The factors described above are delivered into cells using a number of delivery approaches including integrative methods such as lenti- and retrovirus or non-integrative methods such as Sendai virus[38,39].

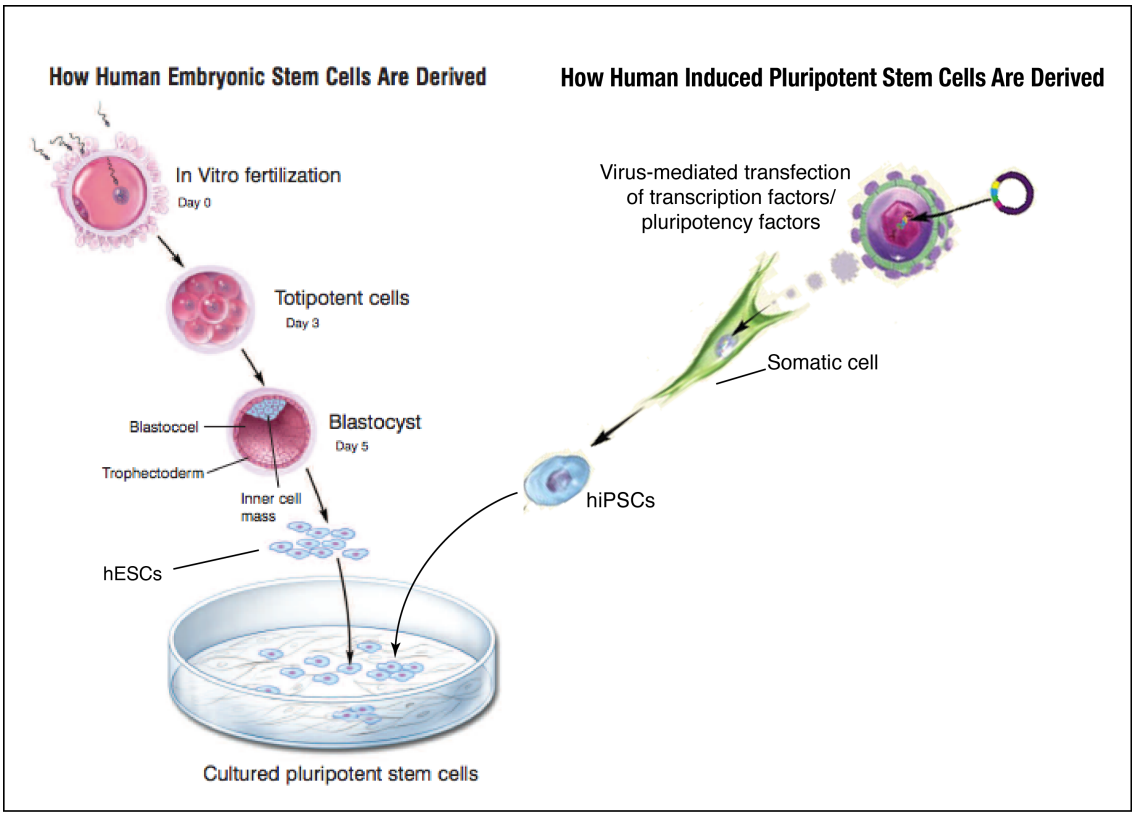

Figure 2. Methods for deriving hESCs and hiPSCS: Diagram showing methods for deriving hPSC cultures from human embryos (hESCs) and somatic cells (hiPSCs). Figures adapted from Regenerative Medicine, 2006, NIH. Copyright Terese Winslow[24].

After hPSCs have been isolated (Figure 2) they require precise culture conditions for maintenance of pluripotency and self-renewal. Pluripotency and stem cell self-renewal are maintained intrinsically by gene expression and are modulated by interactions with extrinsic cues from the environment, such as FGF2 and TGF-β growth factors[40,41]. *Intrinsic gene expression*: the core transcription machinery (OCT4, NANOG, and SOX2) responsible for regulation of both pluripotency and self-renewal is well established in murine ESCs (mESCs) and hESCs and is in fact the basis of the reprogramming process[42,43,44]. However, there are species differences in how the core network is regulated by extrinsic signalling proteins[45,46]. The principal reason for these observed differences is that mESCs are thought to be at a different stage of embryonic development, the so called "naïve" stage of development while hESCs are at a more "primed" developmental state[45,47,48,49,50]. As a consequence the extrinsic requirements differ for mouse and human ESCs[40,45,51]. Accordingly, there have been major efforts to understand the

difference between naïve and primed states, leading to a number of reports describing ways to modulate these states in mouse and human ESCs, using a combination of extrinsic factors in the forms of growth factors such as LIF and FGF2, small molecule inhibitors, and transcription factors (Figure 3)[40,48,52,53]. To understand how these extrinsic signals modulate pluripotency, it is imperative to understand how pluripotency is regulated, and further how a cell exits this state to commit towards a particular lineage. We therefore proceed to an account of the signalling events that regulate pluripotency versus commitment to differentiation.

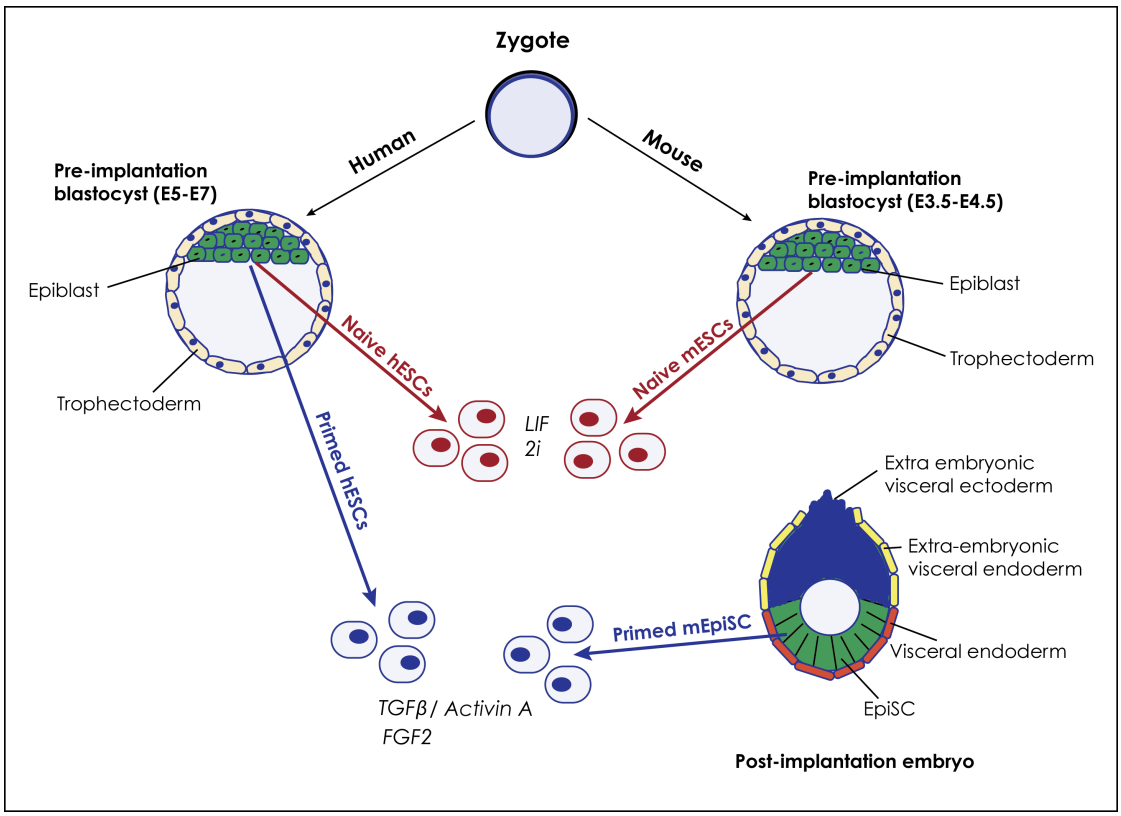

Figure 3. Naïve vs primed stem cells: Naïve and primed pluripotent stem cells are classified by a number of distinguishing features that are maintained by the respective stem cell states *in vitro*. Naïve stem cells express the pluripotency factors SOX2, OCT4, NANOG, and KLFs. Naïve cells have a global DNA hypomethylation profile similar to ICM cells. Self-renewal of naïve PSCs is maintained with the exogenous factors LIF, and 2i (a dual inhibitor of MEK & GSK3). Primed stem cells express the pluripotency factors SOX2, OCT4, and NANOG and require exogenous supplementation of FGF, and TGF-β or Activin A for self-renewal. DNA methylation is up-regulated in primed PSCs. Unlike primed hPSCs, primed mEpiSCs tend to be derived from post-implantation stage mouse epiblasts. Conventional "primed" human ESCs, are distinct from mouse primed EpiSCs and have various naive features[47,48,49,50,52,53].

1.4 Cell Signalling from Pluripotency to Differentiation

For brevity, only the events that lead to endodermal differentiation from a pluripotent state shall be described. This process involves a complex network of pathways that both act independently, and converge through crosstalk. With respect to pluripotency and the exit from pluripotency a multitude of extrinsic factors including, Fibroblast Growth Factors (FGFs), Transforming Growth Factor Beta (TGF-β) family proteins, Wingless-Type MMTV Integration Site (Wnt) proteins, β-catenin signalling proteins, and metabolic regulators such as those of the phosphoinositide 3-kinase/Akt (PI3K/Akt), Mitogen-activated protein kinases (MAPK)/ extracellular signal-regulated kinases (ERK) and mechanistic target of rapamycin (mTOR) pathways, control these events. Below is a summary of the literature pertaining to the signalling events underlying this transition (sections 1.4.1 – 1.5.4).

1.4.1 Regulation of the Pluripotent State

1.4.1.1 Fibroblast Growth Factors

FGFs are a large family of growth factors with numerous functions including angiogenesis, wound healing, embryonic development and various endocrine signalling pathways[54]. In humans there are 22 members that have been identified to date[54]. One member of this family, basic FGF/ FGF2 is used for the *in vitro* maintenance of hPSCs in a state of pluripotency, as high levels of FGF2 specifically promote self-renewal[41,55]. However, the precise mechanisms by which FGF2 maintains pluripotency remains unclear, being further complicated by the observation that FGF is also active in differentiation[56,57,58]. FGF co-regulates self-renewal by acting in concert with Nodal signalling (section 1.5.1) to maintain NANOG expression[41]. Indeed the blocking of FGF2 causes a decline in NANOG levels implicating FGF in maintenance of NANOG expression[58]. Furthermore Nodal signalling induces the expression of FGF2[59].

The influence of FGF and Nodal signalling on NANOG expression indicates interplay between these two factors in pluripotency maintenance. One study showed that chemical inhibition of the FGF receptor (FGFR) could be rescued by increasing the dose of exogenous Activin, while the absence of Activin signalling could not be rescued with a high dose of FGF[41]. Another study using the same FGFR chemical inhibitor combined with FGF2 free culture conditions, found that neither FGF2 nor Activin A could maintain pluripotency on their own, indicating that both are required[59]. Interestingly the role of FGF2 in differentiation appears to be regulated by NANOG.

FGF2 regulates both self-renewal, as well as the expression of genes involved in neuroectoderm (NE) differentiation, however, these NE-signals are blocked in the presence of NANOG[57]. FGF2 also regulates pluripotency through antagonism of Bone Morphogenic Protein (BMP) signalling[55]. This is achieved by expression of FGF2 dependent target genes including Gremlin 1, DAN family BMP antagonist (GREM1), which inhibits BMP4 preventing differentiation[60]. FGF2 has also been shown to modulate BMP4-activity, promoting the formation of mesendoderm (ME) rather than extraembryonic lineages in BMP4-induced differentiation of hESCs[58]. FGF2 is also known to activate the PI3K/Akt and MAPK/ERK signalling pathways[45]. However, there are conflicting reports about the role of these pathways in relationship to FGF-signalling. There is growing evidence that PI3K/Akt signalling is instrumental in maintenance of pluripotency[61,62,63], whereas MAPK/ERK signalling is involved in differentiation[61,64,65,66]. This is demonstrated clearly when Activin A and FGF2 are combined with an ERK1/2 inhibitor to promote hESC self-renewal[65], while activation of ERK1/2 in hESCs is required for neural and mesendodermal differentiation[58,65,66]. Finally FGF2 might also be able prevent differentiation by modulating the effects (Glycogen Synthase Kinase 3) GSK3 inhibition[67]. The overall picture of FGF-signalling therefore suggests that its effects are context-dependent and modulated by the activity of other pathways such as Activin/Nodal, BMP, MAPK/ERK, PI3K/Akt and canonical WNT[56].

1.4.1.2 Metabolic Regulators of Pluripotency

The metabolic state of a cell is divided into anabolic and catabolic processes. Catabolic pathways break down molecules to generate energy (ATP) and reducing power (NADH), through the oxidation of organic compounds[68]. While anabolic pathways utilise the energy released by catabolic processes to drive the synthesis of biological compounds (e.g. proteins, lipids, nucleic acids) that make up the cell. Together the sum of anabolic and catabolic reactions constitute the metabolism of the cell[69].

Metabolic regulation is integral to many cellular processes such as cell survival, cell cycle progression, cell growth and anabolic glucose metabolism, as well as maintenance of pluripotency and self renewal in stem cells[62,63,70,71]. Under nutrient-rich conditions, growth factors such as insulin and insulin-like growth factor-1 (IGF1), epidermal growth factor (EGF), vascular endothelial growth factor (VEGF) stimulate anabolic processes through the PI3K/Akt pathway (Figure 4)[72,73,74].

1.4.1.3 The PI3K/Akt Pathway

The recruitment of Akt to the plasma membrane is primarily mediated through phosphoinositide 3-kinase (PI3K) phosphorylation of phosphatidylinositol (4,5)-bisphosphate (PIP2) to generate phosphatidylinositol (3,4,5)-trisphosphate (PIP3). Subsequently the amino terminal pleckstrin homology (PH) domain of Akt binds to PIP3, promoting its translocation to the plasma membrane where it is phosphorylated and activated[75]. The activity of Akt is regulated via phosphorylation of the threonine 308 (Thr308) and serine 473 (Ser473) residues[76]. On activation, Akt initiates many anabolic processes in the cell, by inhibiting GSK3, which promotes glycogen synthesis by preventing GSK3 from phosphorylating and inhibiting glycogen synthase (GS)[77]. Intriguingly, PI3K/Akt signalling can also promote GSK3 mediated phosphorylation and inhibition of AMPK, a catabolic regulator of cellular energy homeostasis that inhibits anabolic and activates catabolic processes[72]. Akt promotes cell cycle progression by preventing GSK3 from degrading

cyclin D1, and indirectly activating mTOR, which promotes the translation of cyclin D1[78,79]. In addition to its role in cell cycle progression Akt upholds cell survival by inhibiting apoptosis[70]. Akt also activates mTOR complex 1 (mTORC1) by inhibiting the tuberous sclerosis complex (TSC) complex, a negative regulator of the mTOR pathway[75]. The mTOR pathway stimulates cell growth and proliferation through the phosphorylation of the S6K1 and 4E-BP1 proteins, which are involved in ribosome biosynthesis and the initiation of protein translation[80]. The Akt pathway has also been shown to be positively regulated by mTORC2, which can phosphorylate Akt at Ser473, enhancing AKT/mTOR signalling[81,82]. This stimulates cell growth by initiating protein and lipid synthesis[72].

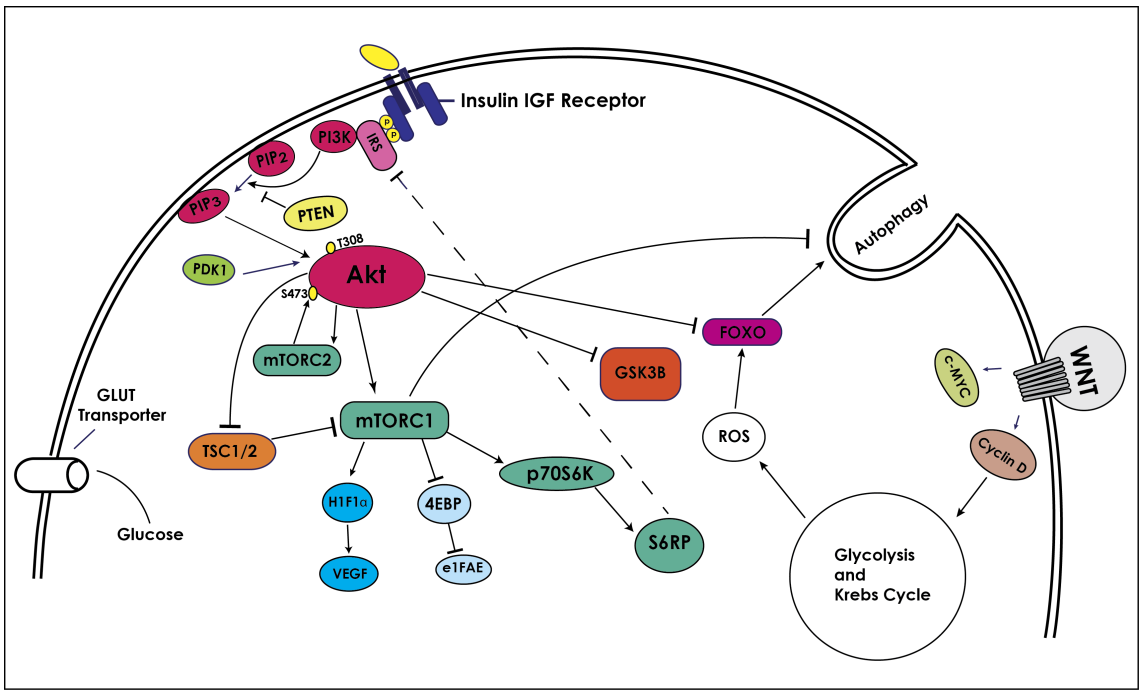

Figure 4. The PI3K/Akt signalling pathway: Akt is phosphorylated and activated by PDK1, and PIP3 through PI3K. PTEN is the major negative regulator of this process. Active Akt inhibits GSK3, and TSC1/2, while promoting anabolic activities through mTOR and inhibiting autophagy[70,82,223] .

In addition to the aforementioned roles, PI3K/Akt is an important signalling component for the maintenance of pluripotency in stem cells. In 2006 McLean *et al*, demonstrated that PI3K antagonizes the ability of hESCs to differentiate in response to endogenous Activin/Nodal signalling, furthermore inhibition of

PI3K efficiently promoted differentiation of hESCs into ME and DE by allowing them to be specified by Nodal signals present in the hESC culture[83].

This is corroborated by previous findings of a requirement for high levels of exogenous Activin for the initiation of mesendodermal differentiation in hESCs. Additionally high levels of Nodal signalling need to be maintained beyond the ME stage for specification of DE rather than mesoderm[84]. Recent research also supports the finding that a ratio of high Nodal to low PI3K/Akt signalling needs to be maintained for initiation of differentiation to ME and continuation toward DE (Figure 5)[63,85,86,87]. Therefore, it appears that PI3K/Akt is required for maintenance of pluripotency by regulating the bi-functional role of Nodal as either a promoter of pluripotency when PI3K/Akt activity is high, or a promoter of endodermal differentiation when PI3K/Akt activity is low[62,63,88].

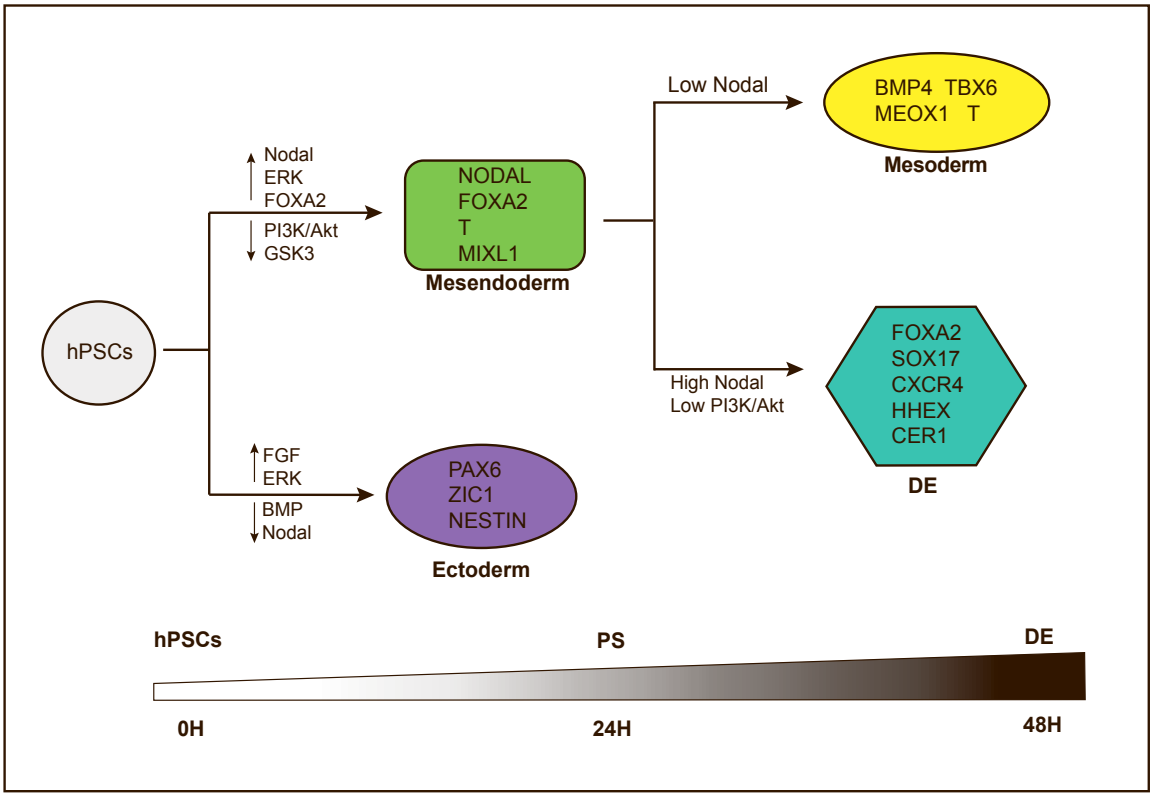

Figure 5. The process of generating DE from hPSCs: The lower panel shows the course of differentiation over 48 hours, with the corresponding embryonic states being recapitulated by the differentiating cells (i.e PS, DE). The upper panel shows the different conditions that give rise to the 3 different germ layers, as well as genes expressed in the different tissues[47,84,98].

1.5 The Fulcrum to Differentiation

1.5.1 Activin/Nodal Signalling

Activin and Nodal are members of the transforming growth factor beta (TGF-β) superfamily, which are a group of secreted ligands that also includes TGF-βs, Growth Differentiation Factors (GDFs), the Bone Morphogenetic Proteins (BMPs), anti-Mullerian hormone, and the Nodal antagonists Lefty1/2[89,90]. The activity of the Activin/Nodal pathway is mediated through type I and type II serine/threonine kinase receptors including activin receptors (ACVRs) and activin receptor like kinases (ALKs)[56]. Nodal signalling is important for both maintenance of pluripotency and induction of ME differentiation, under different conditions[91]. Nodal regulates pluripotency through the downstream effectors Mothers Against Decapentaplegic Homolog 2/3 (Smad2/3) complex, which binds to the OCT4 and NANOG promoter and regulate pluripotency factor expression by forming a nuclear complex with Smad4. The Smad 2/3 complex also regulates expression of NANOG which in turn blocks FGF-induced neuroectoderm differentiation[57,92].

Activin/Nodal signalling also regulates a number of key biological processes pertaining to cell fate decisions and organogenesis[92]. Despite the signalling effects of activins and Nodal often being indistinguishable, activins are not expressed in the PS and are non-essential for early development[92], we will therefore focus on the endogenous expression of Nodal in this study, and refer to Activin/Nodal signalling pathway as Nodal signalling. When conditions shift from maintaining pluripotency to directing differentiation, the Nodal cascade causes the Smad2/3/4 complex to bind to the promoters of signature mesendodermal genes such as Brachury (*T*), *EOMES*, and *MIXL1* to initiate their transcription[83,93]. Several transcriptional co-factors regulate binding of the Smad2/3/4 complex to regulatory elements within the above genes; one such example is TRIM33 a member of the transcriptional intermediary factor 1 (TIF1) family of transcriptional cofactors. TRIM33 facilitates recruitment to the histones H3K9me3 and H3K18ac on the promoters of mesendodermal genes[56]. The TRIM33–Smad2/3 complex makes the Nodal response element

accessible to the Smad2/3/4 complex and RNA polymerase II, leading to increased transcription of Nodal[56]. A detailed description of the co-factors involved is outside the scope of this thesis and can be followed up in the following review *Signaling Control of Differentiation of Embryonic Stem Cells toward Mesendoderm, Lu Wang, Ye-Guang Chen, Journal of Molecular Biology, 2015* [56]. Exactly how Nodal initiates differentiation is not fully understood, but recent research implicates crosstalk between certain metabolic signalling pathways such as PI3K/Akt and mTOR, (section 1.4.1.3).

1.5.2 Bone Morphogenic Proteins

In addition to Nodal, the Bone Morphogenic Proteins (BMPs) are important effectors of differentiation in stem cells. Unlike the FGF and Nodal pathways discussed previously, the BMPs are exclusively involved in differentiation and do not have a dual role in the maintenance of stem cell renewal or pluripotency[94]. Thus to maintain a steady state of pluripotency/self-renewal it is important to maintain a low level of BMP-signaling[94]. One member, BMP4, interacts with OCT4 to specify a particular cell fate depending on the relative concentrations of OCT4 and BMP4[95]; High levels of OCT4 enable hPSC self-renewal in the absence of BMP4, but specify differentiation towards ME when BMP4 is present, while low levels of OCT4 were shown to induce ectoderm differentiation in the absence of BMP4, but specify extraembryonic lineages when BMP4 is present[95]. BMP4 also downregulates the expression of the pluripotency factor SOX2[96]. BMP2 and BMP4 operate by phosphorylating Smad1/5/8, which then binds to Smad4 regulating the transcription of genes related to ME differentiation[56,94]. BMP thus contributes to ME differentiation and the formation of PS, after which point BMP promotes mesoderm differentiation[47,94,97]. High Nodal activity on the other hand drives the differentiation of definitive endoderm from ME[96,98].

1.5.3 The Canonical Wnt pathway

Wnt proteins are an important group of secreted ligands involved in cell proliferation and differentiation. The Wnt-signalling proteins are instrumental in development, and were first identified as morphogens involved in body pattern formation[99,100,101,102]. They constitute a family of morphogenic glycoproteins present in all metazoan animals[99]. In mammals there are 19 Wnt proteins, which are cysteine rich ligands ranging from 350 to 400 amino acids in size and contain an N-terminal secretion peptide[99,101]. The secreted Wnt proteins signal via a relatively complex membrane receptor providing regulation through extensive feed-back control mechanisms[103]. There are three well characterized Wnt-signaling pathways, that promote a wide range of functions including cell polarity, proliferation, migration, cell adhesion, tissue homeostasis in adult organisms, tissue morphogenesis, and through regulation of the state-shift between stem cell self-renewal and differentiation[103,104]. All these pathways are initiated by Wnt-ligands binding to the Frizzled-LRP receptor complex[105]. The signals can then be transduced in two ways: either through the canonical Wnt pathway, which is mediated through β-catenin, or non-canonical Wnt pathways that are independent of β-catenin[104,106]. This thesis will focus on the canonical Wnt/β-catenin pathway, for a description of the non-canonical pathways please see *Sugimura R, Li L. Noncanonical Wnt signaling in vertebrate development, stem cells, and diseases. Birth Defects Research Part C - Embryo Today Review, 2010*[104]*.*

The Wnt/β-catenin (canonical Wnt) pathway regulates the intracellular stability and basal levels of β-catenin. Upon activation of the canonical Wnt signalling pathway, stabilized β-catenin translocates to the nucleus and initiates transcription of Wnt target genes which are involved in regulating cell proliferation, and differentiation[105,100]. The following sections (1.5.3 – 1.5.3.4) give an overview of the key players in canonical Wnt signalling, a finely tuned process that cross-talks with a diverse array of different signalling pathways[103].

When discussing canonical Wnt signalling, it is conventionally divided into two states of signalling. Wnt-signalling is either in an inactive, basal "*Wnt-off state"*

or activated in a **"***Wnt-on state***"** (Figure 6)[105]**.** In the off state, there is an absence of Wnt ligand; under these conditions β-catenin is bound in a multiprotein complex termed the "destruction complex". This complex is made up of adenomatous polyposis coli (APC), casein kinase (CK1) and glycogen synthase kinase (GSK3)[105,107]. CK1 and GSK-3 phosphorylate β-catenin, axis inhibition protein (Axin) and APC in a manner that both enhances the stability of the protein complex, and their ability to bind β-catenin[99]. Trapped β-catenin is then phosphorylated by CK1 and GSK3 protein kinases on serine and threonine residues providing a binding site for E3 ubiquitin ligase, which targets β-catenin for degradation by the proteasome[105,108]. In this state the absence of Wnt signals ensures that β-catenin levels are low enough for Groucho proteins (a transcriptional co-repressor) to bind to T-cell factor/lymphoid enhancer factor (TCF/LEF) and suppress the transcriptional activation of Wnt target genes[105]. Conversely, in the Wnt-on state*,* Wnt ligands interact with a membrane surface receptor complex composed of seven-pass transmembrane protein Frizzled and the single-pass transmembrane proteins low-density lipid receptor LRP5 or LRP6. This triggers the phosphorylation of Dishevelled (Dvl) proteins and promotes their interaction with the Frizzled proteins on the cytoplasmic side of the receptor[105,109]. The resulting complex, known as the LRP6 signalosome, binds and inactivates Axin[110,111]. Exactly how the LRP6-signalosome complex captures Axin and allows β-catenin to accumulate is unclear, but a recent model (Figure 7) suggests that when Wnt is absent, Axin is associated with and phosphorylated by GSK3 in an activated ("open") conformation that promotes the binding/ phosphorylation of β-catenin. This leaves Axin poised for interaction with LRP6. Upon Wnt stimulation, the LRP6-signalosome recruits Axin, inhibiting Axin-bound GSK3. This leads to the inhibition of β-catenin phosphorylation and tips the balance toward Axin dephosphorylation. Dephosphorylated Axin adopts an inactivated ("closed") conformation, becoming incompetent for association with β-catenin and phospho-LRP6, leading to the disassembly of the signalling complex. Phospho-LRP6 is thus freed to undergo another round of recruitment of phosphorylated Axin for inactivation while ignoring dephosphorylated-inactivated Axin, in a reiterative manner that keeps β-catenin phosphorylation suppressed[111,112]. In the Wnt-on

state, active β-catenin can translocate to the nucleus to displace the transcriptional repressor Groucho, forming a complex with TCF/LEF leading to initiation of Wnt target gene expression. These genes are involved in regulating cell proliferation, stem cell maintenance, and differentiation[100,105].

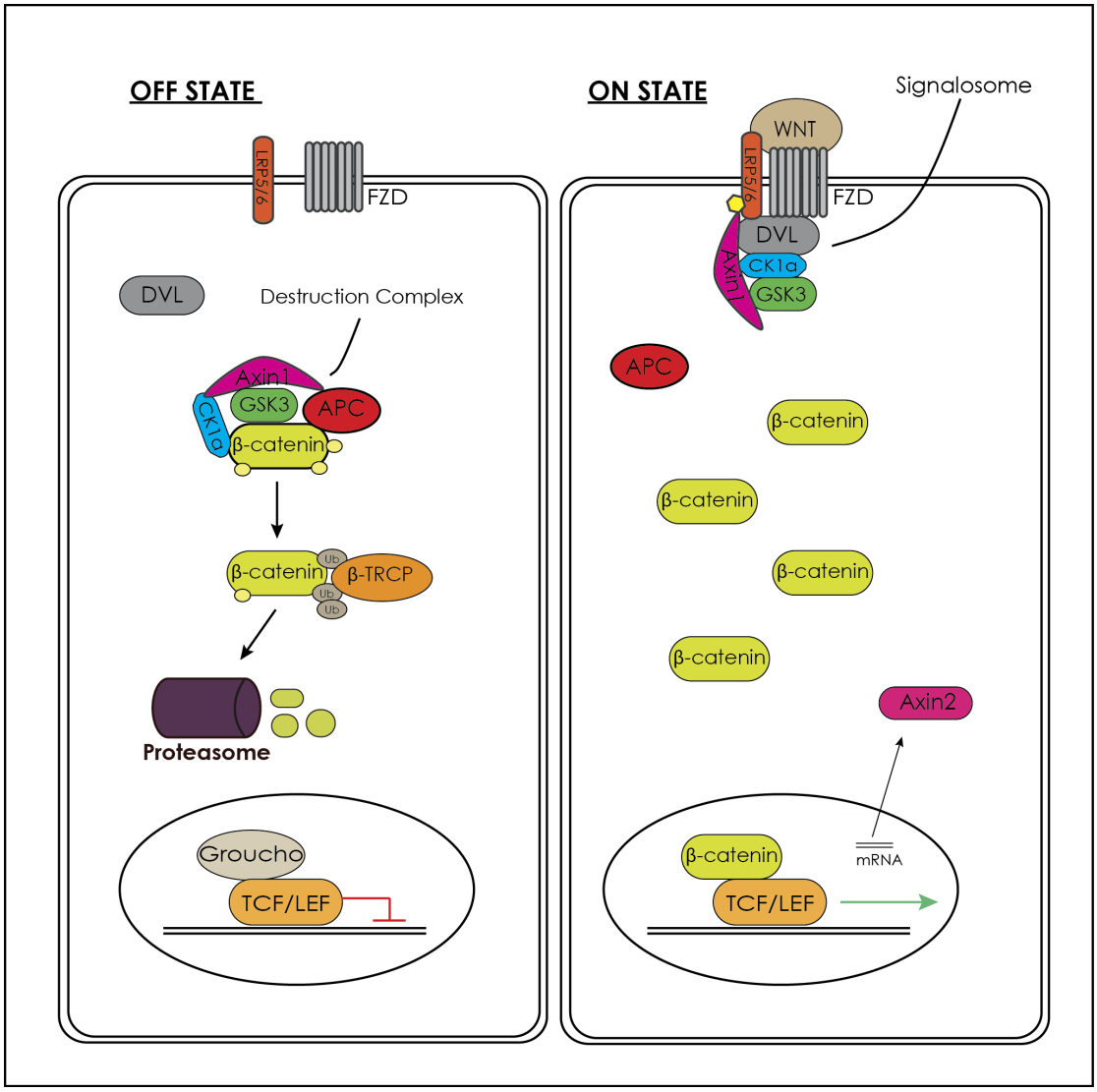

Figure 6. Canonical Wnt pathway: In the "Wnt off state" β-catenin is captured by destruction complexes that target it for ubiquitination and subsequent degradation. In the "Wnt on state" Axin, GSK3 and CK1 are bound to the LRP5/6-signalosome and unable to bind and degrade β-catenin, which then accumulates in the cytoplasm and nucleus[99,101,102,105].

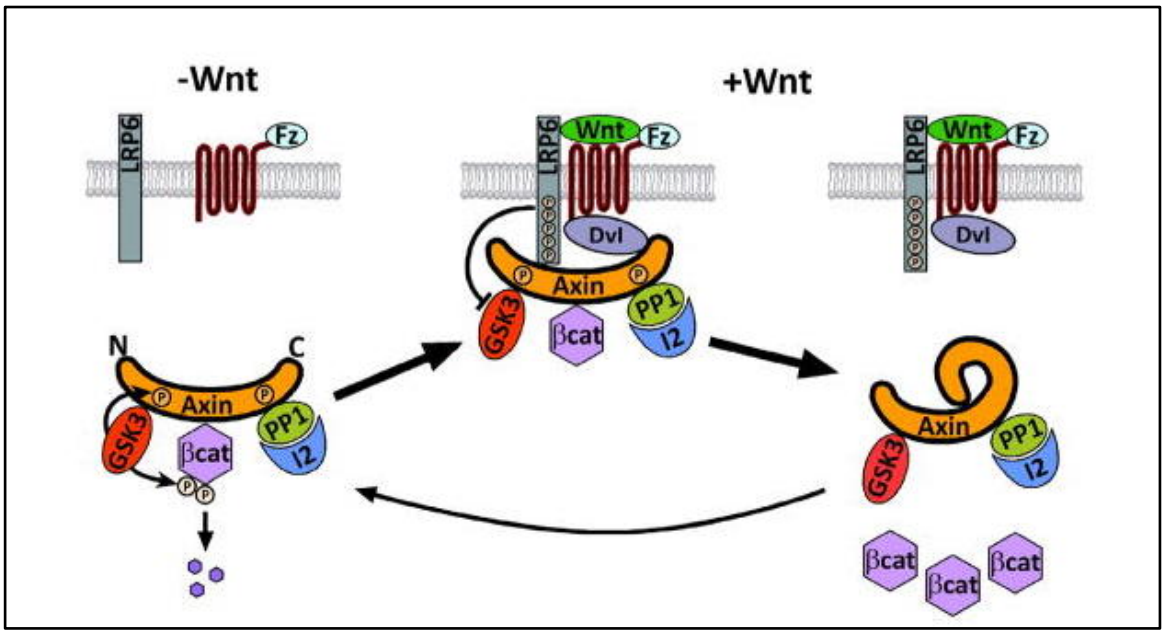

Figure 7. Mechanistic model for Axin-regulated β-catenin destruction: In the absence of Wnt, GSK3 phosphorylates Axin giving it an activated ("open") conformation that promotes the binding and phosphorylation of β-catenin. Upon Wnt stimulation the LRP6-signalosome recruits Axin, inhibiting Axin-bound GSK3, preventing β-catenin phosphorylation and leading to Axin dephosphorylation. Dephosphorylated Axin adopts an inactivated ("closed") conformation that is unable to associate with β-catenin and phospho-LRP6, leading to the disassembly of the signalling complex. Phospho-LRP6 is then freed to recruit more phosphorylated Axin for inactivation while ignoring dephosphorylated (inactivated) Axin in a reiterative manner, preventing β-catenin destruction. Figure taken from Kim et al, Science 2013.[111]

1.5.3.1 Glycogen Synthase Kinase 3

Glycogen synthase kinase 3 (GSK3) is another central player in Wnt signalling[102,113]. GSK3 is a serine/ threonine kinase, originally identified as a negative regulator of glycogen metabolism via its inhibition of glycogen synthase[114]. The functions of GSK3 are mediated through a number of substrates including β-catenin, glycogen synthase (GS), and τ-proteins[115]. GSK3 is also regulated by the metabolic pathway PI3K/Akt, which is activated in response to insulin stimulation; the signalling is transduced through PI3K phosphorylation of Akt, which then catalyzes the inhibition of GSK3 via phosphorylation of both the Serine21 residue on GSK3α and the Serine 9 residue on the GSK3β isoform (Figure 4). The inhibition of GSK3 promotes dephosphorylation and activation of GS, contributing to the stimulation of

glycogen synthesis. Conversely GSK3 activity can be induced by auto-phosphorylation at Tyr279/216 in the absence of negative regulators[116,117].

Other protein kinases such as P70S6K, RSK1 and PKA also act as inhibitors of GSK3[118], but despite the negative regulation of GSK3 by multiple pathways related to metabolism and cell proliferation, current evidence illustrates that insulin and other agents involved in PI3K/Akt signalling do not stabilize β-catenin and are not associated with transcriptional activation of TCF/LEF[119,118,120]. Furthermore insulin does not cause β-catenin accumulation[121]. Therefore, cells seem to be capable of uncoupling the GSK3-dependent regulation of Wnt-signalling from the GSK3 signalling in other pathways, and executing distinct responses accordingly[118]. As there are two forms of GSK3 in mammalian cells, some have considered a potential labour division between the two, where one of the isoforms is involved in Wnt signalling and the other is involved in different pathways[121]. However, despite variations in the relative proportions of the two proteins in certain tissues (there is more GSK3β than GSK3α in the brain for instance)[113], functional studies of GSK3α and GSK3β have shown that the two isoforms exhibit similar expression patterns and remarkable functional redundancy, indicating that they might function in association or at least mediate very similar activities in canonical Wnt signalling and other pathways[113,122].

1.5.3.2 Canonical Wnt Activation through Inhibition of GSK3

The role of canonical Wnt/β−catenin signalling in differentiation and pluripotency has been the subject of controversy due to conflicting reports; some studies have reported that the activation of canonical WNT-signalling through inhibition of GSK3 activity is required for stem cell self-renewal[109,123]. Conversely several studies have found canonical Wnt-signalling to be a promoter of differentiation through the same process of inhibiting GSK3 activity[97,124,125]. Indeed, the methodology for differentiating hPSCs in this thesis is based on the inhibition of GSK3 and the subsequent activation of β-catenin signaling[126-127]. This is achieved with CHIR99021, an ATP-competitive small molecule inhibitor of GSK3. CHIR99021 inhibits GSK3 activity by

adopting an ATP-like binding to hydrogen bonds on “hinge” residues (Val135-NH and Asp133-CO) of the GSK3 molecule, binding to both the GSK3α and the GSK3β isomer[116].

Many studies have looked at the effects of blocking canonical WNT signalling entirely and found that it is not required for stem cell renewal[46,97,128]. A study by the Dalton group (2012), gives a tentative explanation for these observed incongruences, whereby GSK3β inhibition modulates stem cell self-renewal in a dose-dependent manner. They found that supplementation with the GSK3β inhibitor, BIO (6-bromoindirubin-3'-oxime) at concentrations of <1 μM leads to a stabilization of the pluripotency factor c-MYC and had a negligible effect on β-catenin stabilization. Conversely under concentrations of >2.0 μM BIO, they observed a stabilization of β-catenin, concomitant with a decrease in pluripotency markers such as NANOG[46].

Due to the aforementioned involvement of GSK3 in multiple signalling pathways that are incapable of inducing WNT/β-catenin activity, some have proposed that GSK3 is compartmentalized into different pools that might have different activation thresholds[46,121,129,130]. Such a compartmentalization may in fact be attained through the opposing functions of membrane associated GSK3 versus cytoplasmic GSK3. Membrane associated GSK3 is known to phosphorylate LRP6 in conjunction with CK1, providing docking sites for further recruitment of Axin and GSK3 to the LRP6-signalosome complex[131,132]. These two WNT-associated “forms” or “pools” of GSK3s are also functionally uncoupled from the cytoplasmic pool of GSK3 involved in metabolism, which is negatively regulated by Akt[120]. Perhaps, the most pertinent explanation of the role GSK3 in Wnt signalling so far comes from two articles investigating the Wnt mediated inhibition of GSK3[133]. The articles demonstrate that GSK3 is sequestered and inactivated in multivesicular endosomes upon Wnt stimulation (Figure 8)[134,135]. These findings support our experimental observations, and provide a mechanistic explanation for our CHIR99021-based protocol for DE differentiation (see discussion, section 4).

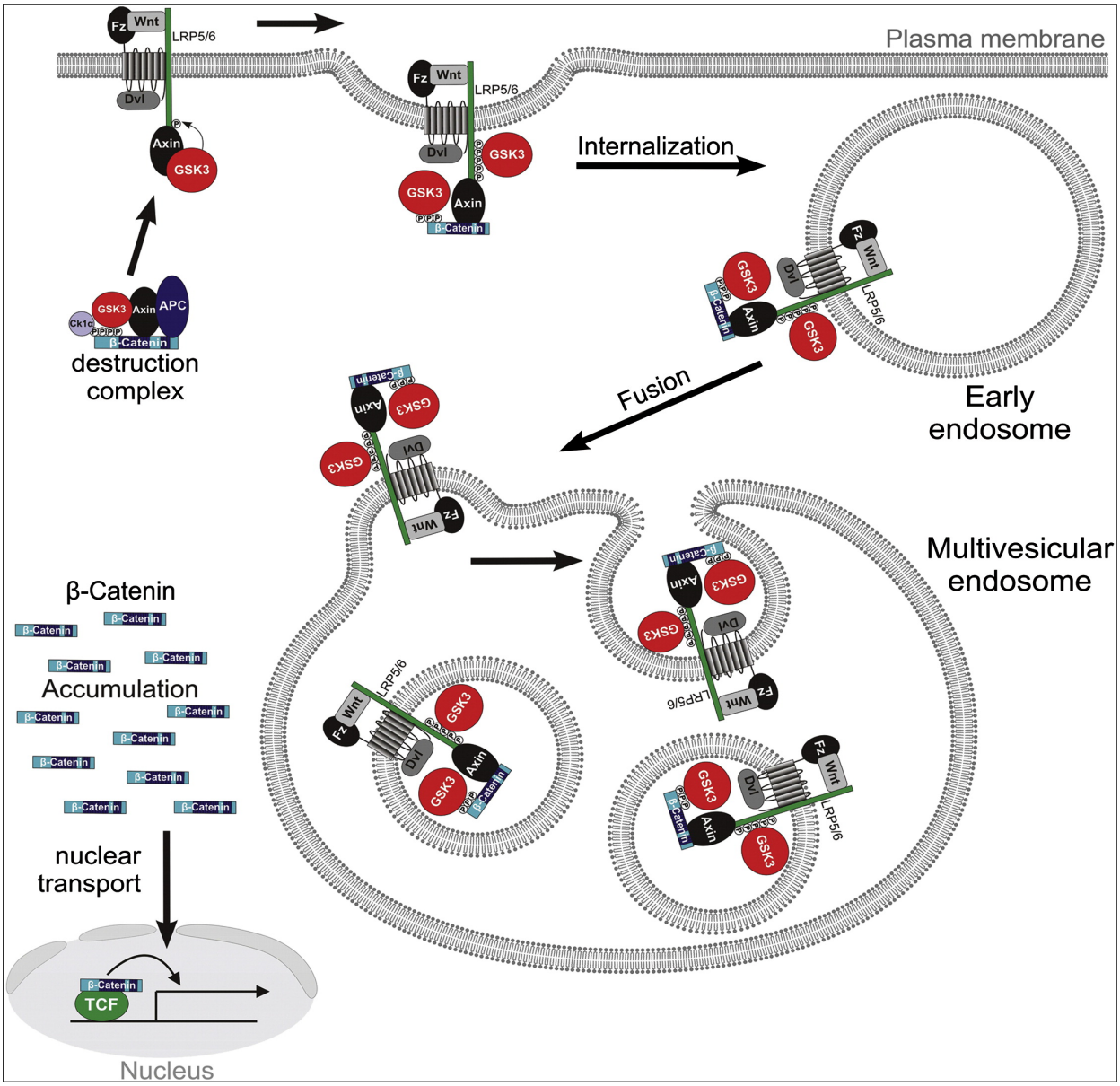

Figure 8. Wnt Induced GSK3 sequestration: Canonical Wnt signalling induces the inhibition of GSK3 activity by sequestration of GSK3 from the cytosol into multivesicular bodies (MVBs), separating GSK3 from its many cytosolic substrates. Figure taken from Taelman et al. Cell, 2010[135].

1.5.3.3 The Axin Homologs

Above we described β-catenin as a positive effector of Wnt signalling, the opposing negative effector of Wnt/β-catenin signalling is Axin. In 2003, a mathematical model of Wnt/β-catenin signalling established Axin as the rate-limiting factor in the β-catenin destruction complex, due to the relatively low concentration of Axin in comparison to other components of the destruction complex[136,137,138]. Prior to this study the role of Axin as key negative regulator of Wnt/β-catenin signalling had already been established by experimental analysis[107,139] and Axin has since been recognized as key negative regulator of Wnt/β-catenin activity[137,140].

There are two homologs of the Axin protein which share 45% nucleotide sequence identity: Axin1 and Axin2 both of which have two isoforms[140,141,142]. Axin1 and 2 are believed to be functionally redundant, pivotal negative regulators of canonical Wnt signalling. Mutations or knockouts of either homolog have been shown to increase β-catenin activity[95,137,140, 144]. However, different studies investigating the function of the Axin homologs have yielded conflicting results, for example the replacement of Axin1 with an Axin2 cDNA knock-in, in mouse embryos, produced viable mice, indicating that the Axin homologs are functionally similar enough to compensate for each other[141]. On the other hand several other studies have shown dissimilarities in the functions of Axin1 and 2 during development. These studies have demonstrated that inactivation of Axin1 is embryonically lethal in mice, causing defects in axis formation and brain patterning[143,145,146], whereas Axin2 inactivation produced viable mice, but lead to craniofacial defects due to excessive osteoblast proliferation and differentiation[143,146]. Axin1 is a constitutively expressed component of the β-catenin destruction complex and is vital for maintenance of low levels of canonical Wnt signalling in the basal (Wnt-off) state[142,143]. By contrast, Axin2 is expressed in a circumscribed manner at certain developmental stages, and in specific tissues[142,143,147].

Given the presumed functional redundancy of the homologs, the disparate effects of Axin1 and Axin2 inactivation are thought to be due to differences in

the expression of their genes[143]. However, this notion has been increasingly challenged as the mechanisms and nuances of Axin-signalling become further elucidated. A recent study found that overexpression of Axin2 could not compensate for knockdown of Axin1 in muscle stem cells, suggesting that they are not entirely redundant[143]. Furthermore, unlike Axin1, Axin2 is a target gene of active β-catenin meaning that transcriptional Axin2 expression is up-regulated by active β-catenin in the nucleus. The expression of Axin2 is therefore an indicator of canonical Wnt pathway activity. Since Axin2 is known to induce β-catenin degradation, its transcriptional activation by β-catenin is believed to be part of a negative feedback loop that regulates canonical Wnt signalling by limiting its duration and intensity[142,143,148,149]. Additionally a recent study uncovered differences in the sensitivity of Axin1 & 2 to binding and inactivation by the upstream Wnt-protein, Dishevelled. The study demonstrated differences in the ability of Dvl2 to block Axin-mediated degradation of β-catenin, showing a clear inhibitory effect on Axin1, in contrast to a rather weak effect on Axin2[149]. The authors hypothesized that the functional division of Axin1 and Axin2 into a constitutive, and an inducible negative regulator, respectively, might allow more fine-tuned responsiveness to Wnt/β-catenin signalling feedback, instead of the abrupt blocking of an important negative regulator of canonical Wnt signalling[149].

1.5.3.4 Tankyrase-Mediated Inhibition of Axin

In 2009, a study investigating the molecular actions of a small molecule inhibitor of canonical Wnt signalling, lead to the identification of a new gene product (*Tankyrase* or telomeric repeat factor TRF1-interacting ankyrin-related adenosine diphosphate ADP-ribose polymerases (TNKS)) that interacted with the Wnt/β-catenin signalling pathway through the promotion of Axin1/2 degradation[150]. TNKS was originally discovered as a protein involved in telomere homeostasis[151], but an expanding number of functions have now been identified including cellular functions, such as mitotic progression, as well as glucose metabolism, stress granule formation, Wnt signalling, and proteasome regulation[136]. TNKS belongs to the family of Diphtheria toxin-like

ADP-ribosyltransferases (ARTDs)[152]. The human Tankyrases: TNKS1 and TNKS2 are multi-domain proteins belonging to a distinct subgroup of the polymer forming ARTDs[136]. The two TNKS share 82% sequence identity and are collectively essential for embryonic development as the TNKS1/TNKS2 double knockout is embryonically lethal in mice. Individually however they are somewhat redundant, as individual knockouts produced viable mice with only mildly defective phenotypes[136,153]. The TNKS1/2 molecular mechanism of action involves the transfer of the ADP-ribose moiety from NAD+ to a specific amino acid residue on substrate proteins[152]. In this way the catalytic ART domain of TNKS1/2 may poly-ADP-ribosylate (PARsylate) Axin[136,150,154,155]. The PARsylated Axin is then recognized by the E3 ubiquitin ligase (RNF146), which adds ubiquitin moieties to Axin, targeting it for proteasomal degradation[156,157,158].

Research into the effects of TNKS inhibition has also further verified its role as an inhibitor of Axin. Inhibition of TNKS via small-molecules or small interfering RNA (siRNA) results in a stabilization of Axin proteins that subsequently leads to an accumulation of destruction complexes[154,159,160]. The accumulation of destruction complexes enhances β-catenin degradation, causing a sharp decrease of canonical Wnt signaling[150,154,140-160]. This accumulation of β-catenin destruction complexes is thought to be mediated by a large increase in, and stabilization of Axin expression[161]. In a recent publication by Yang et al[162], TNKS was shown to have an unanticipated effect on Axin following Wnt stimulation. In this study they found that in addition to controlling Axin levels, TNKS-dependent ADP-ribosylation promoted a functional change in Axin following canonical Wnt stimulation. In both Drosophila and human cells, TNKS was shown to rapidly ADP-ribosylate Axin in the presence of Wnt stimulation, leading to a rapidly increased pool of ADP-ribosylated Axin in the cell. While this would normally lead to its degradation under basal conditions, the ADP-ribosylation of Axin enhanced its ability to bind to the Wnt membrane-receptor LRP6, enabling it to form the LRP6 signalosome (Figure 9)[162]. They further postulate that the initial increase in levels of ADP-ribosylated Axin drives the response to Wnt stimulation by enhancing the Axin-LRP6 interaction, whereas the subsequent decrease in Axin levels

prolongs the duration of signalling by reducing destruction complex assembly. (This is further explored in section 4.1)

In corroboration with other recent publications on the role of Axin in Wnt signalling[163], a model has been proposed where Axin plays a dual role in modulating Wnt signalling: on one hand, Axin scaffolds the β-catenin destruction complex, promoting its degradation and inhibiting Wnt signal transduction; on the other hand, Axin interacts with LRP5/6, facilitating the recruitment of GSK3 to the plasma membrane to promote LRP5/6 phosphorylation and Wnt signalling. The differential assemblies of Axin with these two distinct complexes have to be tightly controlled for appropriate transduction of the "on" or "off" Wnt signal.

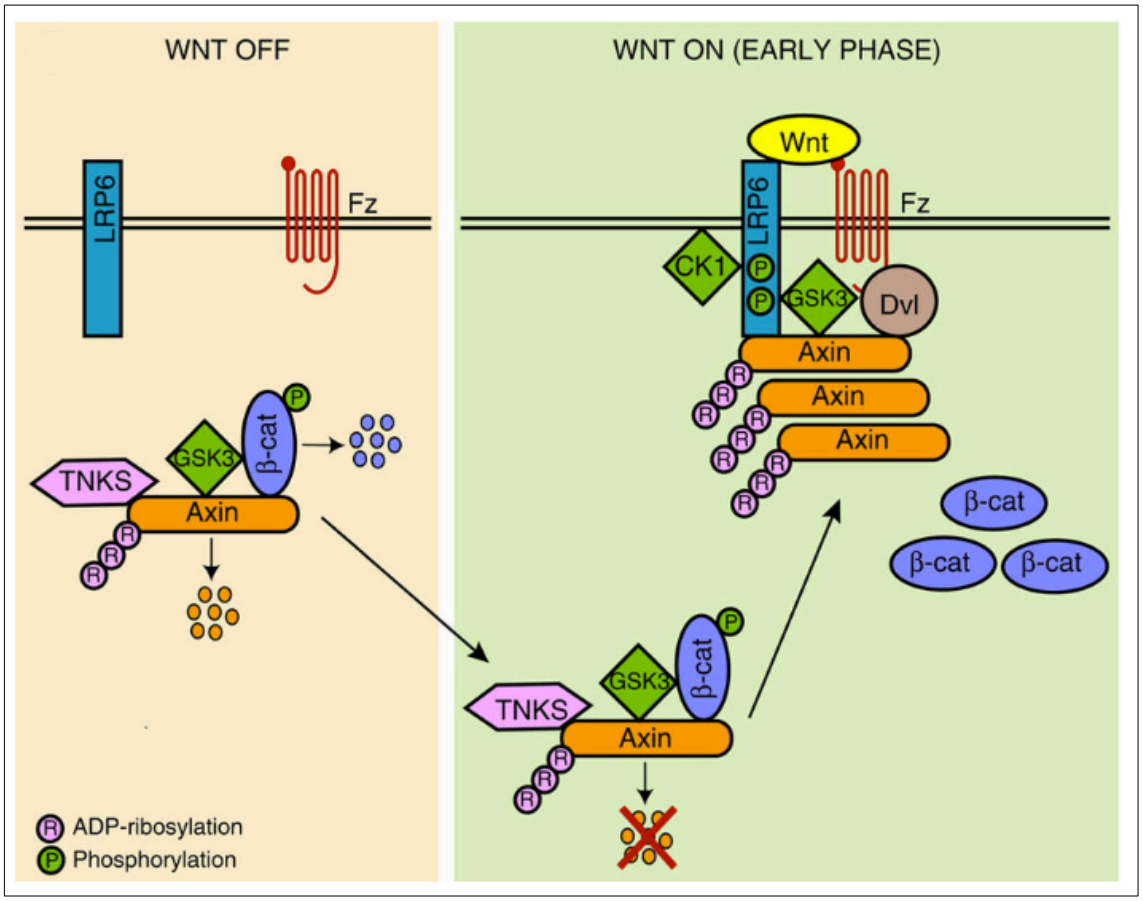

Figure 9. The Wnt-dependent ribosylation of Axin by TNKS: TNKS-mediated ADP-ribosylation targets Axin for proteolysis in the absence of Wnt. The presence of Wnt however sparks a rapid accumulation of ADP-ribosylated Axin by TNKS. Following Wnt stimulation ADP-ribosylation promotes Axin's interaction with LRP6, thereby activating the Wnt pathway. Figure taken from Yang et al, Nature Communications. 2016.[162]

1.5.4 Convergence of PI3K/Akt and AMPK on mTOR

AMP-activated protein kinase (AMPK) is a key regulator of cellular energy homeostasis and metabolic processes[72]. AMPK is a heterotrimeric protein comprised of a catalytic α subunit and regulatory β and γ subunits[164]. It is activated under conditions that heighten the ratio of adenosine monophosphosphate (AMP) to adenosine triphosphate (ATP), such as nutrient-poor conditions or prolonged exercise[165,166]. AMPK can be viewed as the catabolic counterpart to the PI3K/Akt/mTOR mediated activation of anabolic processes (section 1.4.1.3). Indeed Akt and AMPK act as antagonists in many signalling pathways. Akt activates, while AMPK inactivates mTOR activity in stem cells[167,168,169]. Active AMPK suppresses many anabolic pathways such as fatty acid and protein synthesis, and stimulates catabolic pathways such as fatty acid oxidation and glycolysis (Figure 10)[170]. In low-energy conditions AMPK is activated through phosphorylation by liver kinase B1 (LKB1) on threonine-172 (Thr172) in the activating loop of AMPKα. This occurs when AMP binds to the γ subunit of AMPK permitting the binding of AMPK to Axin-LKB1 to form a Axin-LKB1-AMPK complex that facilitates the phosphorylation of AMPK via by LKB1[170]. This leads to a more than 100-fold increase of its kinase activity[170]. Once activated, AMPK phosphorylates a variety of substrates to stimulate catabolic activities that maintain intracellular ATP levels, such as autophagy,[165,169,171]

AMPK and PI3K/Akt both converge on mTOR and are known to be involved in differentiation, but the underlying mechanisms are poorly defined. Under low-energy conditions AMPK together with GSK3 phosphorylates and activates TSC2, which then inhibits mTORC1[167]. Under high-energy conditions PI3K/Akt stimulates the reverse process, inhibiting the TSC1/2 complex to promote mTORC1 activity[168,172]. AMPK and mTOR also have opposing roles in the maintenance of self-renewal in pluripotent stem cells versus differentiation. AMPK has been implicated in the process of differentiation through its enhancement of β-catenin/TCF mediated transcription[173] and by inducing metabolic shifts characteristic of stem cells undergoing differentiation, such as the shift from glycolysis to oxidative phosphorylation (OXPHOS) and

the concomitant maturation of mitochondria[168,174,175,176]. Additionally, the activation of AMPK has been shown to be incompatible with pluripotency[177]. It therefore seems likely that AMPK mediated activation of autophagy might allow differentiating cells to recycle nutrients and undergo cellular "remodelling"[178,179].

mTOR on the other hand has been recently established as an important positive regulator of pluripotency[180,181]. Inhibition of mTOR has been shown to impair pluripotency and prevent cell proliferation, while enhancing mesoderm and endoderm activities in hESCs[180]. Furthermore mTOR has been shown to integrate signals from extrinsic pluripotency-supporting factors and repress the transcriptional activities of a subset of genes involved in endodermal differentiation and devleopment such as *T, GATA4/6, EOMES*, and *SOX17*[180]. In contrast to AMPK, mTOR also negatively regulates autophagy[179,181,]. mTOR exists as two distinct protein complexes, mTOR complex 1 (mTORC1) and mTOR complex 2 (mTORC2), each complex contains the protein mTOR, but are associated with certain shared and complex specific proteins. The core components of mTORC1 are regulatory-associated protein of mTOR (RAPTOR) and mammalian lethal with SEC thirteen 8 (mLST8); whereas, those of mTORC2 are rapamycin-insensitive companion of mTOR (RICTOR), SAPK-interacting 1 (SIN1) and mLST8[171]. Both of the mTOR complexes are positively regulated by PI3K/Akt and interact with it different manners. As previously mentioned PI3K/Akt maintains mTORC1 activity by inhibiting TSC1/2. The mTORC2 pathway is not as well characterized, but was recently found to play an important role in mediating PI3K/Akt driven maintenance of pluripotency in hPSCs. A recent paper demonstrates that PI3K activated mTORC2 attenuates Smad2/3 activity, inhibiting Nodal-induced DE differentiation in hPSCs. At the molecular level, PI3K activation of mTORC2 promotes mTORC2 mediated phosphorylation of Smad2/3 at the linker residue, which enables the recruitment of E3 ubiquitin ligase to the active Smad2/3, resulting in its degradation[182]. This gives a potential mechanistic explanation for the required ratio of high PI3K/Akt to low/moderate Nodal expression in pluripotent stem cells versus low PI3K and high Nodal expression in DE differentiation.

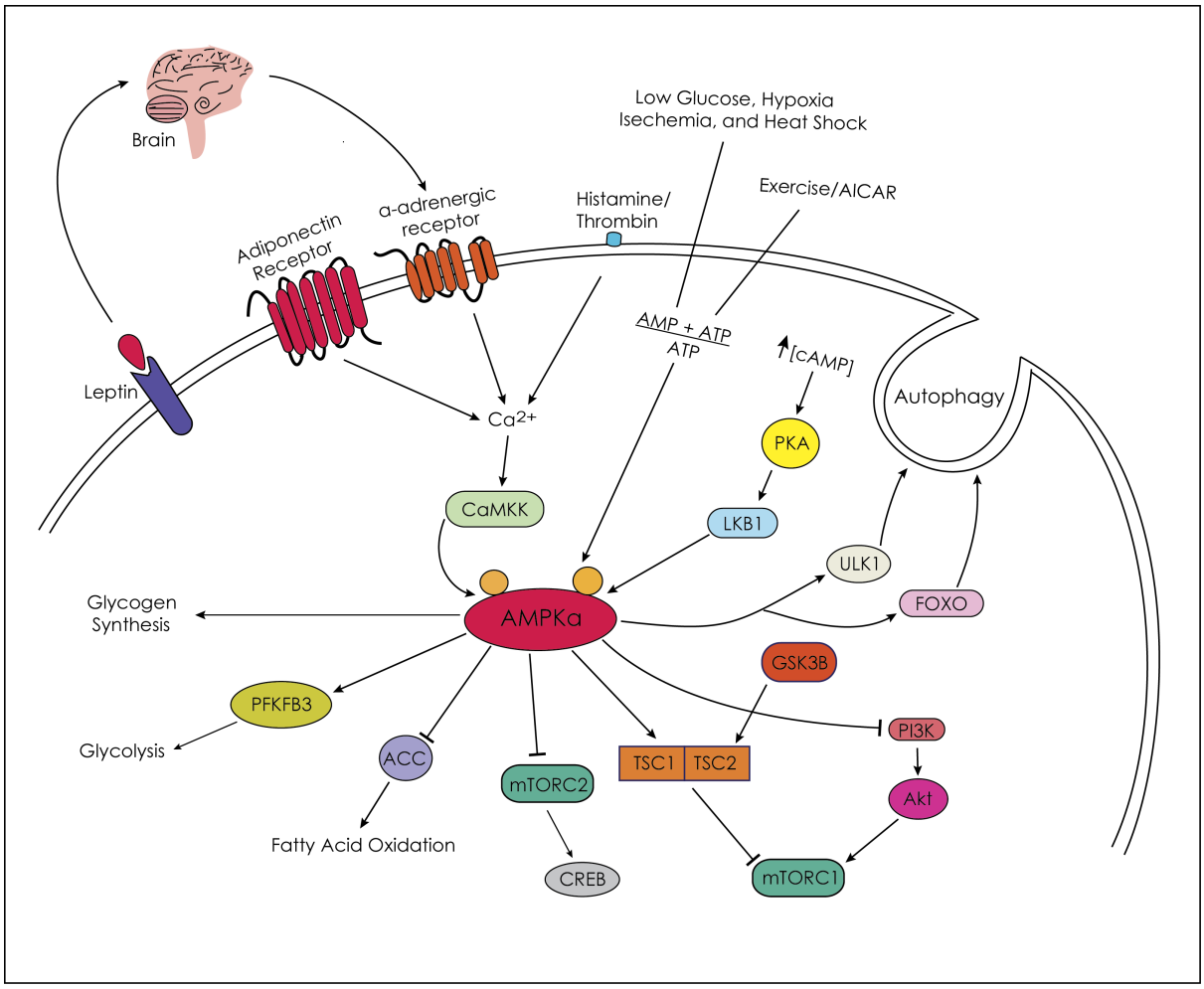

Figure 10. AMPK pathway: Upon nutrient low conditions AMP binds to AMPK allowing for activation of AMPK by LKB1. Active AMPK then inhibits mTORC2, and activates TSC1/2, while promoting catabolic activities such as glycolysis, fatty acid oxidation and autophagy[165,224,225] . Figure inspired by Cell Signaling Technology's AMPK Signaling Pathway[226].

1.6 Aim of the Study

Based on the cell-signalling information above we wanted to examine protein activity and expression dynamics for key extrinsic signalling proteins during the development from hPSCs to DE. The following sections will explain our methodology and reasoning in these attempts.

2 Methods and Materials

2.1 Human Pluripotent Stem Cell (hPSC) Culture and Maintenance

The hESC lines H1 (WiCell), 207 and 307 (Hovatta Lab, Karolinska Institute), and the Sendai virus–derived hiPSC lines AG05836B clone #27 (AG-27, Coriell Institute), Detroit 551 RA, RB and RC (American Type Culture Collection (ATCC CCL-110)) were cultured under feeder free conditions. hPSCs were cultured in Nunc Nucleon 6-well Multidish plates (Thermo Fischer Scientific), coated with Geltrex (Life Technologies) diluted 1:100 with Advanced DMEM F12 (Life Technologies). Cells were fed daily with 2ml / well of Essential 8 medium (Life Technologies), and maintained in a humidified incubator at 37°C and 5% CO2. The cells were routinely passaged at 70-80% confluence, typically every 4-5 days. For routine maintenance the cells were passaged according to our published protocol[183] using EDTA (Life Technologies). All cell-culturing procedures were carried out in a sterile environment. The cell lines were routinely checked for mycoplasma contamination with the MycoAlert™ Mycoplasma Detection Kit (Lonza). (For a list of the materials, buffers, and cell lines used see Tables 4, 5, and 6).

2.1.1 Differentiation of Human Pluripotent Stem Cells Toward DE

The differentiation of hPSCs toward DE was performed according to our published protocols[126,183]. For the work of this thesis, the differentiation proceeded to day 2 (DE stage) as described in our protocol.

To prepare cultures for the differentiation procedure**,** hPSCs were washed with DPBS without Calcium and Magnesium (Life Tech), before being dissociated using Accutase (Life Technologies) and re-plated on Geltrex-coated plates at a density between 40,000 to 50,000 cells per cm^2 depending on the cell line. The optimal seeding density was determined empirically for each line by titrating the cell number and assessing the efficiency of differentiation at each respective density. The cells were re-plated in Essential

8 Medium supplemented with 10μM ROCK inhibitor Y-27632 (Tocris Biosciences) used to enhance hPSC survival by preventing dissociation-induced apoptosis (anoikis)[184]. Cells were allowed to adhere overnight in a 37°C, 5% CO_2 incubator. Before beginning the differentiation, the cells were assessed to determine whether the confluency was correct (ideal confluency for starting differentiation to DE in our hands is approximately 30-40% as reported in Siller et al[126] and Mathapati et al[183]).

To initiate DE differentiation our in-house small molecule driven protocol was utilized. Briefly, the cells were washed with DPBS (without Calcium or Magnesium) (Life Technologies) prior to the addition of RPMI 1640 medium supplemented with B27 either with or without Insulin (both from Life Technologies) and the GSK3 inhibitor CHIR99021 (Stemgent). Importantly, prior to setting up experiments, each hPSC line was assessed for the optimal concentration of CHIR99021 and whether the presence of insulin in the B27 supplement inhibited or enhanced differentiation.

In our hands we have found that the majority of cell lines readily differentiate to DE using 3-4 μM of CHIR99021. In the case of the H1 and AG-27 cell lines, the optimal plating densities were 47,000 and 50,000 cells/cm2, respectively. For H1 we have found that optimal DE is obtained using RPMI supplemented with B27 with insulin and 3 μM CHIR99021. For the hiPSC line AG-27, the optimal conditions for DE differentiation were with RPMI supplemented with B27 without Insulin and 4 μM CHIR99021. Both cell lines were maintained at 37°C, and 5% CO_2 for 24 hours followed by removal of the GSK3 inhibitor and 24-hour treatment with RPMI-B27 media alone (with or without insulin as before). Cells were collected for either qRT-PCR, or Western blot analysis at six different time points: 0, 4, 8, 12, 24 and 48 hours. The cells were observed under a light microscope to ensure expected morphological changes during differentiation. At around 24 hours, the cells formed compact bright clusters indicative of PS formation. By 48 hours the cells displayed a petal shaped morphology indicative of DE.

2.2 Sample Collection

Cells were collected for analysis as follows. For qRT-PCR, 3 wells (from a 6-well plate) were collected for each time point. Cells were washed with DPBS (without Calcium and Magnesium) and then 0.5 ml of TRIzol (Life Technologies) was added to each well. Cells were detached from the plate by manual scraping with a pipette and transferred to an Eppendorf tube. The sample was then either processed for RNA extraction immediately according to the manufacturer´s instructions[185] or stored at -80°C for further processing. Samples collected for western blot analysis were pooled from 5 wells of a 6-well plate. Protein samples were collected for the same time points as RNA collection and processed (as described in western blotting section 2.4).

2.2.1 RNA Isolation

RNA was isolated using TRIzol according to the manufacturer´s instructions. RNA was quantified using a NanoDrop.

2.2.2 cDNA Synthesis

500ng of RNA was used to synthesize cDNA using the High Capacity Reverse Transcriptase kit from Life Technologies.

2.2.3 Quantitative Real Time Polymerase Chain Reaction Analysis

cDNA was analyzed by qRT-PCR using a TaqMan ViiA7 Real Time PCR System with TaqMan primers (See Table 1), and BioRad SsoAdvanced Universal Probes Supermix according to the manufacturer's instructions. All samples were run in triplicate, with *ACTB* serving as a housekeeping gene, control. Data was normalized to undifferentiated hPSC, and all data is expressed as the average of 3 biological replicates +/- the standard deviation.

To analyze the fold change in gene expression we had make the following calculations based on our Ct values: Ct (cycle threshold) value is the cycle number at which the fluorescent signal is significantly higher than the baseline (background) signal[186].

ΔΔ Ct = (Ct target sample - Ct reference sample)

- Ct refrence sample in this case is the β-actin value at 0 hours.

To find the fold change in gene expression we calculate the $2^{(-\Delta\Delta Ct)}$ value for each sample[187], which is designated as its relative quantification (RQ) value. We then calculate the log10 of our RQ value in order to represent the fold change in gene expression on a logarithmic scale.

Table 1. List of gene probes (primers) used for qRT-PCR analysis

Gene Probe	TaqMan Assay ID	Manufacturer
NODAL	Hs00415443_m1	Applied Biosystems
GSC	Hs00906630_m1	Applied Biosystems
T (BRACHYURY)	Hs00610080_m1	Applied Biosystems
MIXL1	Hs00430824_g1	Applied Biosystems
FOXA2	Hs00232764_m1	Applied Biosystems
SOX17	Hs00751752_s1	Applied Biosystems
CER1	Hs001933796_m1	Applied Biosystems
HHEX	Hs00242160_m1	Applied Biosystems
POU5F1P (OCT4)	Hs00999634_gH	Applied Biosystems
SOX2	Hs01053049_s1	Applied Biosystems
NANOG	Hs042600366_g1	Applied Biosystems
MYC	Hs00153408_m1	Applied Biosystems
FOXG1	Hs01850784_s1	Applied Biosystems
PAX6	Hs00240871_m1	Applied Biosystems
NESTIN	Hs04187831_g1	Applied Biosystems
WNT3A	Hs00263977_m1	Applied Biosystems
AXIN1	Hs00394718_m1	Applied Biosystems
AXIN2	Hs00610344_m1	Applied Biosystems
Human *ACTB*	4352667	Applied Biosystems

2.3 Immunofluorescence-Staining & Microscopy

hPSCs were collected at either 0 hours (for pluripotency characterization) or 48 hours (for DE characterization) and washed with DPBS without Calcium and Magnesium before being fixed with a 10 minute treatment of ice-cold methanol at -20°C. Fixed cells were washed in 0.1% PBS-T: PBS containing 0.1% Tween 20 (Sigma Aldrich). The cells were then blocked for 3 hours using 10% normal goat serum (Life Technologies) made up in 0.1% PBS-T. After washing the cells twice with 0.1% PBS-T, cells were treated with primary antibodies diluted in 1% normal goat serum/ 0.1% PBS-T and incubated overnight at 4°C; (see Table 2 for antibody details). Following primary antibody incubation, cells were washed 4 times with 0.1% PBS-T and treated with secondary antibodies (Life Technologies) diluted in PBS for 1 hour at room temperature. Cells were then washed 4 times with PBS-T and three times with PBS before being mounted using Fluoroshield with DAPI (Sigma Aldrich) and glass coverslips (VWR).

2.3.1 Microscopy

For phase contrast microscopy**,** the cells were imaged using a Primovert (Zeiss) microscope and images were obtained using Zen Software (Zeiss). For confocal microscopy, the cells were imaged using a Zeiss LSM700 laser scanning confocal microscope (Zeiss) and Zen software (Zeiss).

Table 2. List of primary and secondary antibodies and reagents used for immunostaining

Target Protein	Manufacturer	Catalogue #	Species	Dilution
OCT4	STEMGENT	09-0023	Rabbit	1:100
SOX2	STEMGENT	09-0024	Rabbit	1:100
NANOG	STEMGENT	09-0020	Rabbit	1:100
SOX17	Abcam	ab84990	Mouse	1:100
FOXA2	Abcam	ab40874	Rabbit	1:1000
Alexaflour 488 anti rabbit	Life Technologies	A21206	Donkey	1:400
Alexafluor 488 anti mouse	Life Technologies	A11059	Rabbit	1:400
Alexafluor 594 anti mouse	Life Technologies	A11005	Goat	1:400
Dye/stain	**Manufacturer**	**Catalogue #**		
Fluoroshield with DAPI	Sigma Aldrich	F6057		

2.4 Western Blotting (Immunoblotting) Protocol

2.4.1 Preparation of Cell Lysates

Western blot analysis was performed on protein samples that were pooled from 5 wells of a 6-well plate for each time point. For each time point the media was aspirated before washing with 2ml of DPBS. The DPBS was then aspirated off so that there was no remaining liquid in the wells. The plates were then flash frozen on dry ice before being stored at -80°C for further processing. cOmplete protease inhibitors and PhosSTOP phosphatase inhibitors (Roche Applied Science) were added to the cell lysis buffer for protein extraction. 1 tablet of each inhibitor was added per 10ml of NP-40 Cell Lysis Buffer (Thermo Fischer Scientific). 150μl of the prepared lysis buffer was then added to each of the 5 wells of the 6-well plate. The cell lysate was collected using cell scrapers (Starstedt) and the lysate was transferred to a 1.5 ml Eppendorf tube, which was centrifuged at 15,000 rpm for 15 min at 4°C. NP-40 was specifically chosen as the lysis buffer, as it allows for the pelleting of nuclei and cell debris to the bottom of the eppendorf tube, while cytoplasmic proteins are suspended in the supernatant. This allowed us to look at the nuclear and cytoplasmic fractions of our cell lysates, separately. After the nuclei had been pelleted to the bottom of the tube, the supernatant containing cytoplasmic proteins was transferred to a new eppendorf tube, and the remaining pellet containing the nuclear fraction, was stored at -20°C. In addition to preparing cell lysates for our 2 main cell-lines (H1 and AG-27) we also prepared cell lysate samples for 5 control hPSC lines (Detroit 551 RA, RB, RC, 207 and 360, see table 6). These were prepared in the same manner as above, with the exception of the cell lysis buffer and the number of collected time points. Since the control cell lines were only used to check if the overall trends of protein expression were conserved across cell lines, we used RIPA Lysis Buffer (Millipore) instead of NP-4. This gave us an aggregate of both cytoplasmic and nuclear proteins. Samples were collected at 0, 4, 8 and 48 hours for the control cell lines.

2.4.1.1 Measuring Protein Concentration for the Cytoplasmic Fraction

Protein concentration was determined using the Pierce Micro BCA Protein Assay Kit (Thermo Fischer Scientific), according to the manufacturers instructions. Briefly, 10µl of protein samples was analysed and quantified using, bovine serum albumin (BSA) protein standards. The absorbance of the solution was then measured with a photo-spectrometer at a wavelength of 562nm. A standard curve was made based on the measured absorbance values for the BSA standards. The resulting ratio was used to calculate the protein concentrations of our cell lysate samples from their absorbance values.

2.4.1.2 Sample Preparation:

After determining the protein concentrations of our cell lysates, we adjusted all cell lysate samples to a final concentration of 0.5µg/µl by diluting samples with NP-40 buffer. The samples were vortexed and incubated at 70°C for 10 min.

2.4.1.3 Sonication and Preparation of Lysates from Nuclear Fractions:

To prepare the nuclear fraction samples for immunoblotting, we added 100µl of RIPA lysis buffer (Millipore) to the previously centrifuged Eppendorf tubes containing the nuclear pellets. These samples were then sonicated in an ultrasonic water bath. The lysates were then prepared for western blotting in the same manner as the cytoplasmic protein fractions described above.

2.4.2 SDS-PAGE:

Gel electrophoresis of the protein samples, was performed using NuPAGE Novex 4-12% Bis-Tris protein gels (Life Technologies) for analysis of proteins under 200kDa, or NuPAGE Novex 3-8% Tris-Acetate protein gels for analysis of proteins above 200kDa. Likewise PageRuler prestained protein ladder (Thermo Fisher Scientific) was used as a molecular weight ladder for proteins under 200 kDa, whereas HiMark Prestained Protein Standard (Thermo Fisher

Scientific) was used for proteins over 200 kDa. 30µl (15µg of protein) of the protein samples were loaded into wells and run in Novex electrophoresis chambers (Life Technologies) at 70 - 130 V, in either NuPAGE MOPS SDS Running Buffer or NuPAGE Tris-Acetate SDS Running Buffer (Life Technologies) depending on the gel.

2.4.3 Semi-Dry Electrophoretic Transfer

After gel electrophoresis the PAGE gel was soaked in transfer buffer (see table 5), while Whatman filter paper (BIORAD) and polyvinylidene fluoride (PVDF) membrane (Immobilon-P^{SQ}, Millipore) were cut to size for transfer of the PAGE gel. The PVDF membrane was soaked in methanol for 2 minutes before being equilibrated in transfer buffer for 5 min. The Whatman paper, PVDF, and PAGE gel were soaked in transfer buffer, before being transferred to the Trans-Blot SD semi-dry electrophoretic transfer cell (Bio-Rad). The materials were placed in the following order from anode to cathode: filter paper, PVDF membrane, protein gel and filter paper. The electrophoretic transfer was then carried out in a cold-room at 4°C either at 25 V for 1.5 hours or overnight (10-18H) at 3W.

2.4.4 Blocking and Incubation of Western Blots

After transfer of proteins from the PAGE gel to the PVDF membrane, the blot was blocked with 5% (non-fat dried) milk (AppliChem) in Tris-buffered saline with Tween 20 (TBS-T, Medicago) for 1-2 hours . The blot was then incubated with primary antibodies of interest and a control antibody (β-actin or GAPDH), in 5% milk and TBS-T overnight at 4°C, or two nights at 4°C depending on the antibody. The blots were then washed with TBS-T, and incubated with the respective secondary antibodies in 5% milk in TBS-T for 1-2 hours at room temperature. (For antibody details see Table 3)

2.4.5 Protein Detection

For detection of proteins, the blots were washed with TBS-T and treated with Amersham ECL Prime reagents (GE Healthcare) according to the manufacturer´s instructions. This enabled detection of protein bands by chemiluminescence imaging in a ChemiDoc Touch Imager System (Bio-Rad).

Table 3. List of primary and secondary antibodies used for western blotting

Primary Antibodies	**Catalogue #**	**Species & Isotype**	**Dilution**	**Manufacturer**
β-actin	SAB5500001-100UL	Rabbit IgG	1:10000	Sigma Aldrich
Akt	#9272	Rabbit IgG	1:1000	Cell Signaling Technology
pAkt (Ser473)	#4060	Rabbit IgG	1:1000	Cell Signaling Technology
pAkt (Thr308)	#9275	Rabbit IgG	1:1000	Cell Signaling Technology
AMPKα	#2793	Mouse IgG	1:500	Cell Signaling Technology
pAMPKα (Thr172)	#2531	Rabbit IgG	1:500	Cell Signaling Technology
Axin1	#2087	Rabbit IgG	1:1000	Cell Signaling Technology
Axin2	#2151	Rabbit IgG	1:1000	Cell Signaling Technology
Non-phospho (active) β-Catenin	#8814	Rabbit IgG	1:1000	Cell Signaling Technology
GSK-3β	#12456	Rabbit IgG	1:1000	Cell Signaling Technology
pGSK-3β (Ser9)	#9323	Rabbit IgG	1:1000	Cell Signaling Technology
mTOR	#2972	Rabbit IgG	1:1000	Cell Signaling Technology
PTEN	#9552	Rabbit IgG	1:1000	Cell Signaling Technology
p70 S6 Kinase	#9202	Rabbit IgG	1:1000	Cell Signaling Technology
S6RP	#2217	Rabbit IgG	1:1000	Cell Signaling Technology
TSC2	#4308	Rabbit IgG	1:1000	Cell Signaling Technology
E-Cadherin	sc-21791	Mouse IgG	1:1000	Santa Cruz Biotechnology
pERK 1/2 (Tyr 204)	sc-101761	Rabbit IgG	1:1000	Santa Cruz Biotechnology
GAPDH	sc-32233	Mouse IgG	1:5000	Santa Cruz Biotechnology
TNKS1/2	sc-8337	Rabbit IgG	1:250	Santa Cruz Biotechnology
Lamin B1	ab16048	Rabbit IgG	1:5000	Abcam
Secondary Antibodies	**Catalogue #**	**Species & Isotype**	**Dilution**	**Manufacturer**
donkey anti-mouse IgG-HRP	sc-2314	Donkey IgG-HRP	1:5000	Santa Cruz Biotechnology
donkey anti-rabbit IgG-HRP	sc-2313	Donkey IgG-HRP	1:5000	Santa Cruz Biotechnology

Table 4. List of materials

Product	Manufacturer	Catalogue Number
hPSC culturing:		
Essential 8 Medium	Life Technologies	A1517001
Essential 8 Supplement	Life Technologies	A15171-01
Geltrex	Life Technologies	A1413302
Nunc Nunclon 6-Well x 3mL MultiDish	Thermo Fisher Scientific	140685
EDTA	Life Technologies	15575-020
ROCK inhibitor Y-27632	Tocris	1254
Advanced (DMEM-F12) Dulbecco's Modified Eagle Medium/Ham's F-12	Life Technologies	12634028
DPBS	Life Technologies	14190
DE differentiation of hPSCs:		
Accutase	Life Technologies	A1115-01
40-µm Corning cell strainer	Sigma Aldrich	CLS431750
50-ml Falcon conical tubes	VWR	734-0453
RPMI Medium 1640, GlutaMAXTM	Life Technologies	61870
B-27 Supplement ± insulin	Life Technologies	17504-044 or A1895601
CHIR99021	STEMGENT	04-0004-10
qRT-PCR		
TRIzol Reagent	Life Technologies	15596026
SsoAdvanced Universal Probes Supermix	Bio-Rad	
High-Capacity cDNA Reverse Transcription Kit	Life Technologies	4368813
Immunofluorescence		
Normal Goat Serum (NGS)	Life Technologies	PCN5000
Tween 20	Sigma Aldrich	P7949
SDS-PAGE		
NP40 Cell Lysis Buffer	Life Technologies	FNN0021

cOmplete, Mini Protease Inhibitor Cocktail	Roche	4693124001
PhosSTOP Easypack Phosphatase Inhibitor Cocktail	Roche	04906837001
Micro BCA Protein Assay Kit	Thermo Fischer Scientific	23235
Nu-PAGE Novex 4-12% Bis-Tris Protein gels, 1.0 mm, 10 well	Life Technologies	EA0375BOX
Nu-PAGE Novex 3-8% Tris-Acetate Protein gels, 1.0 mm, 10 well	Life Technologies	NP0321BOX
Nu-PAGE MOPS running buffer 20X	Life Technologies	NP0001
Nu-PAGE Tris-Acetate SDS running buffer 20X	Life Technologies	LA0041
PageRuler Prestained Protein Ladder	Thermo Fischer Scientific	26616
HiMark™ Pre-Stained Protein Standard	Life Technologies	LC5699
Semi Dry Electrophoretic Transfer and Imaging of Blot		
Extra Thick Blot Filter Paper	Bio-Rad	1703960
Immobilon-P^{SQ} Transfer Membrane	Millipore	ISEQ00010
Nonfat Dried Milk	AppliChem	A0830,0500
TBST - Tablets	Medicago	09-7510-100
Trizma-base	Sigma Aldrich	T1503
Glycine	Sigma Aldrich	G7126
Sodium Dodecyl Sulfate (SDS)	Sigma Aldrich	L3771
Bromophenol Blue Sodium Salt	Sigma Aldrich	B5525
β-Mercaptoethanol	AppliChem	A1108,0100
Sodium chloride (NaCl)	Sigma Aldrich	S3014
Tris hydrochloride (Tris-HCl)	Sigma Aldrich	RES3098T
EDTA	Sigma Aldrich	431788
Amersham ECL Prime Western Blotting Detection Reagent	GE Healthcare Life Sciences	RPN2236

Table 5. List of buffers and solutions used in our protocols

Buffers and Solutions	Components
Essential 8 Medium	500ml Essential 8 Medium 10ml 50X Essential 8 Supplement
Geltrex 6-Well Plate Coating	500-µl of Geltrex stock solution (Pre-diluted in AdvDMEM/F12 medium at 1:1 ratio) Is further diluted in 50ml of cold AdvDMEM/F12.
RMPI/B-27 Medium or RPMI/B-27 Medium with CHIR99021	10 ml B-27 Supplement ± insulin 490 ml RPMI 1640 Medium, GlutaMAX supplement. With or without 3-4 µM of CHIR99021
TBS-T	2 TBS-T tablets (Medicago) per liter of MQ H_2O 0.15 M NaCl, 0.050 M Tris-HCl, 0.05% Tween 20
10X Protein Transfer Buffer (Stock)	30.3g of Trizma-base 144g of Glycine 1000ml MQ H_2O
Transfer Buffer	100ml 10X Protein Transfer Buffer 200ml of Methanol 700ml of MQ H_2O
NP-40 Cell Lysis Buffer	10ml NP-40 Cell Lysis Buffer 1 tablet of Protease inhibitors 1 tablet of Phosphatase inhibitors
SDS Loading Buffer	Sodium dodecyl sulfate (SDS), Glycerol, Bromophenol blue sodium salt, β-Mercaptoethanol, Sodium chloride, Tris-hydrochloride, EDTA. - *SDS Loading Buffer was prepared by our collaborators in the Krauss Cell Signalling Unit, at a concentration of 4X.*
RIPA Lysis Buffer 10X (20-188 Merck Millipore)	Purchased ready-made from manufacturer.

Table 6. List of hPSC cell lines

Cell Line	Type	Source	Reprogramming Method	Reference
H1	hESC	WiCell	N/A	Thomson et al[29]
207	hESC	Hovatta Lab, Karolinska Institute	N/A	Ström et al[188]
360	hESC	Hovatta Lab, Karolinska Institute	N/A	Ström et al[188]
Detroit 551 RA	hiPSC	ATCC, reprogrammed in Sullivan Lab	Yamanaka Factors, Retroviral	Siller et al[126]
Detroit 551 RB	hiPSC	ATCC, reprogrammed in Sullivan Lab	Yamanaka Factors, Retroviral	Siller et al[126]
Detroit 551 RC	hiPSC	ATCC, reprogrammed in Sullivan Lab	Yamanaka Factors, Retroviral	Siller et al[126]
AG05836B (AG-27)	hiPSC	ATCC, reprogrammed in Sullivan Lab	Yamanaka Factors, Retroviral	Mathapati et al[183]

3 Results

In order to verify our hPSC model of mesendodermal and DE differentiation, we analysed a number of relevant markers by qRT-PCR, we also assessed the morphology of our cells to ensure that the CHIR99021-treated time course transitioned through the appropriate developmental trajectories. This developmental sequence is signified by an initial mesendodermal differentiation to PS, which is followed through to DE.

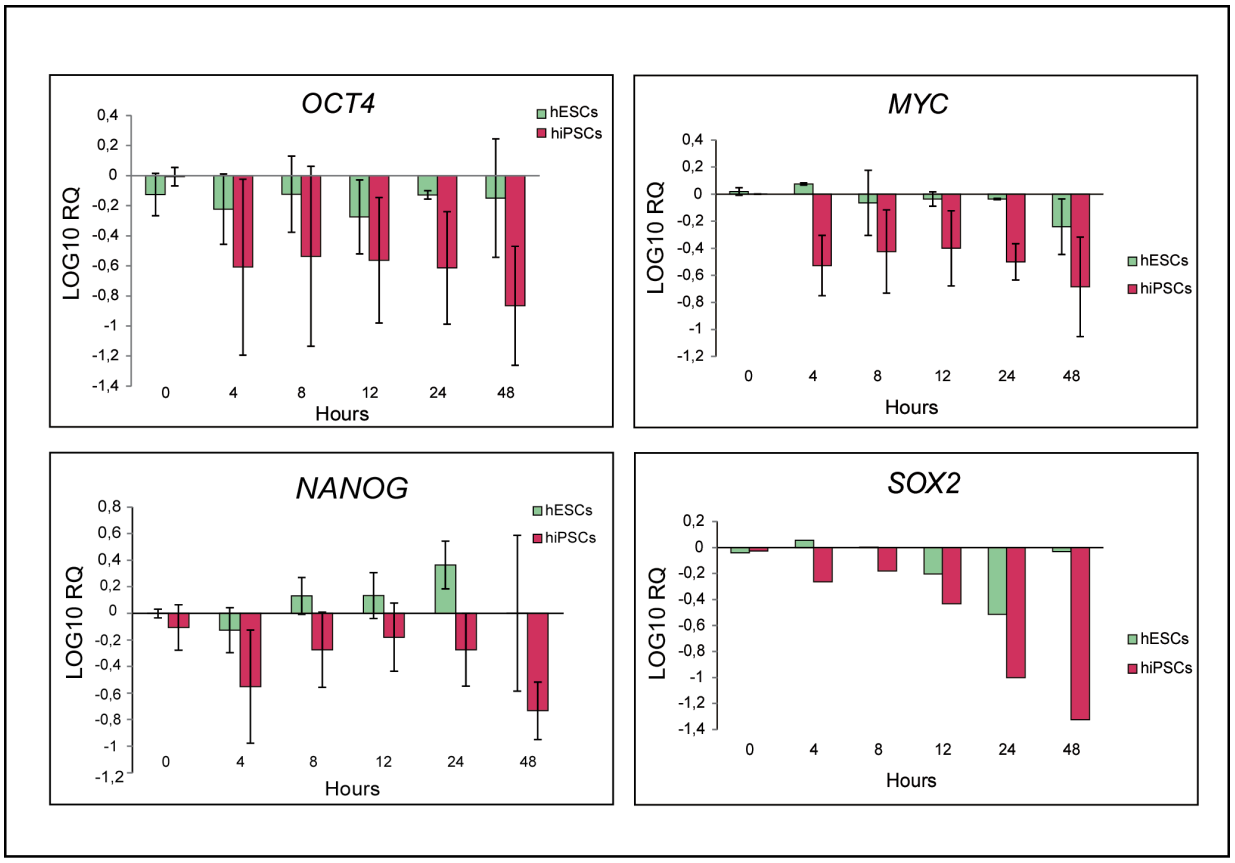

Figure 11. Quantitative RT-PCR analysis of pluripotency factors in differentiating hPSCs: The graphs display gene expression results for marker genes of the pluripotency, factors OCT4, c-MYC, NANOG and SOX2. The graphs represent the averaged results from 3 separate 48-hour time courses (except for MYC in hESCs, which is based on 2 TC's, and SOX2 which is based on 1 TC for both cell lines). Error bars represent the standard deviation between the 3 time courses (SOX2 is only based on one time course for each cell line and therefore does not contain error bars). The hESC cell line (H1) is represented by a green bar, and the hiPSC cell line (AG-27) is represented by a red bar. The X-axis represents the time in hours after the start of the differentiation protocol. The Y-axis shows the log10 of the RQ values derived from qRT-PCR analysis. In all of the graphs, gene expression levels are normalized to β-actin expression in undifferentiated hPSCs (0 hours).

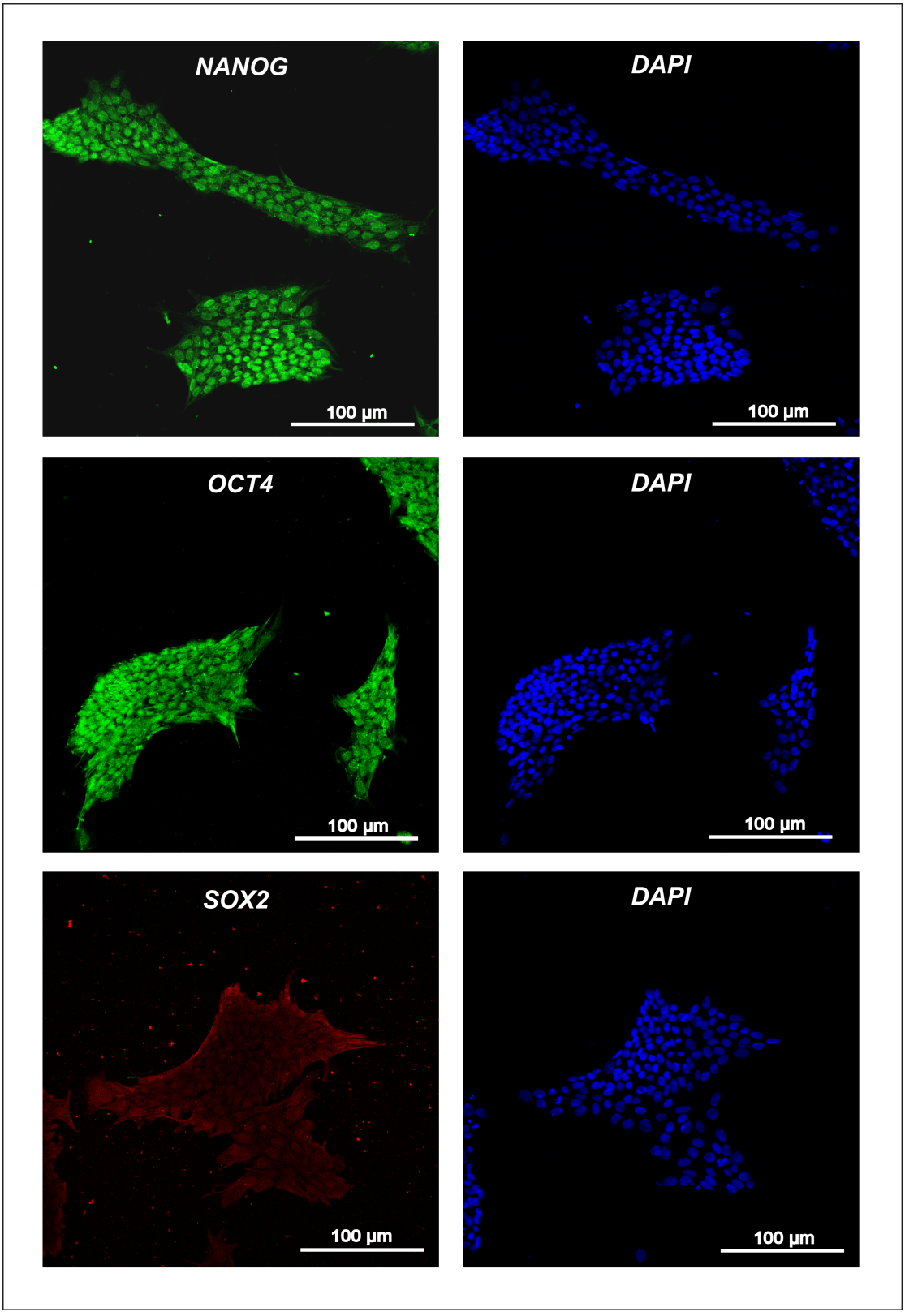

Figure 12. Immunostaining of pluripotency factors at time 0: At 0 hours, before CHIR99021 is added to the media, we see high expression of NANOG, OCT4 and SOX2. DAPI was used as a nuclear counterstain. Magnification 20X.

3.1 Verifying the *in-vitro* hPSC Model of DE Differentiation

To confirm that the hPSCs were differentiating and losing their pluripotent potential over time, we assessed the gene expression of pluripotency factors by qRT-PCR (Figure 11). As expected gene expression levels of pluripotency factors decreased over time, with the exception of *NANOG* expression in H1 cells. However, the error bars for *NANOG* show considerable variance between the time courses. Thus the significance of *NANOG* expression in H1 cells should not be overstated; the data should rather be supplemented by repeating the time course to generate more reliable results for *NANOG* in the H1 cell line. The overall picture confirmed that our hPSCs showed uniform expression of pluripotency factor proteins at 0 hours, and that gene expression of the pluripotency factors decreased with time during the differentiation. To verify that we had high quality, pluripotent populations of hPSCs at the outset of our differentiation, we performed immunostaining for the intrinsic core network of pluripotency factors (NANOG, OCT4 and SOX2) at 0 hours (Figure 12). The immunofluorescence images display high expression levels of the pluripotency factors NANOG, OCT4 and significant expression of SOX2 at 0 hours, prior to the initiation of differentiation. Before initiating the differentiation procedure the cells were observed by phase-contrast microscopy, ensuring desired cell morphology and confluency (Figure 13).

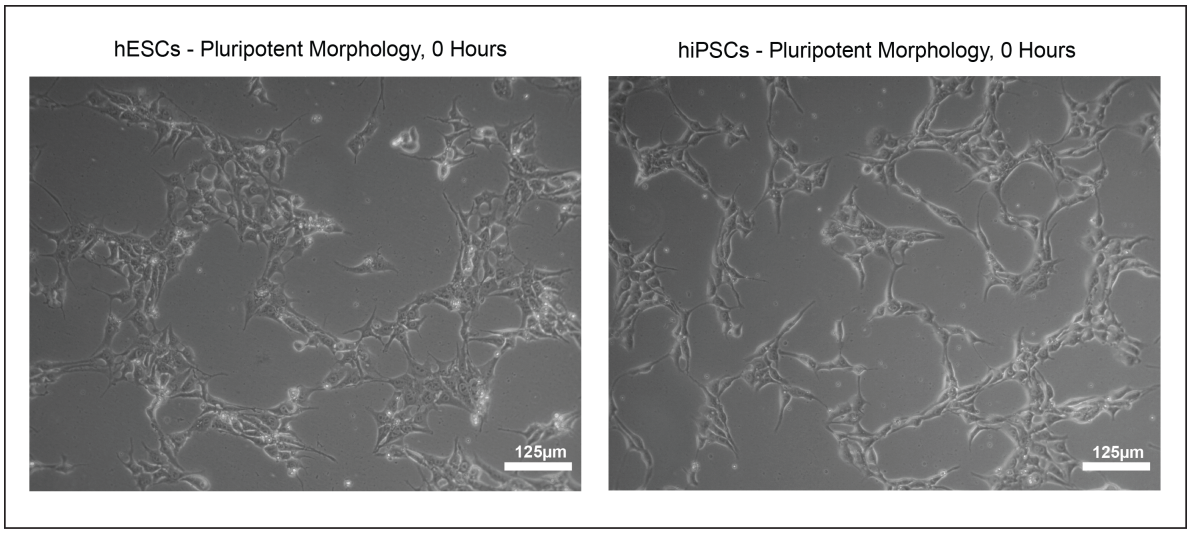

Figure 13. Pluripotent cell morphology: Typical cell morphology of hPSCs at 0 hour time point. Cells seen at desired confluency (approx. 30%) for initiation of DE differentiation. Magnification 10X.

Next we looked at gene expression markers for PS (Figure 14). These include *NODAL*, *GSC, MIXL1, T*, and *FOXA2*. All PS gene expression markers apart from *FOXA2* showed a peak around 24 hours, which is the expected time point for PS-like cell formation using our current protocol. *FOXA2* continued to rise until 48 hours due to its dual role in PS and DE specification. In addition we checked cell morphology, the hPSCs formed dense bright clusters at 24 hours, a morphological hallmark of cells expressing PS gene expression markers (Figure 15).

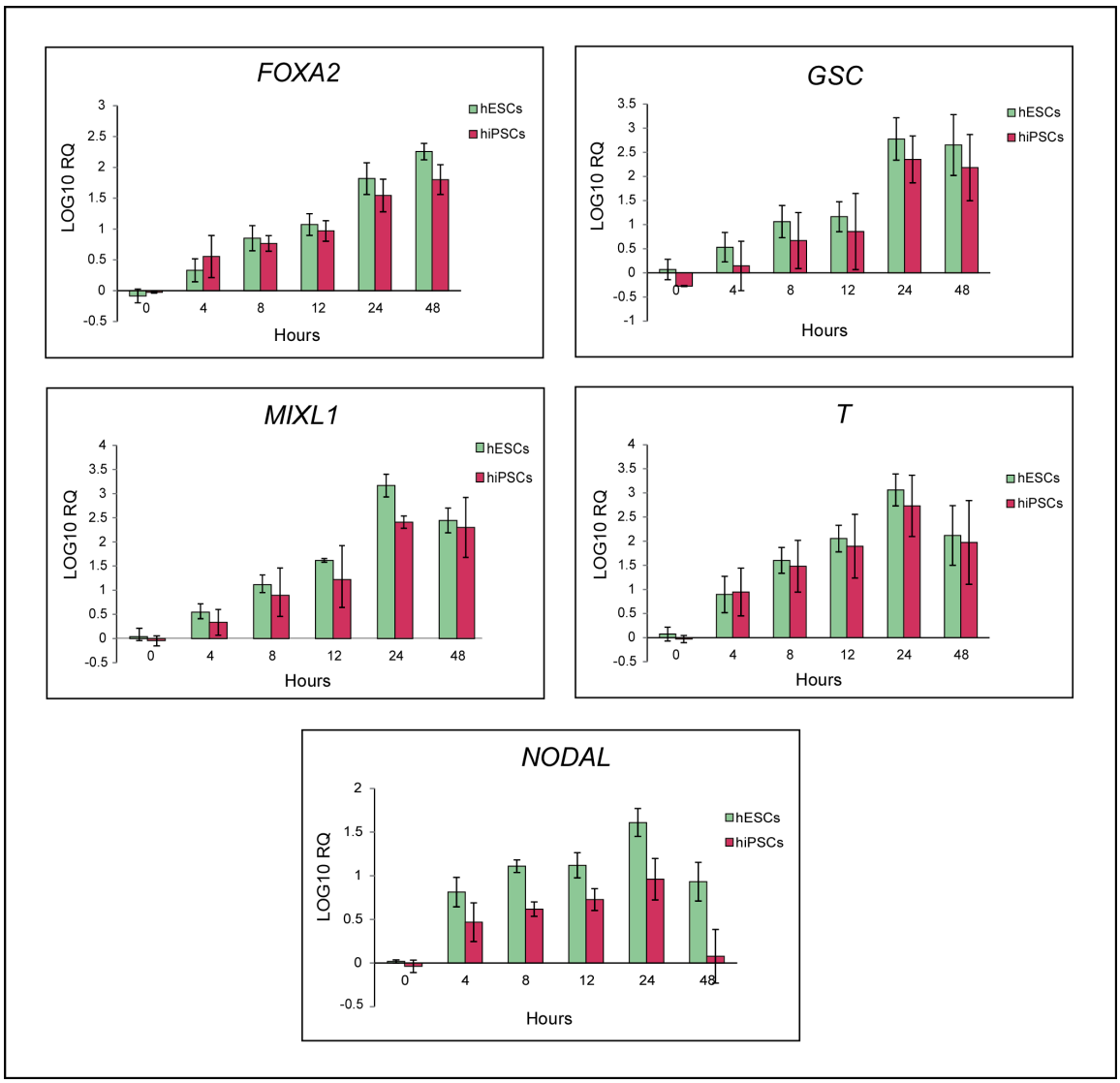

Figure 14. Quantitative RT-PCR analysis of PS markers: The data shows gene expression of the primitive streak marker genes *FOXA2, GSC, MIXL1, T*, and *NODAL* over the time course. The graphs represent the average of 3 separate time courses. Error bars represent the standard deviation between the 3 time courses. The hESC cell line (H1) is represented by a green bar, and the hiPSC cell line (AG-27) is represented by a red bar. The X-axis represents the time in hours after the start of the differentiation protocol. The Y-axis shows the log10 of the RQ values derived from qRT-PCR analysis. In all of the graphs, gene expression levels are normalized to β-actin expression in undifferentiated hPSCs (0 hours).

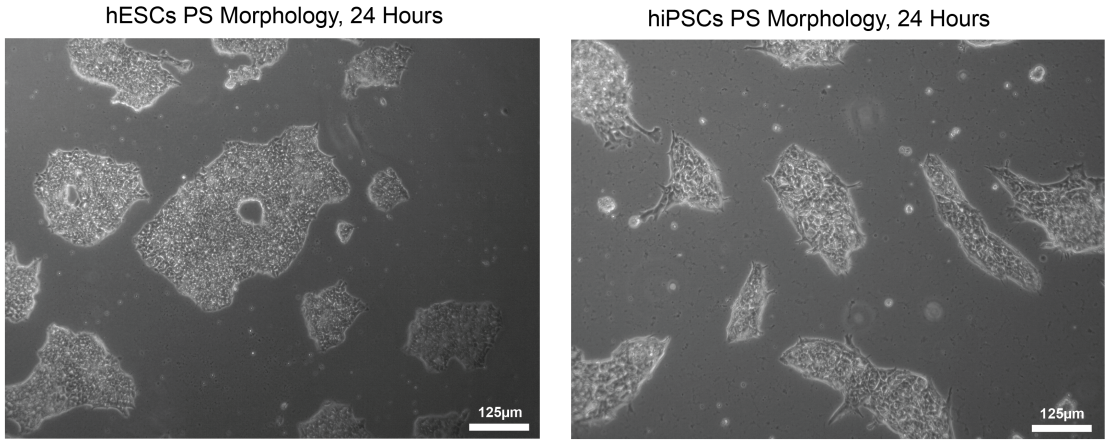

Figure 15. Cell morphology during PS-like state: At 24 hours the cells formed dense bright clusters characteristic of the PS-like state. 10X Magnification.

3.1.1 Early Time-Points of Differentiation

The role of PS-markers and pluripotency factors was assessed during the early time points of differentiation from 0 and 4.5 hours, taking samples every 30 minutes. These experiments (data not shown) showed an insignificant change in the levels of many primitive streak markers, and an expected initial expression of pluripotency factors followed by a decrease at the later time points (around 4 hours). Interestingly the early time points did show significant and rapid up-regulation of *NODAL* and *FOXA2*, two important regulators of ME differentiation (Figure 16) (explored in greater detail in section 4.1).

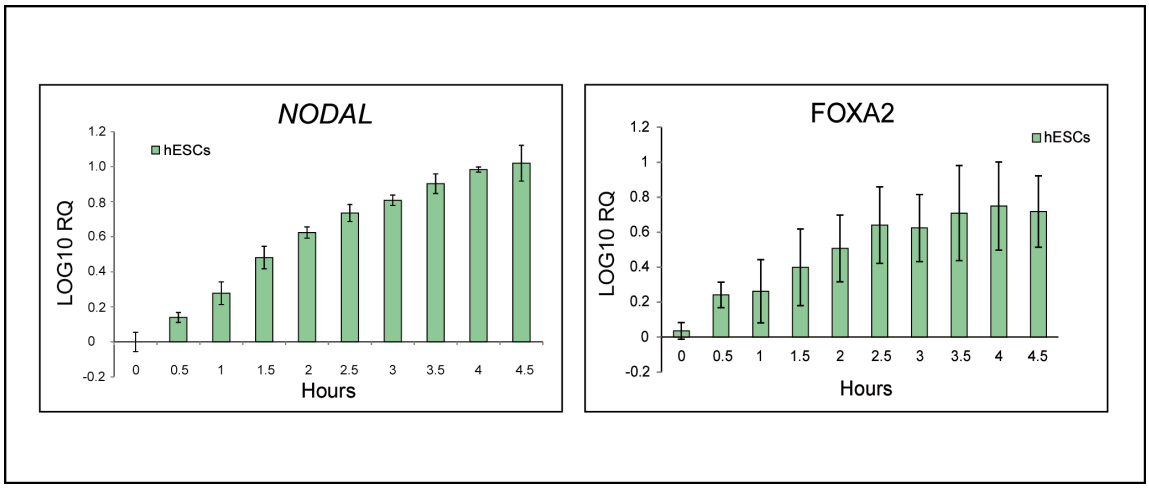

Figure 16. Early up-regulation of *NODAL* and *FOXA2*: The graphs display gene expression results for the PS marker genes *NODAL* and *FOXA2* during the initial 0 - 4.5 hours of differentiation. This was done for the hESC cell line only. Time points were collected in triplicate every 30 minutes for the first 4 hours and 30 minutes of CHIR99021 treatment. All graphs represent the averaged result from 3 separate time courses. Error bars represent the standard deviation between the 3 time courses. The X-axis shows the time points, with samples taken every 30 min. The Y-axis shows the log10 of the RQ values derived from qRT-PCR analysis. In all of the graphs, gene expression levels are normalized to β-actin expression in undifferentiated hPSCs (0 hours).

3.1.2 End-Point Definitive Endoderm

Lastly in our verification process, we characterised by qRT-PCR, cell morphology and immunostaining at 48 hours to confirm efficient derivation of DE cell populations. The qRT-PCR analysis (Figure 17) revealed up-regulation of the DE markers *FOXA2*, *SOX17*, *HHEX* and *CER1* at the later time points in the time course, reaching peak expression at 48 hours (our empirically determined stage of DE formation).

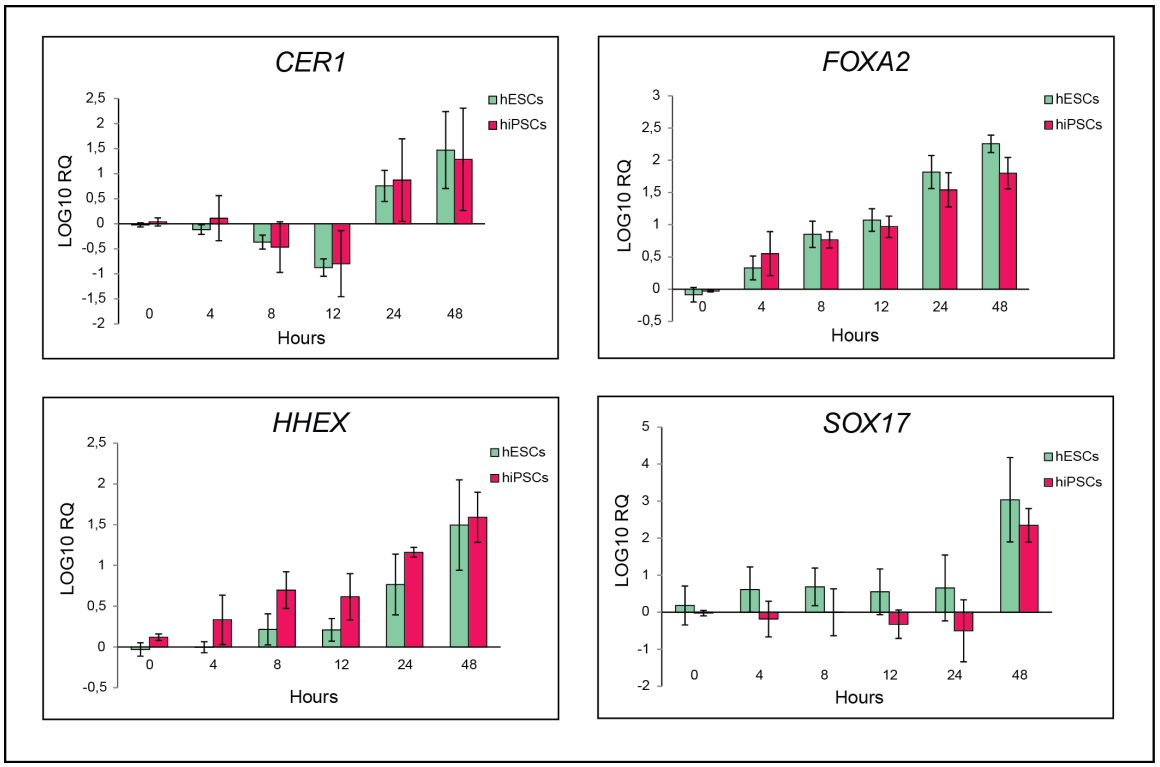

Figure 17. Quantitative RT-PCR analysis of DE marker genes: The graphs display qRT-PCR results for gene expression of the DE marker genes, *CER1, FOXA2, HHEX,* and *SOX17*. The graphs represent the average expression levels of 3 separate time courses. Error bars represent the standard deviation between the 3 time courses. The hESC cell line (H1) is represented by green bars, and the hiPSC cell line (AG-27) is represented by red bars. The X-axis represents the time in hours after the start of the differentiation protocol. The Y-axis shows the log10 of the RQ values derived from qRT-PCR analysis. In all of the graphs, gene expression levels are normalized to β-actin expression in undifferentiated hPSCs (0 hours).

To confirm that our cell population was efficiently differentiated to DE and did not consist of a mixed cell population, we assessed gene expression levels of the early ectoderm markers *PAX6* and *NESTIN* as well as the neuroectoderm marker *FOXG1* (Figure 18). On the whole, these markers show low expression levels, as would be expected. However, the second time-course repeat for H1, did show moderate levels of *FOXG1* expression, with significant fluctuations between the different time points reflected in the error bars, and lower expression levels at the later time points. This might indicate that this time-course initially contained *FOXG1* expressing cells that were selected against as the time course progressed.

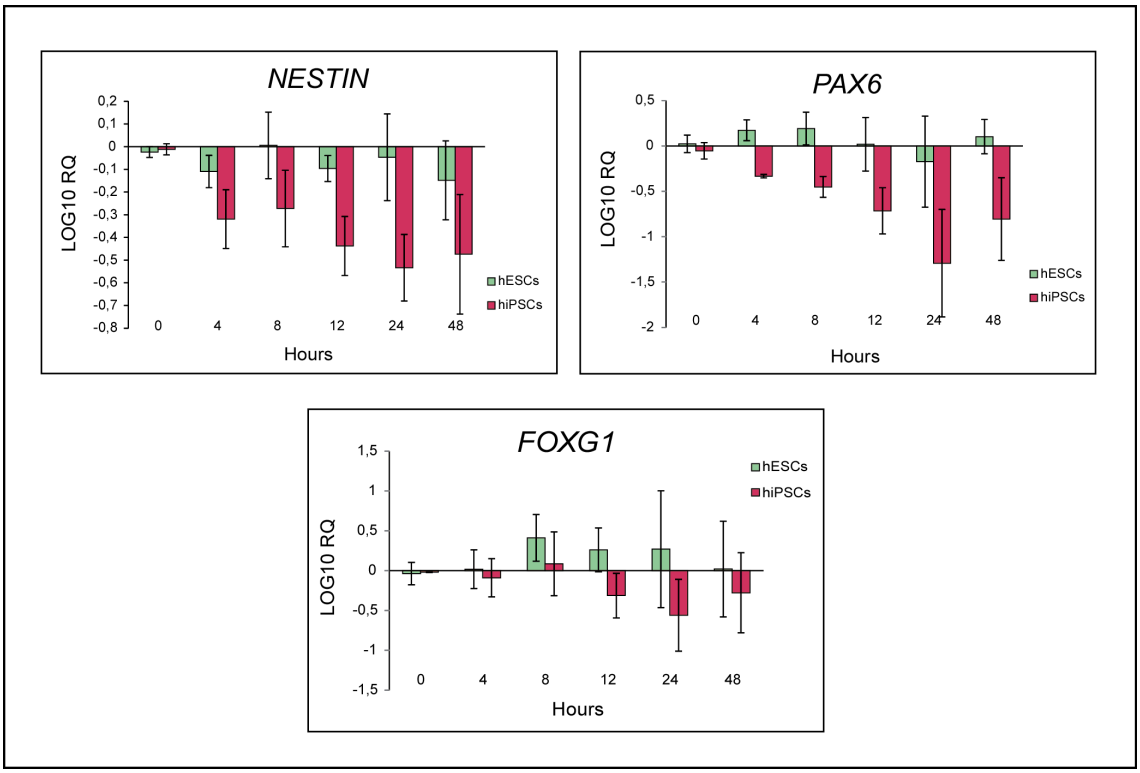

Figure 18. Quantitative RT-PCR analysis of ectoderm marker genes: The graphs display qRT-PCR results for gene expression of the ectodermal marker genes, *NESTIN, PAX6*, and *FOXG1*. The graphs represent the average expression levels of 3 separate time courses. Error bars represent the standard deviation between the 3 time courses. The hESC cell line (H1) is represented by a green bar, and the hiPSC cell line (AG-27) is represented by a red bar. The X-axis represents the time in hours after the start of the differentiation protocol. The Y-axis shows the log10 of the RQ values derived from qRT-PCR analysis. In all of the graphs, gene expression levels are normalized to β-actin expression in undifferentiated hPSCs (0 hours).

Next, we analysed cell morphology at 48-hours and observed the typical petal-shape of hPSC derived DE cells (Figure 19C). Finally, immunofluorescence staining showed high expression of both FOXA2 and SOX17 in the cell population at 48 hours (Figure 19) indicating a uniform DE population, as SOX17 is a DE-specific marker and not associated with mesoderm[84,189,190]. Thus we have successfully replicated previous experiments by the Sullivan group[126], and established our hPSC model of CHIR99021 driven DE differentiation, which follows the developmentally relevant trajectory through PS to DE.

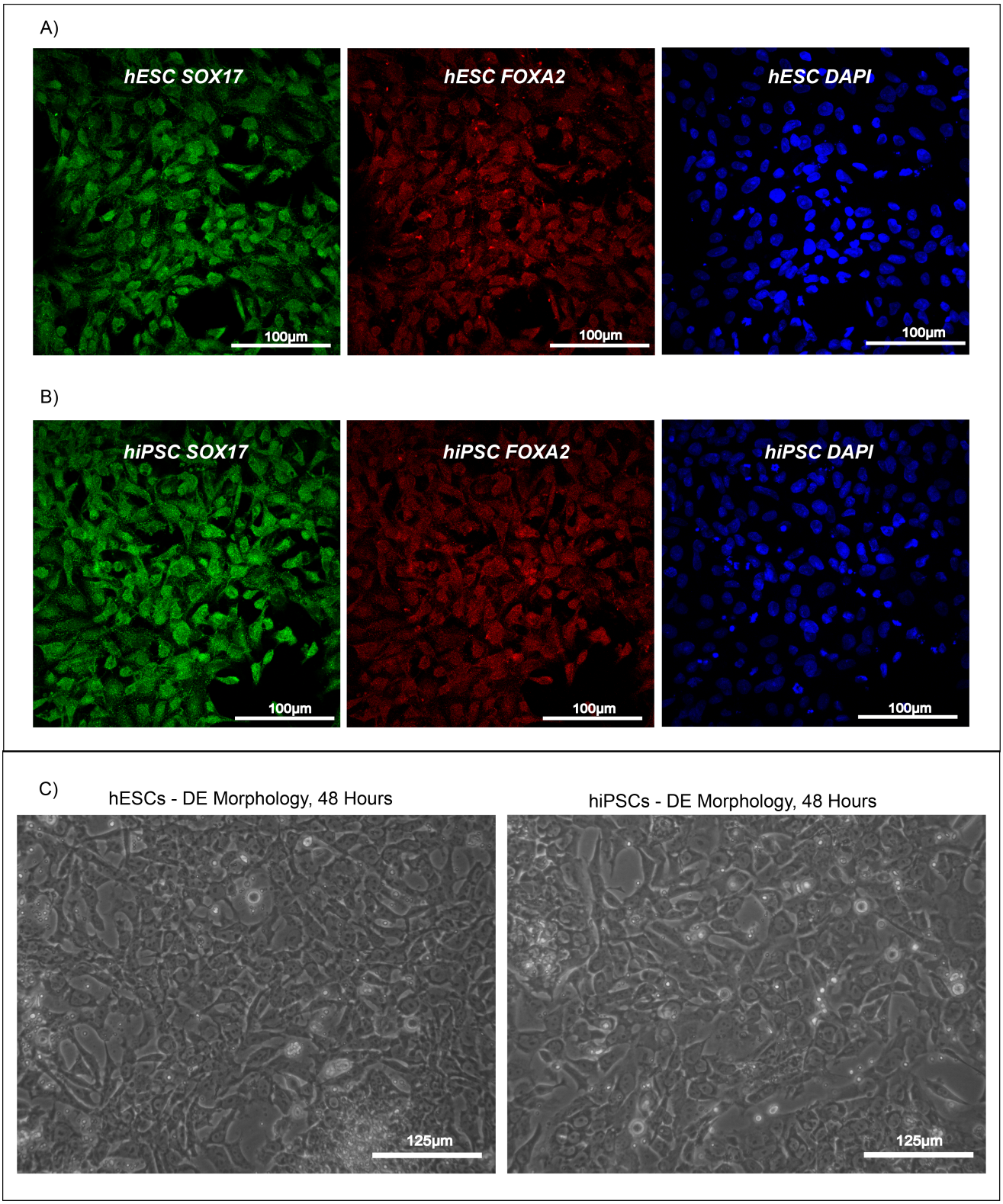

Figure 19. DE characterization: Characterization of hPSC derived DE cell population by immunoflourescence staining and phase contrast imagining of cell morphology: Expression of FOXA2, SOX17 and DAPI in **A)** hESCs (H1 cell line) and **B)** hiPSCs (AG-27 cell line) at the 48-hour time-point after treatment with CHIR99021. Imaged using fluorescent microscopy. Fluorescence images taken at 40X magnification. **C)** Petal-like cell morphology characteristic of *in-vitro* DE cells, at 48-hour time point. Phase contrast images taken at 20X magnification.

3.2 Western Blot Analysis of Key Signalling Proteins in DE Regulation

The transition from a state of pluripotency to the initiation of mesendodermal differentiation in hPSCs is modulated by complex interactions between extrinsic signalling pathways in the cellular environment. Many important regulators of DE such as Nodal and FGF2 have dual context-dependent functions, maintaining pluripotency under one set of conditions, and promoting differentiation under another. To arrive at a better understanding of these processes we analysed protein expression levels for key signalling pathways by western analysis. Cell lysates were prepared and separated by centrifugation into cytoplasmic and nuclear fractions (see section 2). These samples were collected at the same six time points as for qRT-PCR set-up; 0, 4, 8, 12, 24 and 48 hours. Unless stated otherwise the western blot figures display protein levels in the cytoplasmic fraction of the cell lysates. A smaller number of proteins were analysed in the nuclear fraction due to low sample yield. This system allows us to investigate the signals of DE differentiation in an *in-vitro* model of human development.

3.3 The Wnt/β-catenin Pathway

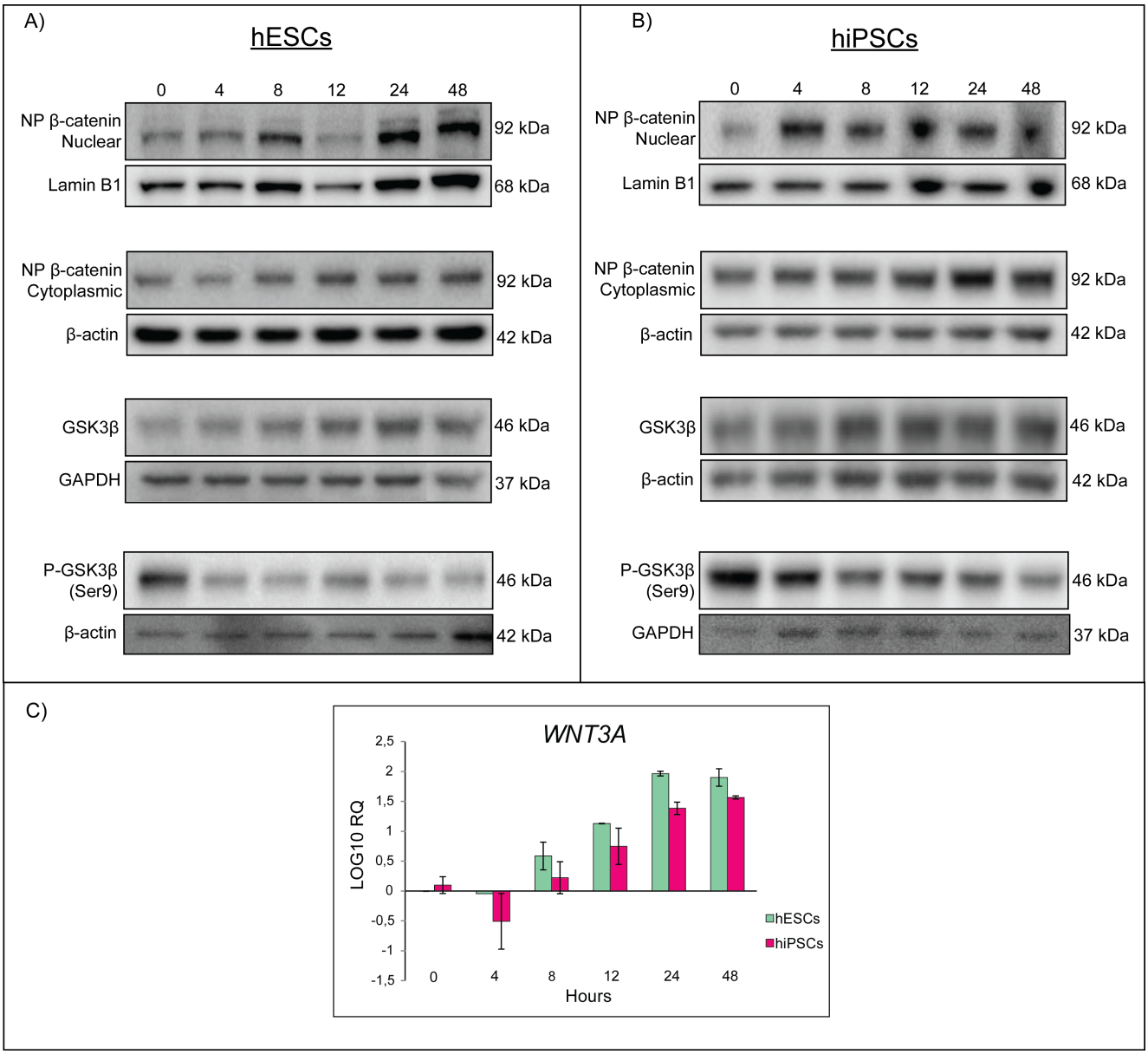

Figure 20. Western blot analysis of key proteins of the WNT/β-catenin pathway: Expression of non-phospho (active) β-catenin in nuclear and cytoplasmic protein extracts, as well as total GSK3β and (inhibited) phospho-GSK3β (Ser9) in the cytoplasmic fraction of the hPSC cell lysates. **A)** Shows protein expressions for the hESCs (H1 cell line). GAPDH and β-actin were used as loading controls for the cytoplasmic fraction, while Lamin B1 was used as a loading control in the nuclear fraction. **B)** Shows protein expression for the hiPSCs (AG cell line) for which β-actin was used as a loading control in the cytoplasmic fractions and Lamin B1 for the nuclear fraction. Cell samples were collected for protein extraction at 0, 4, 8, 12, 24, and 48 hours respectively. **C)** Shows gene expression levels of *WNT3A* given as the average of 3 separate time courses (hESC values are based on 2 repeats). Error bars represent the standard deviation between the 3 time courses. The hESC cell line (H1) is represented by a green bar, and the hiPSC cell line (AG-27) is represented by a red bar. The X-axis represents the time in hours after the start of the differentiation protocol. The Y-axis shows the log10 of the RQ values derived from qRT-PCR analysis. In all of the graphs, gene expression levels are normalized to β-actin expression in undifferentiated hPSCs (0 hours).

We first examined protein expression levels of Wnt/β-catenin related proteins (Figure 20). This revealed expected patterns of protein expression for non-phospho (active) β-catenin (NP-β-catenin). NP-β-catenin accumulates and is stabilized over time in both the nuclear and cytoplasmic fractions. This complies with our model of Wnt/β-catenin activation through GSK3-inhibition[135,134]. We also see an increase in *WNT3A* gene expression over time in the CHIR99021 based protocol (Figure 20C). CHIR99021-mediated inactivation of GSK3 therefore imitates the effects of Wnt-induced sequestration and inhibition of GSK3, causing a significant increase in *WNT3A* over time. Analysis of the total amount of GSK3β in our cell lysates showed a moderate increase in GSK3β over time (Figure 20). We also looked at the levels of p-GSK3β (Ser9), (the inhibited form of GSK3) and observed decreasing levels over time, in a manner that mirrors the decrease in active forms of Akt (see section 4.2).

To assess whether our observed expression patterns were cell line specific or not, we examined NP-β-Catenin, GSK3β, and p-GSK3β (Ser9) expression in 5 more hPSC lines (Figure 21). We assessed three additional hiPSC lines (Detroit 551 RA, RB, and RC), and two additional hESC cell lines, 207 and 360. (GSK3β was only analyzed in the hiPSC cell lines). The samples were collected in the same manner as described in the methods and materials section, however these control cell lines were collected at only 4 time points: 0, 4, 8 and 48 hours, and lysed with RIPA buffer, the samples therefore represent the aggregate of nuclear and cytoplasmic proteins in the cell cultures. These additional cell lines exhibit the same trends in protein expression as our model cell lines (H1 and AG-27) corroborating the trends that we have observed, demonstrating that they are not cell line specific.

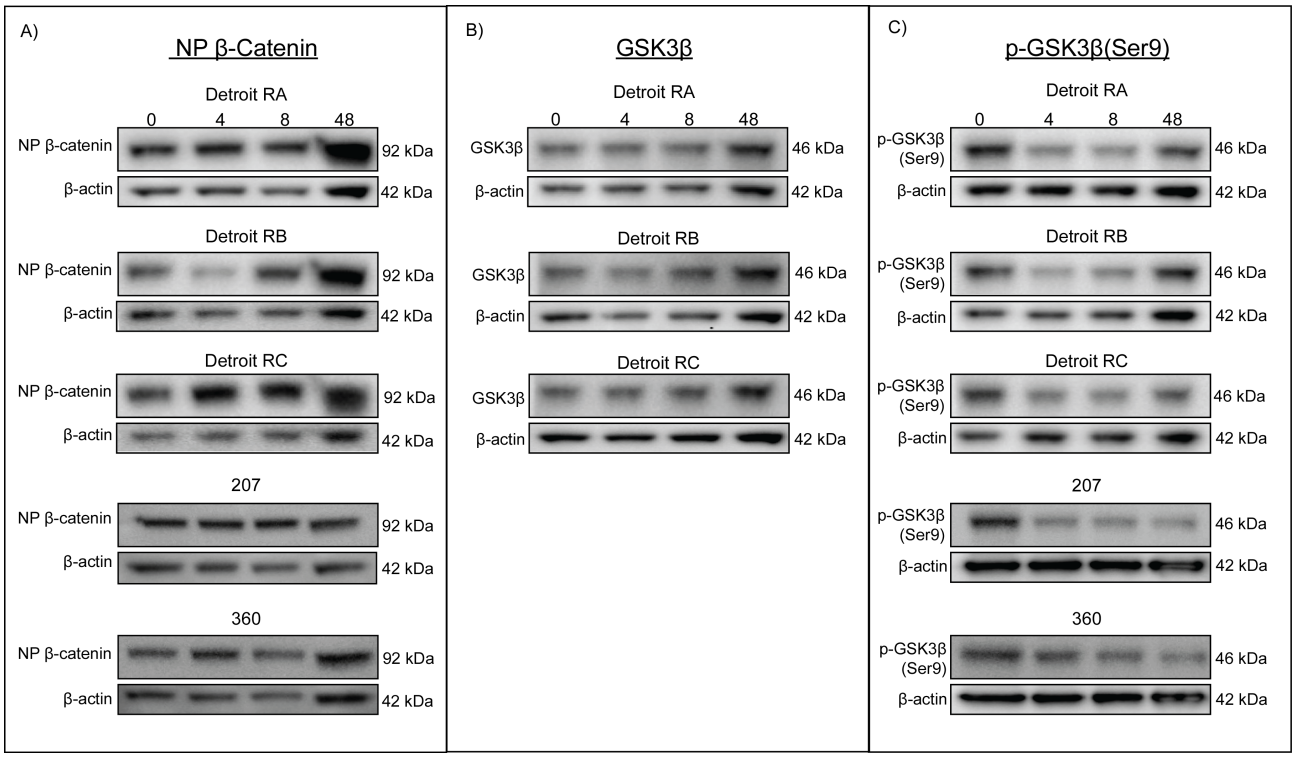

Figure 21. Western blot analysis of key Wnt/β-catenin proteins in additional cell lines: To test if the trends we observed in H1 and AG-27 cells are conserved in other cell lines, the expression of non-phospho (active) β-catenin, GSK3β, and (inhibited) phospho-GSK3β (Ser9) were assessed in 5 additional cell lines. Detroit RA, RB and RC are hiPSC lines, while 207 and 360 are hESC lines. All hPSC lysates were prepared with RIPA. **A)** Shows protein expression patterns for NP β-catenin. **B)** Shows protein expression patterns for GSK3β (only the hiPSC lines were tested due to time constraints). **C)** Shows p-GSK3β (Ser9) protein expression levels. β-actin was used as a loading control. Cell samples were collected for protein extraction at 0, 4, 8, 48 hours respectively.

3.4 Axin and Tankyrase Signalling

We also analysed expression of the Wnt pathway protein Axin, looking at each of its homologs (Axin1 and Axin2) as well as its negative regulator TNKS1/2 (Figure 22). Axin is an important negative regulator of Wnt signalling, interacting with APC, Dvl, β-catenin, GSK3 and LRP5/6. Due to the importance of aberrant Wnt signalling in cancer etiology, experimental research into the effects of TNKS on Axin, and the effects of TNKS inhibition on canonical Wnt signalling are largely based on cancer cell lines[142,136]. Thus, there was a clear interest for looking into the effects of TNKS and Axin in our hPSCs model of differentiation.

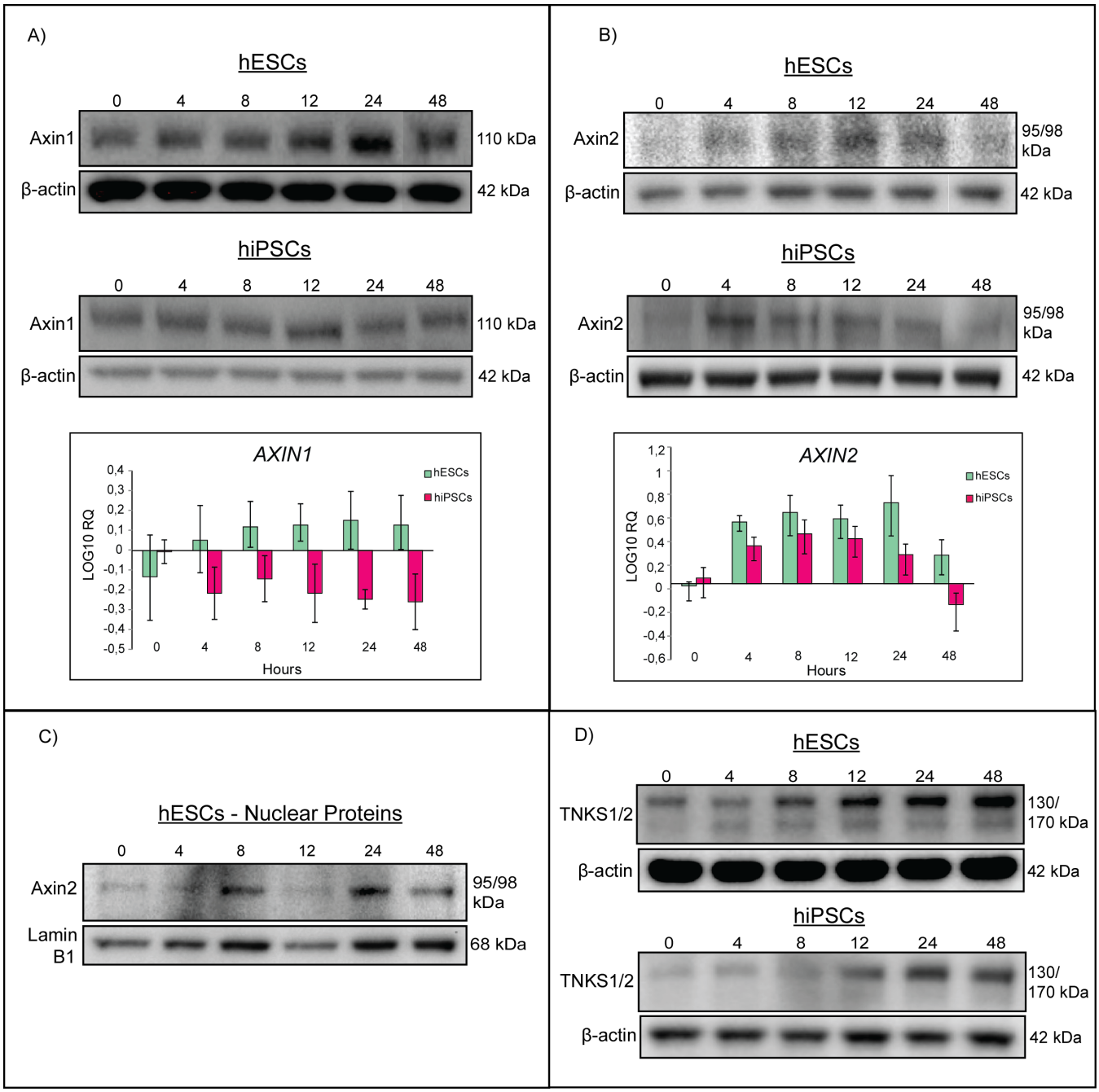

Figure 22. Western blot analysis of Axin1, Axin2 and TNKS1/2, with qRT-PCR analysis of Axins: Protein and gene expression of Axin1 and 2. **A)** Protein and gene expression of Axin1 in the cytoplasm of the H1 and AG-27 cell lines. **B)** Protein and gene expression of Axin2 in the cytoplasm of the H1 and AG-27 cell lines. **C)** Protein expression for Axin2 in the nuclear fraction of hESC (H1) cell line. **D)** TNKS1/2 protein expression in H1 and AG-27s. β-actin was used as a loading control for cytoplasmic samples. Lamin B1 was used as the loading control for nuclear samples.

As expected Axin1 exhibited stable constitutive expression (Figure 22A and B), as it is maintains low Wnt/β-catenin activity in the basal (Wnt off) state[142]. Axin2 also shows an expected up-regulation in response to increased β-catenin concentrations (Figure 22B) as it is believed to act as a negative feedback agent for Wnt signalling[142,149]. However to our surprise we saw a very strictly timed and conserved pattern of Axin2 expression in every time course. Axin2 was essentially undetectable at 0 hours, followed by a rapid up-regulation by 4 hours and maintained expression until 24 hours, after which a decrease was observed. Thus we see a bounce or "pulse" of Axin2 signalling in every time course we examined. This was also verified in 5 additional hPSC lines, which show stable expression of Axin1 throughout the time course, and a pulse of Axin2, which is undetectable at 0 and 48 hours but up-regulated at 4 and 8 hours (Figure 23). Interestingly the qRT-PCR data for *AXIN1* and *AXIN2* gene expression patterns follow the protein expression patterns, with *AXIN1* staying fairly stable around the baseline, and *AXIN2* being upregulated at 4 hours before going down at 24 hours (Figures 22A & B).

Another notable finding in these results is the progressive up-regulation of TNKS1/2 protein expression over the duration of the time course (Figure 22D). The increase in TNKS1/2 coincides with the decrease in Axin2 after 24 hours, but does not correlate with Axin1 expression, which remains stable for the entire time course.

Since Axin is known to contain nuclear import/export sequences and undergoes nuclear shuttling, we looked at levels of Axin2 in the nuclear fraction of our cell lysates Figure 22C). Our results show an accumulation of Axin2 in the nucleus that resembles the accumulation of Axin2 in the cytoplasm. There is a slight dip in expression levels at 12 hours, but this is due to low sample concentration as we can see from the Lamin B1 loading control.

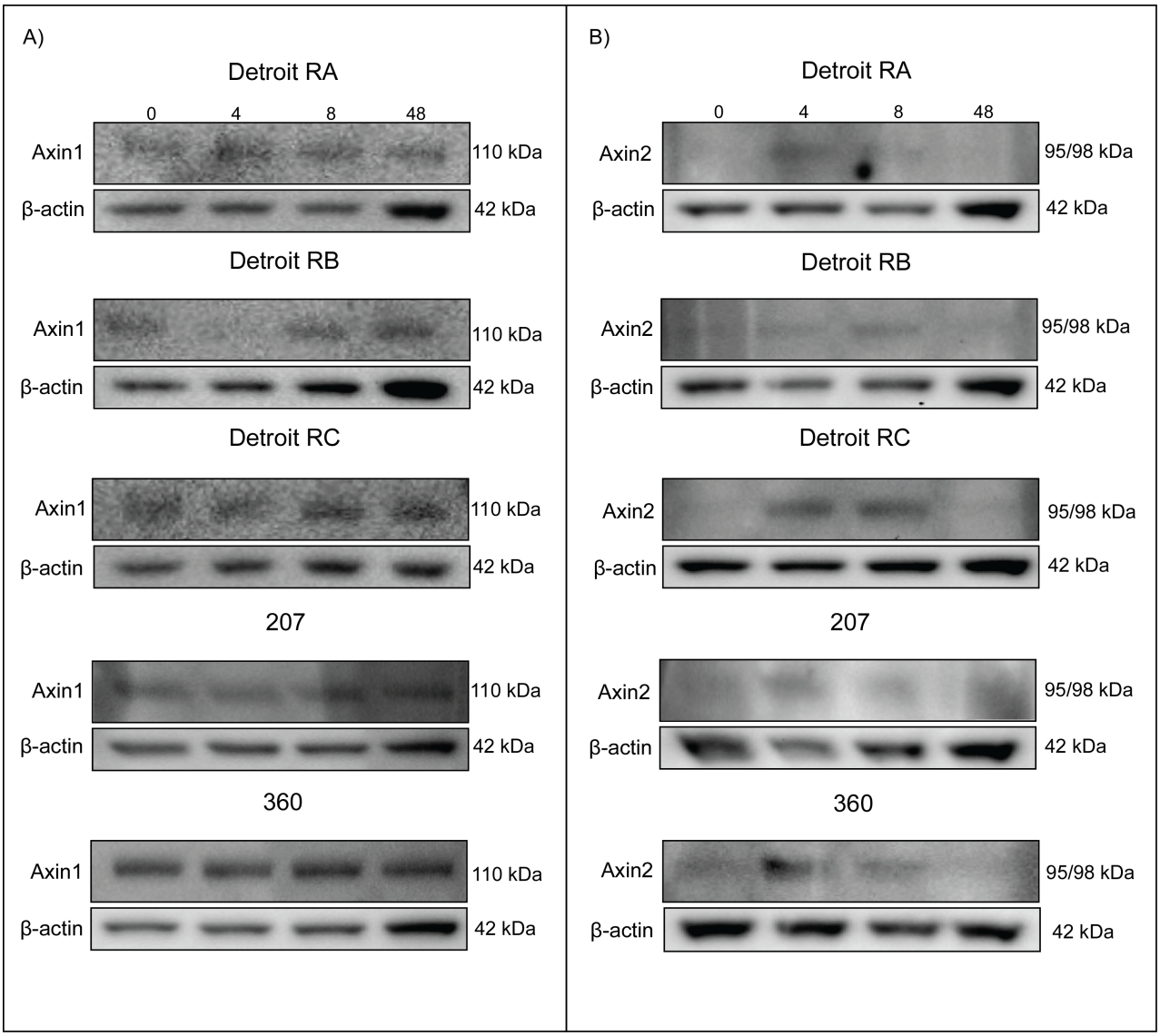

Figure 23. Western blot analysis of Axin1 and Axin2 in additional hPSC lines: To test if the trends we see in our H1 and AG-27 cells are conserved in other cell lines, we assessed the expression of Axin1, and Axin2, in 5 additional hPSC lines. Detroit RA, RB and RC are hiPSC lines, while 207 and 360 are hESC lines **A)** Protein expression patterns for Axin1 which remains stable throughout the time course**. B)** Protein expression patterns for Axin2, which are upregulated at 4 and 8 hours, and low at 0 and 48 hours. β-actin was used as a loading control. Cell samples were collected for protein extraction at 0, 4, 8, 48 hours.

3.5 Akt, PTEN, AMPK, ERK, and E-cadherin Signalling

Next we investigated modulators of metabolism known to be involved in differentiating stem cells (Figure 24). Akt, ERK, and AMPK have established roles in modulating pluripotency and differentiation (see sections 1.4 & 1.5) while regulating the metabolic changes observed in differentiating stem cells. We observed a striking trend in Akt activity in all time courses, namely a rapid, progressive down-regulation of active (phosphorylated) Akt. This was observed for both threonine 308 and serine 473 phosphorylations of Akt in H1 and AG-27 cell lines. Additionally we observed the same conserved pattern of rapid decrease in p-Akt (Ser473) in the previously described 5 additional hPSC lines (Figure 25). When examining the total expression of Akt protein we observed low expression levels throughout the time course as expected, however a conserved increase in Akt occurs at 48 hours (Figures 24 & 25). We also examined the protein expression of PTEN, the main negative regulator of PI3K/Akt activity[191]. PTEN demonstrated high and stabile expression throughout the time-course even at 0 hours (Figure 24). There might however be a qualitative difference between the phospho-status of the protein before and after CHIR99021 is added to the cells and GSK3 is inhibited (see section 4.2 & 4.3). ERK is another metabolic protein, with an important role in promoting differentiation[63,65,66,]. Interestingly, we observed a rise in p-ERK1/2 protein levels during differentiation, in accordance with other recent studies[65] (Figure 24B, and Fig. S10). In the AG-27 line p-ERK1/2 (the active form of ERK) increases in a phasic manner after the 0 hour time point, with higher expression of p-ERK1/2 at 4 and 12 hour time points relative to other time points, and low expression at the 0H and 48H time points. However, cell-line differences in ERK expression were observed. This is possibly due to the presence of insulin (an activator of ERK) in H1 cell line medium[192,193]. Thus we observed clear phasic patterns of increase in p-ERK1/2 levels between the 0 and 48 hour time points in the AG-27 line, and less conserved patterns of expression for the H1 line (Figure S10).

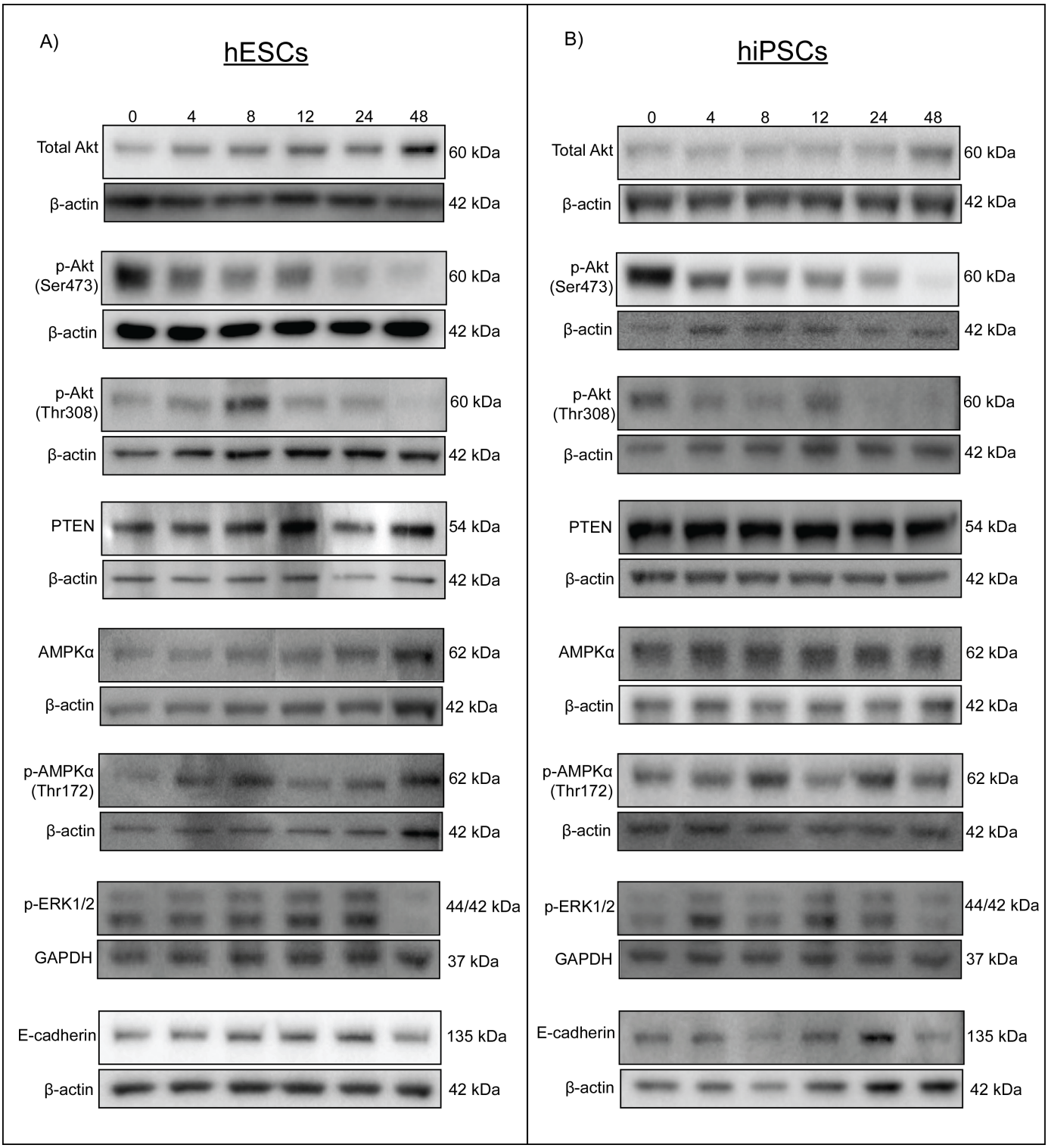

Figure 24. Western blot analysis of key metabolic proteins and E-cadherin: This figure shows protein expression of total Akt, p-Akt (Ser473), p-Akt (Thr308), PTEN, AMPKα, P-AMPKα (Thr172), p-ERK1/2 and E-cadherin. **A)** Protein expression in the hESCs (H1 cell line). **B)** Protein expression in the hiPSC cell line (AG-27). β-actin was used as a loading control in all samples, apart from p-ERK1/2 for which we used GAPDH as a loading control.

To examine the process of EMT in differentiating hPSCs and investigate a recent model of a regulatory network involving β-catenin, E-cadherin, PI3K/Akt and Slug[194] (see section 4.2), we looked at protein expression levels of E-cadherin. Expression levels of E-cadherin (an epithelial adhesion protein) were stable throughout the time course, in all time courses (Figure S10). We also performed gene expression studies by qRT-PCR analysis for *CDH1* (E-cadherin) and *CDH2* (N-cadherin) (Figure S1). Our results show dynamic fluctuations in E-cadherin vs. N-cadherin at the gene expression level, with relative up-regulation of N-cadherin (a mesenchymal adhesion protein) compared to E-cadherin over time, as expected.

Finally to investigate the activation of catabolic processes during differentiation, we looked at AMPKα and its active form p-AMPKα (Thr172) (Figure 24). The expression of total AMPKα resembled the protein loading controls; the active form of p-AMPKα (Thr172) however, demonstrates a phasic expression pattern, increasing at the 8 hour time point and again at later time points (often at 24 hours for AG-27's, and 36 hours for H1's) with some variation in the H1 cell line (Figures S9 and S10).

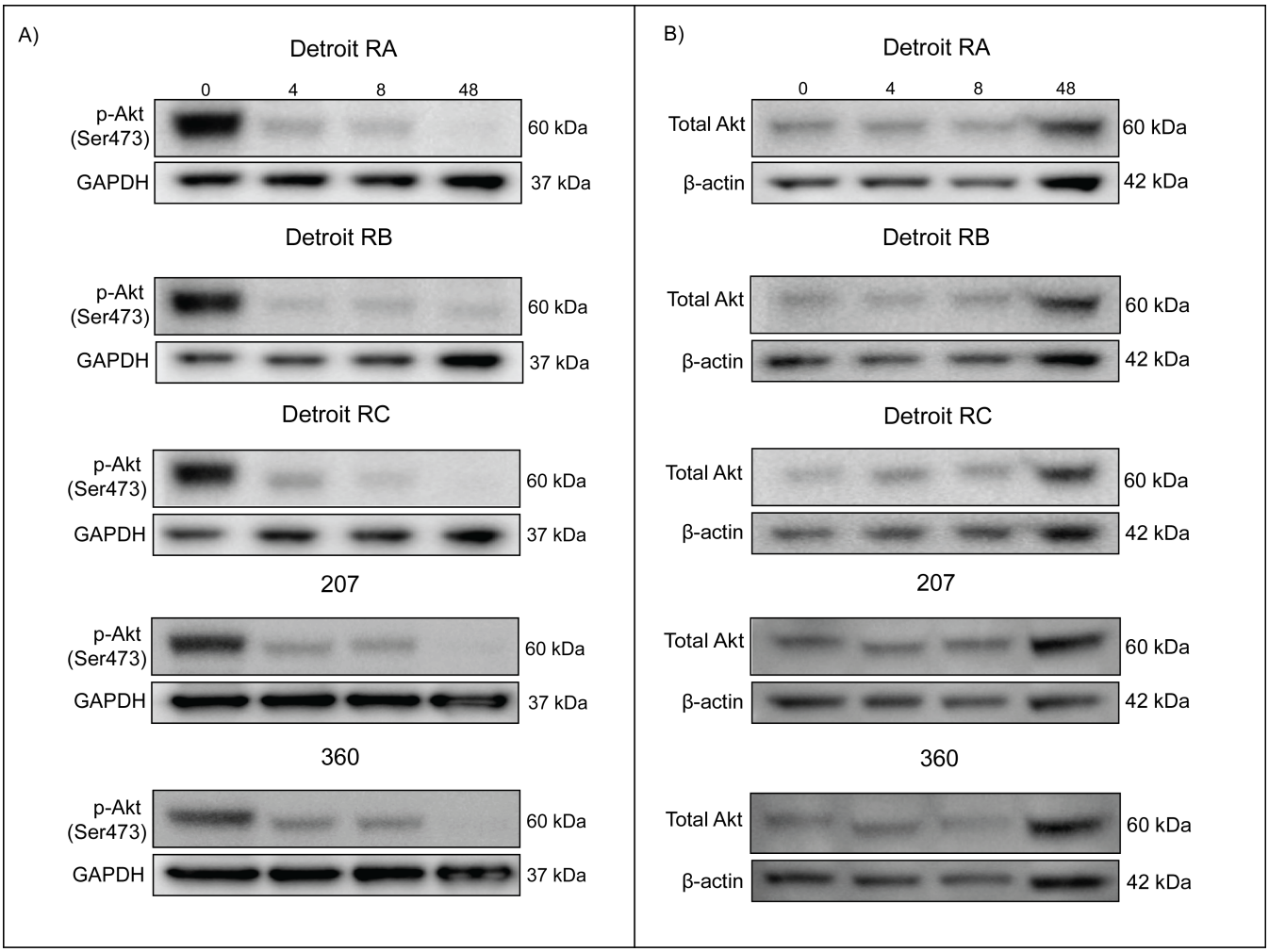

Figure 25. Western Blot analysis of p-Akt (Ser473) and Akt in additional hPSC lines: To test if the trends observed in our H1 and AG-27 cells were conserved, we analysed the expression of p-Akt (Ser473), and total Akt in 5 additional hPSC lines: the Detroit RA, RB and RC lines are hiPSCs, while 207 and 360 are hESCs. **A)** Protein expression patterns for p-Akt (Ser473), which is clearly going down over time. **B)** Protein expression patterns for all 3 non-phosphorylated isoforms of Akt. Total Akt expression remains low throughout most of the time course, but increases at 48 hours. β-actin was used as loading control for p-Akt (Ser473) and GAPDH was used as a loading control for total Akt. Cell samples were collected for protein extraction at 0, 4, 8, 48 hours.

3.6 Metabolic Proteins of the mTOR Pathway

Lastly, we examined the metabolic signalling proteins of the mTOR pathway. mTOR has been increasingly recognized to be involved in the maintenance of pluripotency[180].

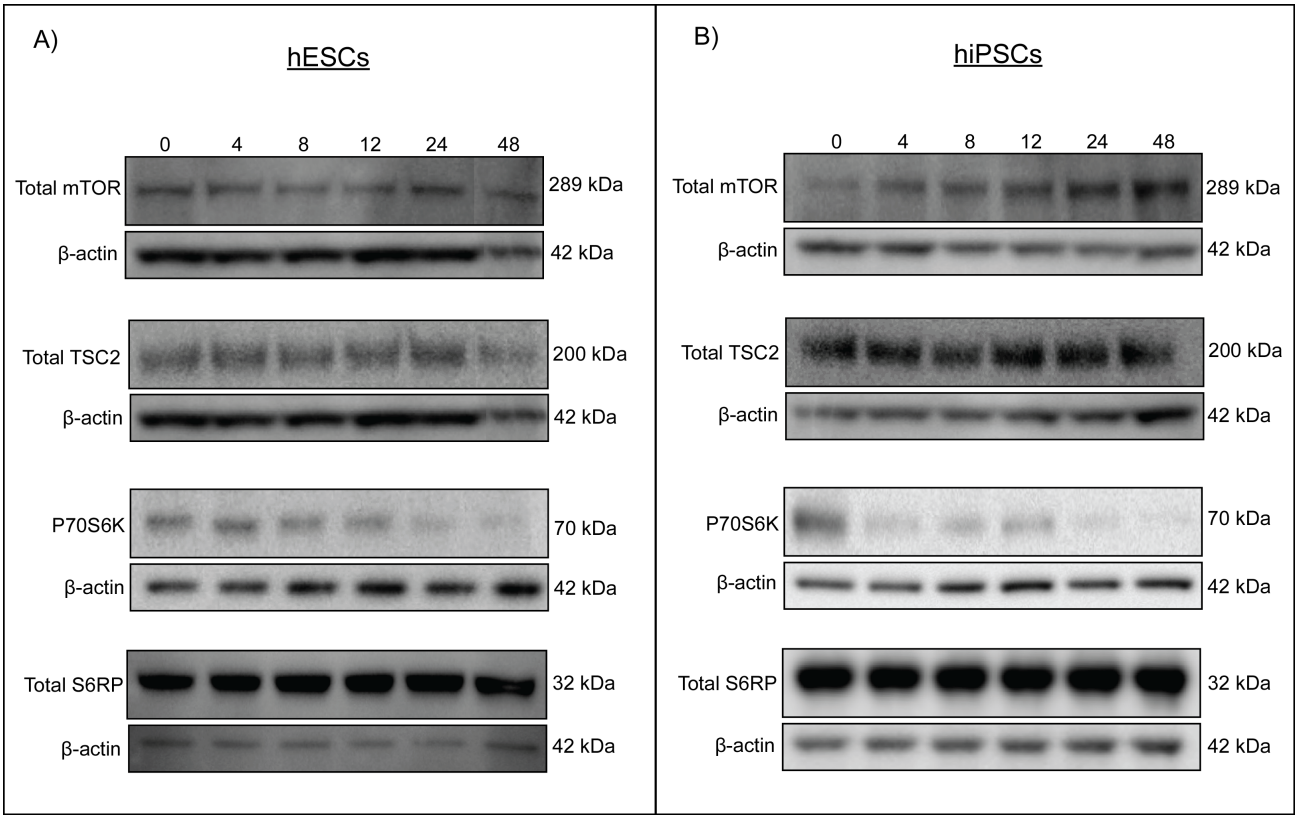

Figure 26. Western Blot analysis of key proteins in the mTOR pathway: protein expression levels of mTOR, TSC2, P70S6K, and S6RP. **A)** Protein expression levels observed in the hESC line, H1. **B)** Protein expression observed in the hiPSC line AG-27. β-Actin was used as a loading control in all samples.

Our results show stable expression of both total mTOR protein levels, and protein levels of the mTOR inhibitor TSC2 (Figure 26). The value of this information is somewhat limited however, as it does not tell us if TSC2 is present in an activated or inactivated form, nor does it tell us about specific phosphorylations or modulations of the different mTOR complexes. The results do however show a clear drop in P70S6K levels over time (Figure 26). P70S6K is a downstream marker of mTOR activity[195,196]. Another indicator of mTOR activity is S6-RP; surprisingly (in light of the drop in p-Akt levels) we observe high expression of S6RP throughout the time course. The

phosphorylated (active) forms of pS6-RP (Ser240/244) and pS6-RP (Ser235/236) were assessed to determine if S6-RP activity really did remain highly and steadily expressed throughout the differentiation (data not shown). They did indeed show the same profile, a high level of protein expression throughout the time course.

4 Discussion

4.1 Regulation of Differentiation through the Wnt and TGFβ pathways

In the course of our efforts to map and analyse gene and protein expression during endodermal differentiation, one of the first and most interesting findings was the rapid up-regulation of gene expression for *NODAL* and *FOXA2* (Figure 16). Both *NODAL* and *FOXA2* are important drivers of anterior PS formation[27]. In particular the rapid increase in *NODAL* expression by CHIR99021 treatment at such an early stage is quite noteworthy, as CHIR99021 is primarily thought to drive differentiation through activation of the Wnt/β-catenin pathway[63]. Nodal is a TGFβ family protein, which is known to cooperate with WNT signalling to initiate ME formation, through unknown interactions[27]. Recent research suggest that the interaction between the Wnt and TGFβ pathways might be mediated though Smad4[197]. In this model Smad4 is inhibited by GSK3, but activated by Wnt mediated GSK3 sequestration and FGF-signalling in combination with active MAPK/ERK[197]. A different study also demonstrated that Wnt signaling increases the half-life of Smad4 resulting in increased TGFβ signaling[135]. This process of Nodal activation through either Wnt signalling or the subsequent reduction in GSK3 is supported by our findings, and provides an avenue for future investigations. The immediate up-regulation of *NODAL* expression in our experiments suggests that canonical WNT signalling and the resulting inhibition of GSK3 in itself are enough to spark the change in conditions that activate Nodal signalling.

Next, we observed protein expression levels of GSK3β to determine how our CHIR99021 mediated inhibition of GSK3 is impinging on protein expression levels of GSK3β. We observed a moderate increase in GSK3β over time, for multiple cell lines (Figures 20 & 21). This could be due to a compensatory mechanism where the cell produces more GSK3 in response to the inactivation of GSK3 by CHIR99021. To garner a deeper understanding of the mechanisms underlying our CHIR99021 driven differentiation, it would be of great interest to know if the GSK3 proteins reside freely in the cytoplasm with reduced catalytic activity after CHIR99021 inhibition, or if they are sequestered in multivesicular endosomes in a similar fashion to Wnt/β-catenin mediated GSK3 sequestration[134,135,]. For p-GSK3β (Ser9), (the inhibited form of GSK3β), we observed a down-regulation of protein expression over time, in a manner that mirrors the decrease in active Akt. When Akt is activated (phosphorylated at the serine 473 or threonine 308 residues) it in turn phosphorylates and inhibits GSK3 on the serine residue of its N-terminus (serine 9 of GSK3β)[121]. Since active Akt was rapidly down-regulated (Figures 24, 25, S8 and S9) the decrease in Akt activity might be a direct cause of the decrease in p-GSK3β (Ser9). Interestingly, the decrease in p-GSK3β (Ser9), contradicts an expected trend where ERK activity increases due to the fall in active Akt and subsequently primes GSK3β for phosphorylation by ribosomal S6 kinases (RSKs)[63,198]. Despite the observed rise in active ERK (Figure 24 & S10), active ERK was not able to mediate an inhibitory effect via phosphorylation of GSK3β. This might be due to steric hindrance from the binding of CHIR99021 to GSK3. Alternatively, since *WNT3A* expression increases (Figure 20) over the course of the protocol, the lack of p-GSK3β (Ser9) could be explained by vesicular sequestration of GSK3[135].

Our results for NP-β-catenin showed an accumulation of NP-β-catenin in the cytoplasm and nucleus (Figures 20, 21 and S5) supporting the model of Wnt activation through GSK3 inhibition. Remarkably, Wnt/β-catenin signalling did not decrease in accordance with the increase of Axin2, as assessed by NP-β-catenin blots and *WNT3A* gene expression levels (Figure 20). These results suggest that Axin2 might not be acting as an effective negative regulator of Wnt/β-catenin signalling during DE differentiation. This highlights the need for

further investigations into potential alternative functions of Axin2 during differentiation. A recent study on the role of Axin2 in mouse embryos investigated the effects of a gain of function mutation of Axin2[147]. This mutation produced a more stable form of Axin2 that was less susceptible to degradation; the study was also supplemented with experiments using TNKS inhibition to prevent Axin2 degradation in normal embryos. They found that the Axin2 mutation led to decreased Wnt signalling in most tissues, but a paradoxical increase in canonical Wnt activity in the late PS of all Axin2 mutant embryos. Furthermore their treatment of wild-type embryos with a TNKS inhibitor, stabilized Axin causing an inhibition of Wnt signalling in most of the embryo, but resulted in increased Wnt signalling in the PS[147]. This might suggest that Axin2 has a different role in PS formation than it does elsewhere during normal development, and might explain the observed pulse in Axin2 in our results.

The results for protein expression levels of TNKS1/2 show a progressive rise in TNKS1/2 throughout the time course. The concurrent drop in Axin2 around 24 hours, when TNKS1/2 is highly up-regulated suggests that TNKS1/2 mediated ADP-ribosylation might lead to the degradation of Axin2 after 24 hours, but is unable to influence Axin1 levels. Furthermore Axin2 does not show an immediate response to increased levels of TNKS1/2. This is in agreement with an aforementioned study, which demonstrated that ADP-ribosylated Axin levels are rapidly increased in an evolutionarily conserved manner in response to Wnt-stimulation[162]. This study proposed a mechanism whereby Wnt activity either rapidly increases the rate of TNKS mediated ADP-ribosylation of Axin, or inhibits the proteasomal degradation of ADP-ribosylated Axin. They also found that ADP-ribosylation of Axin enhanced its ability to bind to the Wnt membrane-receptor LRP6, enabling it to form the LRP6 signalosome[162]. They further postulate that the initial increase in levels of ADP-ribosylated Axin spurs the response to Wnt stimulation by enhancing the Axin-LRP6 interaction, whereas the subsequent decrease in Axin levels prolongs the duration of signalling by reducing destruction complex assembly[162]. These results indicate that rather than simply targeting Axin for proteolysis, TNKS also has a Wnt-dependent role in modulating Axin activity

under certain conditions. They also provide another potential explanation for the role of Axin under Wnt stimulation. Since TNKS-inhibitors can effectively block canonical Wnt signalling by increasing destruction complex activity, and impeding signalosome assembly[150,154,158,162] the ADP-ribosylation of Axin during Wnt exposure, might be causing Axin to bind to the LRP6 signalosome and thus be sequestered and inactivated. This model is limited, in that it only explains how Axin2 could be inactivated by TNKS1/2 under Wnt exposure, in order to prevent the negative regulation of Wnt/β-catenin signalling. This interpretation seems improbable in light of the positive role Axin2 plays in Wnt-activation in the PS of mouse embryos[147], and its strictly conserved pattern of expression during ME differentiation (Figures S3 & S4) . Also pertinent to this discussion are the findings of our collaborators in the Krauss Unit for Cell Signaling. Following our differentiation procedure for hESCs, they added a small-molecule inhibitor of TNKS1/2 was added to the media and observed a pronounced up-regulation in protein expression of Axin1 and Axin2 for all time points, as well as diminished gene expression for both homologs of Axin. Furthermore, hESCs differentiated to PS but could not develop further towards DE, staying locked in a PS state[199]. This suggests that the observed drop in Axin2 after 24-hours in our experiments may be necessary for progression to DE. It is therefore evident that Axin2 merits closer examination into its potential effects in stimulating canonical Wnt signaling and other pathways involved in differentiation.

To examine one such potential function of Axin2, we looked at levels of Axin2 in the nuclear fraction of our cell lysates (Figures 21C & S5). Axin is known to contain nuclear import and export sequences and undergo nuclear shuttling. Moreover its accumulation in the nucleus has been shown to be associated with increased robustness of β-catenin/TCF signalling against fluctuations in Wnt activity, and β-catenin levels[200,201]. Our results show an accumulation of Axin2 in the nucleus that resembles the accumulation of Axin2 in the cytoplasm. Nuclear Axin2 has recently been shown to form an Axin2/β-catenin/TCF complex, which acts to repress *MYC* expression[202]. The c-MYC protein that the *MYC* gene encodes is involved in pluripotency and cell proliferation[203,204,205]. Intriguingly a recent study looking at haploinsufficient

(Myc+/–) mice with reduced *MYC* expression, discovered an increase in AMPK activity, coupled with decreased activities of Akt, TOR, and S6K[206]. These findings are very pertinent to our results for metabolic signalling proteins (section 4.2) as we also see decreased activities of Akt and P70S6K.

4.2 Metabolic Regulation of Differentiation

The role of PI3K/Akt in maintaining pluripotency is well established[62], and several publications use LY294002 a small-molecule inhibitor of PI3K/Akt-signalling in order to enhance the efficiency of DE differentiation from hESCs[83,85]. The finding that Akt signalling is rapidly down-regulated in the CHIR99021 directed protocol was nonetheless unexpected and of great interest to us. To the best of our knowledge, this is the first observation of a negative regulation of Akt in a solely CHIR99021 based treatment. This indicates that Akt activity is either being supressed through Wnt/β-catenin expression or by the decrease in GSK3 activity. In reviewing the literature it has been difficult to find any prospective links between the canonical Wnt and PI3K/Akt pathways. In fact much of the literature investigating this issue supports the conclusion that PI3K/Akt and canonical Wnt signalling are functionally uncoupled and that sequestration or compartmentalization of GSK3 prohibits crosstalk between the PI3K/Akt and the canonical Wnt pathways[102,120,121,129].

However, we did investigate an alternative model based on a recent publication, which proposes that pluripotency versus differentiation is governed by a regulatory network involving β-catenin, E-cadherin, PI3K/Akt and Slug[194]. In this model short-term activation of Wnt/β-catenin signaling enhances hESC self-renewal by up-regulating of E-cadherin at cell-cell junctions, leading to PI3K/Akt activation. The enhanced E-cadherin expression then serves as a β-catenin “sink” reducing the accumulation of free cytoplasmic β-catenin and favouring hESC self-renewal. On the other hand, long-term activation of Wnt/β-catenin increases free cytoplasmic β-catenin, which then exceeds the binding capacity of E-cadherin, leading to

nuclear accumulation of β-catenin, and increased expression of the E-cadherin suppressor Slug. The up-regulated Slug further inhibits E-cadherin expression and reinforces the accumulation of β-catenin, leading hESC differentiation. This explanation had to be rejected for our differentiation model, as it did not fit with our results (Figure S10). Furthermore there are important differences between the protocol described in the article and the one we use. For example, their long-term Wnt/β-catenin treatment entails treatment with the GSK3 inhibitor BIO for 4 days, whereas short-term treatment is 6 hours. They do not see activation of β-catenin/TCF activity after short-term treatment; our results on the other hand show stabilization of NP-β-catenin in the nucleus already at 4 hours, along with up-regulation of Axin2.

Since EMT is an important hallmark of gastrulation, PS-formation and differentiating hPSCs, under which E-cadherin is down-regulated and N-cadherin is up-regulated[207,208,209,210]. We assessed whether there was E-cadherin mediated crosstalk between the PI3K/Akt and β-catenin pathways. The original study looks at E-cadherin levels after long-term exposure to Wnt/β-catenin signalling i.e. BIO-treatment for 4 days. They found a significant down-regulation of E-cadherin combined with a decrease in PI3K/Akt activity[194]. Our results show dynamic fluctuations in E-cadherin versus N-cadherin at the gene expression level with relative up-regulation of N-cadherin (*CDH2*) compared to E-cadherin (*CDH1*) as expected for differentiating cells undergoing EMT (Figure S1)[210]. However, our observed levels of E-cadherin protein expression show stable expression throughout all time courses (Figure S10). This does not fit with the assumption that a decrease in PI3K/Akt activity and rise in β-catenin is driven by a fall in E-cadherin levels. This E-cadherin centered model was therefore ruled-out as a potential explanation of our results.

In looking for an alternative explanation for CHIR99021 mediated decrease in Akt activity, it is worth noting that PTEN the main negative regulator of PI3K/Akt activity is inhibited and destabilized by GSK3 and casein kinase 2 (CK2) mediated phosphorylations[191,211,212,213]. Our results show stable and high expression of PTEN at every time point (Figures S8 & S9), however

there might be differences in the phosphorylation status of PTEN before and after GKS3 inhibition (see section 4.3).

Interestingly Akt1 has also been shown to be required for specifying anterior definitive endodermal identity (ADE) though its effects on ECM composition, which in turn patterns the endoderm[214]. The rise in (total) Akt at 48 hours (Figures 25, S8 and S9) might be indicative of an Akt up-regulation as the naïve DE further differentiates into the foregut (ADE), midgut, and hindgut[214,215].

The role of MAPK/ERK-signalling in hPSC differentiation has been controversial. In contrast to mouse ES cells, p-ERK1/2 levels were reported to be inhibited during differentiation[65,88]. Conversely, recent publications have demonstrated a requirement for ERK activation during ME differentiation[63,65]. Our results display an increase in p-ERK1/2 activity during differentiation (Figure S10) in accordance with recent research on the role of ERK in ME differentiation. ERK has been shown to suppress BMP signalling and prevent extraembryonic differentiation[65], while FGF2 and p-ERK1/2 together have been shown to promote ME differentiation under conditions of high Nodal expression[65]. ERK signalling through p-ERK1/2 has also been shown to stimulate the expression and/or nuclear translocation of active β-catenin[198,216]. ERK is also known to prime GSK3β for inhibitory phosphorylation at the serine 9 residue[63,198]. This has been suggested a potential mechanism by which ERK stimulates differentiation together with Wnt, however the low levels of p-GSK3β (Ser9) expression in our results (Figures 21, S3 and S4) indicate that this is non-essential for DE differentiation as it is not observed in the CHIR99021 based differentiation process.

Exactly how the phasic expression of p-AMPKα (Ser172) (Figures S8 & S9) is affecting the differentiation process is unknown to us, however our collaborators in the Simonsen Autophagy Group have seen interesting patterns of phasic up-regulation for key autophagy markers that appear to correspond with our results for active AMPK (personal communication, Kulbhushan Sharma).

Lastly, we examined the metabolic signalling proteins of the mTOR pathway. mTOR has been increasingly recognized to be involved in maintenance of pluripotency[180] and the exact roles of the two different mTORC complexes is only beginning to be unravelled. Being metabolic sensors and regulators, the mTOR complexes facilitate a great range of different activities and interactions, they also have many binding and phosphorylation sites that modulate their activity[171].

mTORC1 is involved in the following processes: it phosphorylates ribosomal S6K which subsequently activates S6RP to promote ribosome biogenesis. mTORC1 also phosphorylates and inhibits 4E-BP resulting in translation initiation. It also stimulates nucleotide and lipid synthesis and inhibits autophagy by phosphorylating ULK1, (which is activated AMPK)[171]. mTORC2 is also involved in anabolic processes, and is an important regulator of Akt signalling. It co-translationally phosphorylates Akt to prevent its ubiquitination and degradation, and post-translationally phosphorylates Akt at Ser473[171]. mTORC2 activity is in turn positively regulated by the PI3K/Akt pathway[182,217]. A recent study suggests that PI3K/Akt activated mTORC2 is responsible for phosphorylating Smad2/3, priming it for degradation and thereby attenuating Nodal signaling[182]. When PI3K/Akt is inhibited however mTORC2 activity is reduced, allowing Smad2/3 to relay Nodal signals[181,182]. This offers a mechanistic explanation for the dual role of Nodal in maintaining pluripotency in the presence of PI3K/Akt–signalling, and initiating differentiation when PI3K/Akt is inhibited[63]. Based on this information and our results for Nodal and Akt signalling we would expect to see mTORC2 inhibition and the subsequent activation of Nodal to be occurring in our differentiation time course.

Our results show stable expression protein levels for total mTOR, and the mTOR inhibitor TSC2 (Figures 26, S6 and S7). These results do not tell us if TSC2 is present in an activated or inactivated form, nor do they tell us about specific phosphorylations or modulations of the different mTOR complexes. The results do however show a clear drop in expression levels of P70S6K (a

downstream marker of mTOR activity[195,196] over time. The drop in P70S6K expression corroborates the drop in PI3K/Akt signalling (Figures 25, S8, and S9), which as previously mentioned is an inducer of mTOR activity. Viewed in combination with the phasic rise of active AMPKα, the drop in P70S6K might signify a fall in mTOR activity and rise in AMPK-triggered catabolic processes such as autophagy. We do see high and stable expression levels of S6RP throughout the time course (Figures S6, and S7). This might suggest that mTOR activity is being modulated in an intricate manner, whereby some functions are downregulated and others are maintained. In line with this notion Wnt/β-catenin signalling might be stimulating certain aspects of mTOR activity, while other activities are diminished in the absence PI3K/Akt signaling. Wnt signalling has indeed been found to enhance S6K phosphorylation, decrease 4EBP1 mobility, and stimulate protein translation *via* GSK-3 and TSC1/2 inactivation[172,80]. Finally it is difficult to gauge from our results whether TSC2 is active or not. While the fall in PI3K/Akt levels removes one inhibitory regulator of TSC2, its known route of activation requires phosphorylations by AMPK in concert with GSK3[167], which is inhibited in our differentiation procedure. Previous studies have also shown that Wnt signalling inhibits TSC2 through its inhibitory effects on GSK3[80], making it doubtful whether TSC2 is active and mediating any kind of inhibition on mTOR in our experiments.

4.3 Future Investigations

To further elucidate the mechanisms behind the crosstalk and interplay observed in our results, we would like to see further research into the following issues:

To gain a deeper understanding of the mechanisms that mediate crosstalk between the TGFβ and canonical Wnt pathways, we would like to investigate the interactions between FGF, ERK, Smad4 and Nodal signalling, before and during our differentiation process. Both FGF/MAPK and Wnt/GSK3 pathways have been reported to converge on Smad4[218]. To determine if Smad4

mediates the crosstalk between the Wnt/GSK3 and TGFβ pathways and the subsequent increase in gene expression of Nodal, we would like to perform loss-of-function studies on FGF2, ERK and Smad4 during differentiation, to see how Nodal expression levels are affected.

To obtain a better understanding of how CHIR99021-mediated inhibition of GSK3 is affecting other signalling pathways, we would like to label the GSK3 proteins and view them by microscopy to determine if GSK3 becomes sequestered in multivesicular endosomes or remains in the cytosol in an inhibited state. The rise of *WNT3A* gene expression over time (Figure 20C) adds an interesting dimension to this question, as a rise in active Wnt3a in our differentiating cell population should theoretically lead to the secretion of Wnt3a[219] which would then bind to the Wnt membrane receptors of other cells leading to the sequestration of GSK3 in multivesicular endosomes[135]. We would like to investigate this by performing an ELISA assay or western blotting analysis of the cell media during differentiation. Since the CHIR99021 based protocol is thought to initiate differentiation through GSK3 inhibition, which in turn is thought to mimic the effects of canonical Wnt signalling; it would be of interest to perform a control experiment using Wnt3a or Wnt1 instead of CHIR99021. This could confirm whether or not GSK3 inhibition triggers the same gene expression and cell signalling profiles as Wnt ligands.

Two fundamental questions were raised by our characterization of the signalling events in DE differentiation:

The first question regards how the inhibition of GSK3 led to a down-regulation of active Akt. An interesting possibility to investigate is whether GSK3 promotes Akt signalling, through its inhibitory phosphorylations of PTEN[220]. We would therefore like to examine the phosphorylated states of PTEN before and during differentiation. Another aspect we could investigate is how PI3K might be affected by during differentiation. To examine this we could perform immuneprecipitations of PI3K, to see which proteins it interacts with before and after differentiation is initiated.

The second question concerns the role of Axin2 and TNKS in the PS. To understand the role of Axin2 during this critical period, we would like to perform immune-precipitations of Axin2 to identify interacting proteins. We would also like to phospho-map Axin2 to understand how its behaviour might be modulated during differentiation. It would be interesting to see if the observed pulse of Axin2 expression is specific to PS. To determine this, we could investigate the Axin2 expression profile in mature differentiated cells upon Wnt stimulation, as well as the Axin2 expression profile for ectodermal differentiation.

Furthermore, we would also like to determine the role of mTORC2 in attenuating SMAD2/3 signalling and blocking differentiation, and would like to specifically inhibit mTOR1 and mTORC2 individually.

Finally to delineate the timing of metabolic changes known to occur in differentiation of stem cells[221,222], we would like to measure the kinetics, and the degree to which our differentiating stem cells undergo metabolic changes such as mitochondrial maturation, and the shift from glycolysis to oxidative phosphorylation over the 48 hours of DE differentiation.

5 Conclusion

In summary, we demonstrate that the Wnt-mimicking process of GSK3 inhibition drives DE differentiation, mediating crosstalk between pathways previously established to be important for DE development but not known to be regulated or initiated by canonical Wnt-signalling specifically. These pathways include the TGFβ signalling pathway as seen by up-regulation of Nodal gene expression, and the PI3K/Akt pathway as illustrated by the rapid down-regulation of active Akt. Furthermore we highlight an interesting pattern of Axin2 and TNKS signalling in DE differentiation, whereby Axin2 is rapidly up-regulated, before being down-regulated after approx. 20 hours, seemingly due to increased TNKS expression. We also show that these events are

conserved across different hPSC lines. Thus canonical Wnt/GSK3 signalling acts as a master-regulator and initiator of mesendodermal differentiation. Schematic models summarizing the cell signalling events occurring during the pluripotent state (Figure 27), mesendodermal differentiation (Figure 28), and definitive endoderm (Figure 29) are given below.

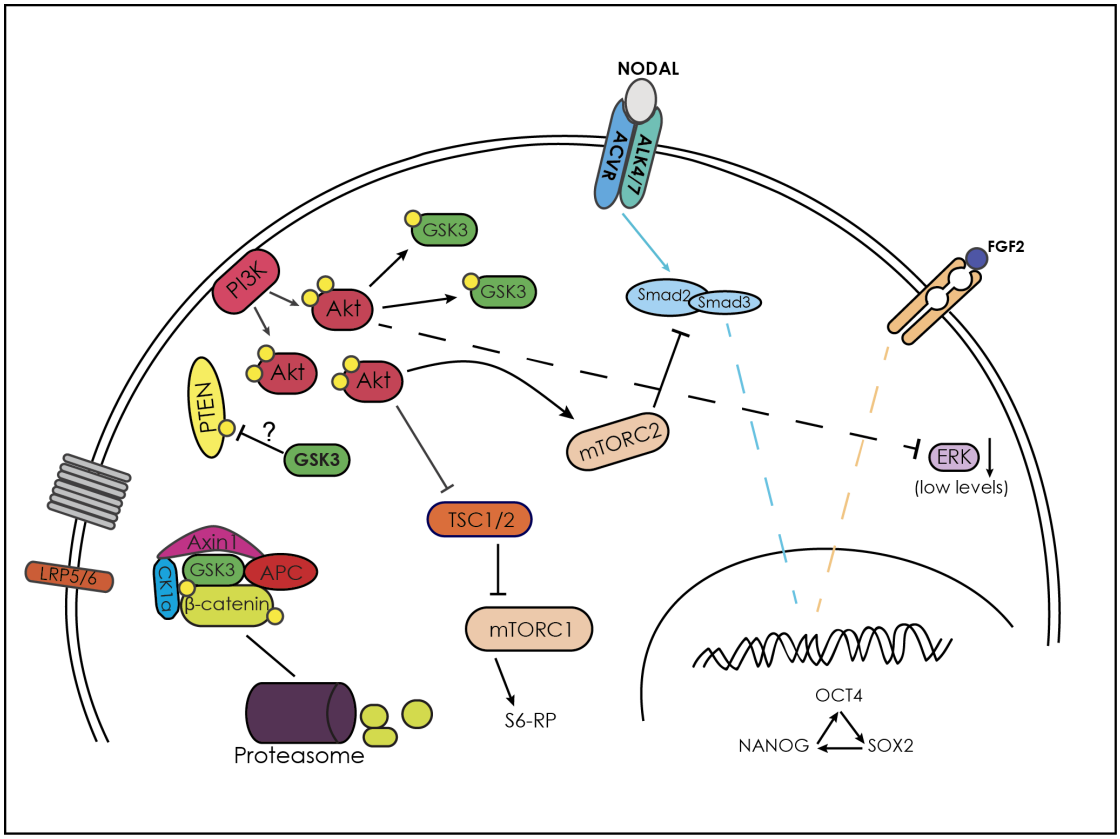

Figure 27. Cell signalling model for the pluripotent state: The pluripotent stem cell state is characterized by active destruction complexes mediating β-catenin proteolysis, high levels of active Akt, low levels of ERK, expression of pluripotency factors, and moderate to high levels of Nodal and high FGF signaling[92,65,182].

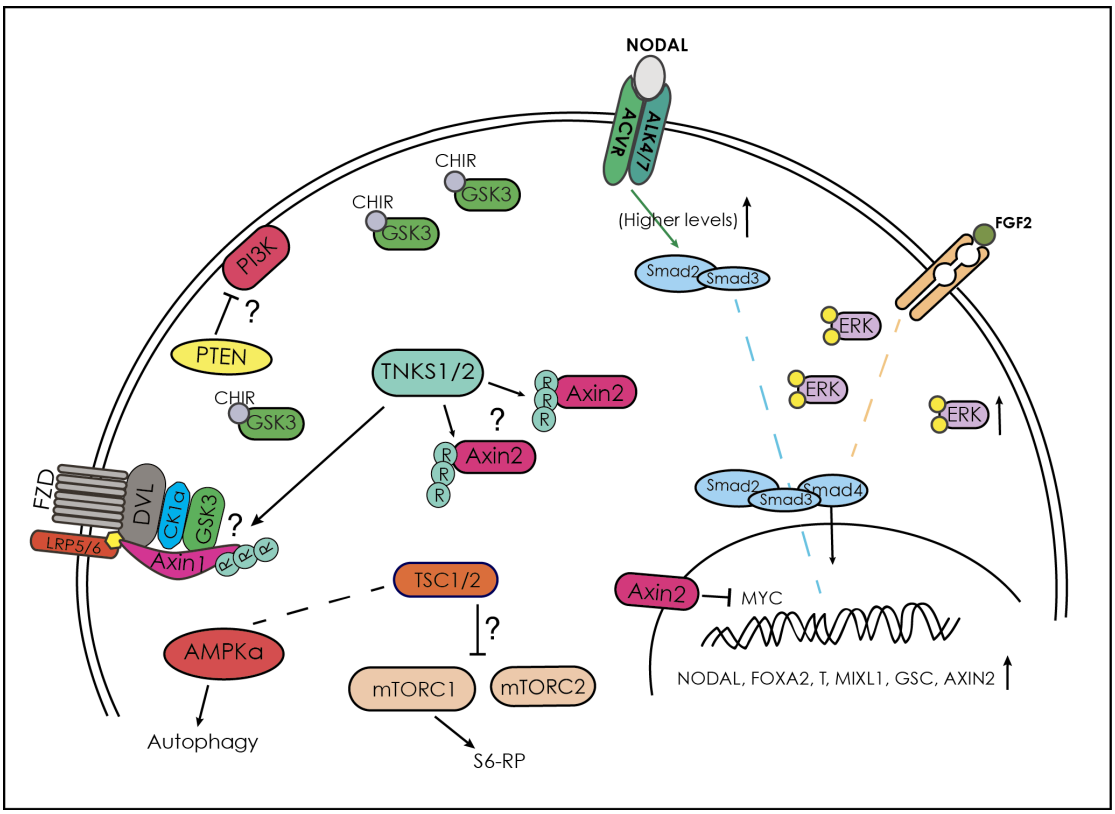

Figure 28. Cell signalling model for mesendodermal differentiation: The shift toward ME differentiation and PS formation is characterized by β-catenin accumulation, a sharp decrease in active Akt levels, a sharp increase in Axin2 expression, increasing levels of TNKS1/2, increasing levels of ERK, high levels of Nodal, active FGF signaling, and expression of PS marker genes[63,162.182,218,211].

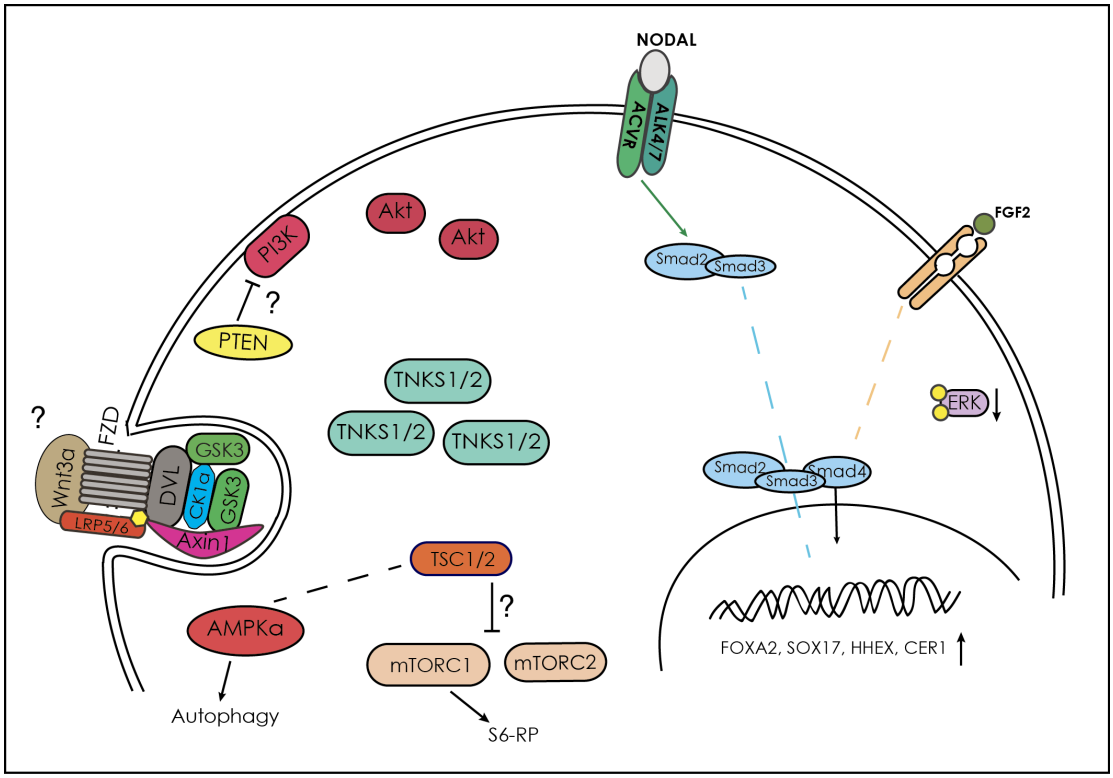

Figure 29. Cell signalling model for DE: The DE state is characterized by increased levels of TNKS1/2, a sharp decrease in Axin2 levels, a drop in Nodal expression relative to 24 hours, increased (non-phospho) Akt expression and expression of DE marker genes. As *WNT3A* is highly expressed at this time point there is also a possibility that GSK3 is sequestered in multivesicular endosomes[135,214,

6 References

1. Lerche-Langrand C, Toutain HJ. Precision-cut liver slices: characteristics and use for in vitro pharmaco-toxicology. *Toxicology* 2000;153(1–3):221-253. doi:http://dx.doi.org/10.1016/S0300-483X(00)00316-4.
2. Soldatow VY, LeCluyse EL, Griffith LG, Rusyn I. In vitro models for liver toxicity testing. *Toxicol. Res. (Camb).* 2013;2(1):23-39. doi:10.1039/C2TX20051A.
3. FDA, Food and Drug Administration. *Innovation or Stagnation: Challenge and Opportunity on the Critical Path to New Medical Products*.; 2004. Available at: http://www.fda.gov/oc/initiatives/criticalpath/whitepaper.html.
4. Mak IW, Evaniew N, Ghert M. Lost in translation: animal models and clinical trials in cancer treatment. *Am. J. Transl. Res.* 2014;6(2):114-8.
5. Perel P, Roberts I, Sena E, et al. Comparison of treatment effects between animal experiments and clinical trials: systematic review. *BMJ* 2007;334(7586):197. doi:10.1136/bmj.39048.407928.BE.
6. Hackam DG, Redelmeier DA. Translation of Research Evidence From Animals to Humans. *Jama* 2006;296(14):1727-1732. doi:10.1001/jama.296.14.1731.
7. Martignoni M, Groothuis GMM, de Kanter R. Species differences between mouse, rat, dog, monkey and human CYP-mediated drug metabolism, inhibition and induction. *Expert Opin. Drug Metab. Toxicol.* 2006;2(6):875-94. doi:10.1517/17425255.2.6.875.
8. Odom DT, Dowell RD, Jacobsen ES, et al. Tissue-specific transcriptional regulation has diverged significantly between human and mouse. *Nat. Genet.* 2007;39(6):730-2. doi:10.1038/ng2047.
9. Jack J, Rotroff D, Motsinger-Reif A. Cell Lines Models of Drug Response: Successes and Lessons from this Pharmacogenomic Model. *Curr. Mol. Med.* 2014;14(7):833-840.
10. Yasuda SU, Zhang L, Huang S-M. The Role of Ethnicity in Variability in Response to Drugs: Focus on Clinical Pharmacology Studies. *Clin. Pharmacol. Ther.* 2008;84(3):417-423. doi:10.1038/clpt.2008.141.
11. Bale SS, Vernetti L, Senutovitch N, et al. In Vitro Platforms for Evaluating Liver Toxicity. *Exp Biol Med* 2014;239(9):1180-1191. doi:10.1177/1535370214531872.
12. Orlando G, Soker S, Stratta RJ, Atala A. Will regenerative medicine replace transplantation? *Cold Spring Harb. Perspect. Med.* 2013;3(8). doi:10.1101/cshperspect.a015693.
13. Hynds RE, Giangreco A. The Relevance of Human Stem Cell-Derived Organoid Models for Epithelial Translational Medicine. *Stem Cells* 2012;31(1):417-422. doi:10.1002/stem.1290.
14. Fatehullah A, Tan SH, Barker N. Organoids as an in vitro model of human development and disease. *Nat. Cell Biol.* 2016;18(3):246-54. doi:10.1038/ncb3312.
15. Luni C, Serena E, Elvassore N. Human-on-chip for therapy development and fundamental science. *Curr. Opin. Biotechnol.* 2014;25:45-50. doi:10.1016/j.copbio.2013.08.015.
16. Bhatia SN, Ingber DE. Microfluidic organs-on-chips. *Nat. Biotechnol.* 2014;32(8):760-772. doi:10.1038/nbt.2989.
17. Zhang C, Zhao Z, Abdul Rahim NA, van Noort D, Yu H. Towards a human-on-chip: culturing multiple cell types on a chip with compartmentalized microenvironments. *Lab Chip* 2009;9(22):3185-3192. doi:10.1039/b915147h.
18. Knowlton S, Tasoglu S. A Bioprinted Liver-on-a-Chip for Drug Screening Applications. *Trends Biotechnol.* 2016;34(9):681-682.

doi:10.1016/j.tibtech.2016.05.014.
19. Hall BK. Germ Layers and the Germ-Layer Theory Revisited. In: Hecht MK, Macintyre RJ, Clegg MT, eds. *Evolutionary Biology*. Boston, MA: Springer US; 1998:121-186. doi:10.1007/978-1-4899-1751-5_5.
20. Kalinka AT, Tomancak P. The evolution of early animal embryos: Conservation or divergence? *Trends Ecol. Evol.* 2012;27(7):385-393. doi:10.1016/j.tree.2012.03.007.
21. Martindale MQ, Pang K, Finnerty JR. Investigating the origins of triploblasty: "mesodermal" gene expression in a diploblastic animal, the sea anemone Nematostella vectensis (phylum, Cnidaria; class, Anthozoa). *Development* 2004;131(10):2463-74. doi:10.1242/dev.01119.
22. Schoenwolf GC, Bleyl SB, Brauer PR, Francis-West PH. Larsen's human embryology. In: *Larsen's Human Embryology*.; 2014:307-312. doi:10.1016/B978-0-443-06811-9.10011-9.
23. Luckey CJ, Lu Y, Marto JA. Understanding the first steps in embryonic stem cell exit from the pluripotent state. *Transfusion* 2011;51(SUPPL. 4). doi:10.1111/j.1537-2995.2011.03374.x.
24. Junying Y, James A. T. *Regenerative Medicine 2006*.; 2006. Available at: http://stemcells.nih.gov/staticresources/info/scireport/PDFs/Regenerative_Medicine_2006.pdf.
25. Mohammadnia A, Yaqubi M, Pourasgari F, Neely E, Fallahi H, Massumi M. Signaling and Gene Regulatory Networks Governing Definitive Endoderm Derivation From Pluripotent Stem Cells. *Journal of Cellular Physiology*. 2016.
26. Lawson KA, Meneses JJ, Pedersen RA. Clonal analysis of epiblast fate during germ layer formation in the mouse embryo. *Development* 1991;113:891-911. doi:VL - 113.
27. Gadue P, Huber TL, Paddison PJ, Keller GM. Wnt and TGF-beta signaling are required for the induction of an in vitro model of primitive streak formation using embryonic stem cells. *Proc. Natl. Acad. Sci. U. S. A.* 2006;103(45):16806-16811. doi:10.1073/pnas.0603916103.
28. Loh KM, Ang LT, Zhang J, et al. Efficient endoderm induction from human pluripotent stem cells by logically directing signals controlling lineage bifurcations. *Cell Stem Cell* 2014;14(2):237-252. doi:10.1016/j.stem.2013.12.007.
29. Thomson JA. Embryonic Stem Cell Lines Derived from Human Blastocysts. *Science (80-.).* 1998;282(5391):1145-1147. doi:10.1126/science.282.5391.1145.
30. Richter KS, Harris DC, Daneshmand ST, Shapiro BS. Quantitative grading of a human blastocyst: Optimal inner cell mass size and shape. *Fertil. Steril.* 2001;76(6):1157-1167. doi:10.1016/S0015-0282(01)02870-9.
31. Dhar D, Ho JHE. Stem cell research policies around the world. *Yale J. Biol. Med.* 2009;82(3):113-115.
32. Murugan V. Embryonic Stem Cell Research: A Decade of Debate from Bush to Obama. *Yale J. Biol. Med.* 2009;82(3):101-103.
33. Takahashi K, Yamanaka S. A decade of transcription factor-mediated reprogramming to pluripotency. *Nat Rev Mol Cell Biol* 2016;17(3):183-193. doi:10.1038/nrm.2016.8.
34. González F, Boué S, Belmonte JCI. Methods for making induced pluripotent stem cells: reprogramming à la carte. *Nat Rev Genet* 2011;12(4):231-242. doi:10.1038/nrg2937.
35. Raab S, Klingenstein M, Liebau S, Linta L. A Comparative View on Human Somatic Cell Sources for iPSC Generation. *Stem Cells Int.* 2014;2014. doi:10.1155/2014/768391.
36. Takahashi K, Yamanaka S. Induction of Pluripotent Stem Cells from Mouse Embryonic and Adult Fibroblast Cultures by Defined Factors. *Cell*

2006;126(4):663-676. doi:10.1016/j.cell.2006.07.024.
37. Yu J, Vodyanik MA, Smuga-Otto K, et al. Induced pluripotent stem cell lines derived from human somatic cells. *Science* 2007;318(5858):1917-20. doi:10.1126/science.1151526.
38. Toivonen S, Ojala M, Hyysalo A, et al. Comparative Analysis of Targeted Differentiation of Human Induced Pluripotent Stem Cells (hiPSCs) and Human Embryonic Stem Cells Reveals Variability Associated With Incomplete Transgene Silencing in Retrovirally Derived hiPSC Lines. *Stem Cells Transl. Med.* 2013;2(2):83-93. doi:10.5966/sctm.2012-0047.
39. Wang J, Hao J, Bai D, et al. Generation of clinical-grade human induced pluripotent stem cells in Xeno-free conditions. *Stem Cell Res. Ther.* 2015;6(1):223. doi:10.1186/s13287-015-0206-y.
40. Pera MF, Tam PPL. Extrinsic regulation of pluripotent stem cells. *Nature* 2010;465(7299):713-20. doi:10.1038/nature09228.
41. Vallier L, Alexander M, Pedersen R a. Activin/Nodal and FGF pathways cooperate to maintain pluripotency of human embryonic stem cells. *J. Cell Sci.* 2005;118(Pt 19):4495-4509. doi:10.1242/jcs.02553.
42. Yeo J-C, Ng H-H. The transcriptional regulation of pluripotency. *Cell Res.* 2013;23(1):20-32. doi:10.1038/cr.2012.172.
43. Loh KM, Lim B. A precarious balance: Pluripotency factors as lineage specifiers. *Cell Stem Cell* 2011;8(4):363-369. doi:10.1016/j.stem.2011.03.013.
44. Boyer LA, Lee TI, Cole MF, et al. Core transcriptional regulatory circuitry in human embryonic stem cells. *Cell* 2005;122(6):947-56. doi:10.1016/j.cell.2005.08.020.
45. Sui L, Bouwens L, Mfopou JK. Signaling pathways during maintenance and definitive endoderm differentiation of embryonic stem cells. *Int. J. Dev. Biol.* 2013;57(1):1-12. doi:10.1387/ijdb.120115ls.
46. Singh AM, Bechard M, Smith K, Dalton S. Reconciling the different roles of Gsk3β in “naïve” and “primed” pluripotent stem cells. *Cell Cycle* 2012;11(16):2991-2996. doi:10.4161/cc.21110.
47. Vallier L, Touboul T, Chng Z, et al. Early cell fate decisions of human embryonic stem cells and mouse epiblast stem cells are controlled by the same signalling pathways. *PLoS One* 2009;4(6). doi:10.1371/journal.pone.0006082.
48. Weinberger L, Ayyash M, Novershtern N, Hanna JH. Dynamic stem cell states: naive to primed pluripotency in rodents and humans. *Nat Rev Mol Cell Biol* 2016;17(3):155-169. Available at: http://dx.doi.org/10.1038/nrm.2015.28.
49. Hanna J, Cheng AW, Saha K, et al. Human embryonic stem cells with biological and epigenetic characteristics similar to those of mouse ESCs. *Proc. Natl. Acad. Sci. U. S. A.* 2010;107(20):9222-9227. doi:10.1073/pnas.1004584107.
50. Guo G, von Meyenn F, Santos F, et al. Naive Pluripotent Stem Cells Derived Directly from Isolated Cells of the Human Inner Cell Mass. *Stem Cell Reports* 2016;6(4):437-446. doi:10.1016/j.stemcr.2016.02.005.
51. Schnerch A, Cerdan C, Bhatia M. Distinguishing between mouse and human pluripotent stem cell regulation: The best laid plans of mice and men. *Stem Cells* 2010;28(3):419-430. doi:10.1002/stem.298.
52. Nichols J, Smith A. Naive and Primed Pluripotent States. *Cell Stem Cell* 2009;4(6):487-492. doi:10.1016/j.stem.2009.05.015.
53. Davidson KC, Mason EA, Pera MF. The pluripotent state in mouse and human. *Development* 2015;142(18):3090 LP-3099.
54. Ornitz DM, Itoh N. Fibroblast growth factors. *Genome Biol.* 2001;2(3):REVIEWS3005. doi:10.1186/gb-2001-2-3-reviews3005.
55. Levenstein ME, Ludwig TE, Xu R-H, et al. Basic fibroblast growth factor support of human embryonic stem cell self-renewal. *Stem Cells*

2006;24(3):568-74. doi:10.1634/stemcells.2005-0247.
56. Wang L, Chen Y-G. Signaling Control of Differentiation of Embryonic Stem Cells toward Mesendoderm. *J. Mol. Biol.* 2015;428(7):1409-1422. doi:10.1016/j.jmb.2015.06.013.
57. Vallier L, Mendjan S, Brown S, et al. Activin/Nodal signalling maintains pluripotency by controlling Nanog expression. *Development* 2009;136(8):1339-49. doi:10.1242/dev.033951.
58. Yu P, Pan G, Yu J, Thomson JA. FGF2 sustains NANOG and switches the outcome of BMP4-induced human embryonic stem cell differentiation. *Cell Stem Cell* 2011;8(3):326-334. doi:10.1016/j.stem.2011.01.001.
59. Xu RH, Sampsell-Barron TL, Gu F, et al. NANOG Is a Direct Target of TGFβ/Activin-Mediated SMAD Signaling in Human ESCs. *Cell Stem Cell* 2008;3(2):196-206. doi:10.1016/j.stem.2008.07.001.
60. Greber B, Lehrach H, Adjaye J. Fibroblast growth factor 2 modulates transforming growth factor beta signaling in mouse embryonic fibroblasts and human ESCs (hESCs) to support hESC self-renewal. *Stem Cells* 2007;25:455-464. doi:10.1634/stemcells.2006-0476.
61. Paling NRD, Wheadon H, Bone HK, Welham MJ. Regulation of embryonic stem cell self-renewal by phosphoinositide 3-kinase-dependent signaling. *J. Biol. Chem.* 2004;279(46):48063-48070. doi:10.1074/jbc.M406467200.
62. Watanabe S, Umehara H, Murayama K, Okabe M, Kimura T, Nakano T. Activation of Akt signaling is sufficient to maintain pluripotency in mouse and primate embryonic stem cells. *Oncogene* 2006;25(19):2697-2707. doi:10.1038/sj.onc.1209307.
63. Singh AM, Reynolds D, Cliff T, et al. Signaling network crosstalk in human pluripotent cells: A Smad2/3-regulated switch that controls the balance between self-renewal and differentiation. *Cell Stem Cell* 2012;10(3):312-326. doi:10.1016/j.stem.2012.01.014.
64. Dalton S. Signaling networks in human pluripotent stem cells. *Curr. Opin. Cell Biol.* 2013;25(2):241-246. doi:10.1016/j.ceb.2012.09.005.
65. Na J, Furue MK, Andrews PW. Inhibition of ERK1/2 prevents neural and mesendodermal differentiation and promotes human embryonic stem cell self-renewal. *Stem Cell Res.* 2010;5(2):157-169. doi:10.1016/j.scr.2010.06.002.
66. Sui L, Mfopou JK, Geens M, Sermon K, Bouwens L. FGF signaling via MAPK is required early and improves Activin A-induced definitive endoderm formation from human embryonic stem cells. *Biochem. Biophys. Res. Commun.* 2012;426(3):380-385. doi:10.1016/j.bbrc.2012.08.098.
67. Ding VMY, Ling L, Natarajan S, Yap MGS, Cool SM, Choo ABH. FGF-2 modulates Wnt signaling in undifferentiated hESC and iPS cells through activated PI3-K/GSK3β signaling. *J. Cell. Physiol.* 2010;225(2):417-428. doi:10.1002/jcp.22214.
68. Cooper G. *The Cell: A Molecular Approach*. 2nd Editio. Sunderland (MA): Sinauer Associates; 2000; 2000.
69. Alberts B, Johnson A, Lewis J, Raff M, Roberts K, And Walter P. *Molecular Biology of the Cell*.; 2008. doi:10.1002/1521-3773(20010316)40:6<9823::AID-ANIE9823>3.3.CO;2-C.
70. Brazil DP, Yang ZZ, Hemmings BA. Advances in protein kinase B signalling: AKTion on multiple fronts. *Trends Biochem. Sci.* 2004;29(5):233-242. doi:10.1016/j.tibs.2004.03.006.
71. Manning BD, Cantley LC. AKT/PKB Signaling: Navigating Downstream. *Cell* 2007;129(7):1261-1274. doi:10.1016/j.cell.2007.06.009.
72. Suzuki T, Bridges D, Nakada D, et al. Inhibition of AMPK catabolic action by GSK3. *Mol. Cell* 2013;50(3):407-419. doi:10.1016/j.molcel.2013.03.022.
73. Shah BH, Neithardt A, Chu DB, Shah FB, Catt KJ. Role of EGF receptor transactivation in phosphoinositide 3-kinase-dependent activation of MAP

kinase by GPCRs. *J. Cell. Physiol.* 2006;206(1):47-57. doi:10.1002/jcp.20423.
74. Olsson A, Dimberg A, Kreuger J, Claesson-Welsh L. VEGF receptor signalling — in control of vascular function. *Nat. Rev. Mol. Cell Biol.* 2006;7(5):359-371. doi:10.1038/nrm1911.
75. Altomare DA, Khaled a R. Homeostasis and the importance for a balance between AKT/mTOR activity and intracellular signaling. *Curr. Med. Chem.* 2012;19(22):3748-3762. doi:10.2174/092986712801661130.
76. Alessi DR, Andjelkovic M, Caudwell B, et al. Mechanism of activation of protein kinase B by insulin and IGF-1. *EMBO J.* 1996;15(23):6541-51.
77. Cross D a, Alessi DR, Cohen P, Andjelkovich M, Hemmings B a. Inhibition of glycogen synthase kinase-3 by insulin mediated by protein kinase B. *Nature* 1995;378(6559):785-9. doi:10.1038/378785a0.
78. Alao JP. The regulation of cyclin D1 degradation: roles in cancer development and the potential for therapeutic invention. *Mol. Cancer* 2007;6:24. doi:10.1186/1476-4598-6-24.
79. Hay N, Sonenberg N. Upstream and downstream of mTOR. *Genes Dev.* 2004;18(16):1926-1945. doi:10.1101/gad.1212704.
80. Jin T, George Fantus I, Sun J. Wnt and beyond Wnt: Multiple mechanisms control the transcriptional property of β-catenin. *Cell. Signal.* 2008;20(10):1697-1704. doi:10.1016/j.cellsig.2008.04.014.
81. Sarbassov DD, Guertin D a, Ali SM, Sabatini DM. Phosphorylation and regulation of Akt/PKB by the Rictor-mTOR complex. *Science* 2005;307(5712):1098-1101. doi:10.1126/science.1106148.
82. Hemmings BA, Restuccia DF. PI3K-PKB/Akt pathway. *Cold Spring Harb. Perspect. Biol.* 2012;4(9). doi:10.1101/cshperspect.a011189.
83. McLean AB, D'Amour K a, Jones KL, et al. Activin a efficiently specifies definitive endoderm from human embryonic stem cells only when phosphatidylinositol 3-kinase signaling is suppressed. *Stem Cells* 2007;25(1):29-38. doi:10.1634/stemcells.2006-0219.S.
84. Zorn AM, Wells JM. Vertebrate endoderm development and organ formation. *Annu. Rev. Cell Dev. Biol.* 2009;25:221-51. doi:10.1146/annurev.cellbio.042308.113344.
85. Teo AKK, Arnold SJ, Trotter MWB, et al. Pluripotency factors regulate definitive endoderm specification through eomesodermin. *Genes Dev.* 2011;25(3):238-250. doi:10.1101/gad.607311.
86. Diekmann U, Lenzen S, Naujok O. A reliable and efficient protocol for human pluripotent stem cell differentiation into the definitive endoderm based on dispersed single cells. *Stem Cells Dev.* 2015;24(2):190-204. doi:10.1089/scd.2014.0143.
87. Bernardo AS, Faial T, Gardner L, et al. BRACHYURY and CDX2 mediate BMP-induced differentiation of human and mouse pluripotent stem cells into embryonic and extraembryonic lineages. *Cell Stem Cell* 2011;9(2):144-155. doi:10.1016/j.stem.2011.06.015.
88. Armstrong L, Hughes O, Yung S, et al. The role of PI3K/AKT, MAPK/ERK and NFκβ signalling in the maintenance of human embryonic stem cell pluripotency and viability highlighted by transcriptional profiling and functional analysis. *Hum. Mol. Genet.* 2006;15(11):1894-1913. doi:10.1093/hmg/ddl112.
89. Sakaki-Yumoto M, Katsuno Y, Derynck R. TGF-β family signaling in stem cells. *Biochim. Biophys. Acta* 2013;1830(2):2280-2296. doi:10.1016/j.bbagen.2012.08.008.
90. Guo X, Wang X-F. Signaling cross-talk between TGF-β/BMP and other pathways. *Cell Res.* 2009;19(1):71-88. doi:10.1038/cr.2008.302.
91. Brown S, Teo A, Pauklin S, et al. Activin/Nodal signaling controls divergent transcriptional networks in human embryonic stem cells and in endoderm progenitors. *Stem Cells* 2011;29(8):1176-1185. doi:10.1002/stem.666.

92. Pauklin S, Vallier L. Activin/Nodal signalling in stem cells. *Development* 2015;142(4):607-19. doi:10.1242/dev.091769.
93. Izumi N, Era T, Akimaru H, Yasunaga M, Nishikawa S-I. Dissecting the molecular hierarchy for mesendoderm differentiation through a combination of embryonic stem cell culture and RNA interference. *Stem Cells* 2007;25(7):1664-1674. doi:10.1634/stemcells.2006-0681.
94. Li Z, Chen Y-G. Functions of BMP signaling in embryonic stem cell fate determination. *Exp. Cell Res.* 2012;319(2):113-119. doi:10.1016/j.yexcr.2012.09.016.
95. Wang Z, Oron E, Nelson B, Razis S, Ivanova N. Distinct lineage specification roles for NANOG, OCT4, and SOX2 in human embryonic stem cells. *Cell Stem Cell* 2012;10(4):440-454. doi:10.1016/j.stem.2012.02.016.
96. Teo AKK, Ali Y, Wong KY, et al. Activin and BMP4 synergistically promote formation of definitive endoderm in human embryonic stem cells. *Stem Cells* 2012;30(4):631-642. doi:10.1002/stem.1022.
97. Sumi T, Tsuneyoshi N, Nakatsuji N, Suemori H. Defining early lineage specification of human embryonic stem cells by the orchestrated balance of canonical Wnt/beta-catenin, Activin/Nodal and BMP signaling. *Development* 2008;135(17):2969-2979. doi:10.1242/dev.021121.
98. Faial T, Bernardo AS, Mendjan S, et al. Brachyury and SMAD signalling collaboratively orchestrate distinct mesoderm and endoderm gene regulatory networks in differentiating human embryonic stem cells. *Development* 2015;142(12):2121-35. doi:10.1242/dev.117838.
99. MacDonald BT, Tamai K, He X. Wnt/β-Catenin Signaling: Components, Mechanisms, and Diseases. *Dev. Cell* 2009;17(1):9-26. doi:10.1016/j.devcel.2009.06.016.
100. Rao TP, Kühl M. An updated overview on Wnt signaling pathways: A prelude for more. *Circ. Res.* 2010;106(12):1798-1806. doi:10.1161/CIRCRESAHA.110.219840.
101. Clevers H, Nusse R. Wnt/β-catenin signaling and disease. *Cell* 2012;149(6):1192-1205. doi:10.1016/j.cell.2012.05.012.
102. McNeill H, Woodgett JR. When pathways collide: collaboration and connivance among signalling proteins in development. *Nat. Rev. Mol. Cell Biol.* 2010;11(6):404-413. doi:10.1038/nrm2902.
103. Nusse R, Nusse R. Wnt signaling in disease and in development. *Cell Res.* 2005;15(1):28-32. doi:10.1038/sj.cr.7290260.
104. Sugimura R, Li L. Noncanonical Wnt signaling in vertebrate development, stem cells, and diseases. *Birth Defects Res. Part C - Embryo Today Rev.* 2010;90(4):243-256. doi:10.1002/bdrc.20195.
105. Barker N. The Canonical Wnt/b-Catenin Signalling Pathway. In: *Wnt Signaling, Volume I: Pathway Methods and Mammalian Models*.Vol 468.; 2008:5-15. doi:10.1007/978-1-59745-249-6.
106. Veeman MT, Axelrod JD, Moon RT. A second canon: Functions and mechanisms of β-catenin-independent Wnt signaling. *Dev. Cell* 2003;5(3):367-377. doi:10.1016/S1534-5807(03)00266-1.
107. Kikuchi A. Roles of axin in the Wnt signalling pathway. *Cell. Signal.* 1999;11(11):777-788. doi:10.1016/S0898-6568(99)00054-6.
108. Nusse R, Fuerer C, Ching W, et al. Wnt signaling and stem cell control. In: *Cold Spring Harbor Symposia on Quantitative Biology*.Vol 73.; 2008:59-66. doi:10.1101/sqb.2008.73.035.
109. Miki T, Yasuda S, Kahn M. Wnt/β-catenin signaling in embryonic stem cell self-renewal and somatic cell reprogramming. *Stem Cell Rev.* 2011;7(4):836-46. doi:10.1007/s12015-011-9275-1.
110. Bilic J, Huang Y-L, Davidson G, et al. Wnt induces LRP6 signalosomes and promotes dishevelled-dependent LRP6 phosphorylation. *Science*

2007;316(5831):1619-1622. doi:10.1126/science.1137065.
111. Kim S-E, Huang H, Zhao M, et al. Wnt Stabilization of β-Catenin Reveals Principles for Morphogen Receptor-Scaffold Assemblies. *Science (80-.).* 2013;340(6134):867-870. doi:10.1126/science.1232389.
112. Willert K, Shibamoto S, Nusse R. Wnt-induced dephosphorylation of Axin releases β-catenin from the Axin complex. *Genes Dev.* 1999;13(14):1768-1773. doi:10.1101/gad.13.14.1768.
113. Kockeritz L, Doble B, Patel S, Woodgett JR. Glycogen synthase kinase-3--an overview of an over-achieving protein kinase. *Curr. Drug Targets* 2006;7(11):1377-88.
114. Frame S, Cohen P. GSK3 takes centre stage more than 20 years after its discovery. *Biochem. J.* 2001;359(1):1-16. doi:10.1042/bj3590001.
115. Rayasam GV, Tulasi VK, Sodhi R, Davis JA, Ray A. Glycogen synthase kinase 3: More than a namesake. *Br. J. Pharmacol.* 2009;156(6):885-898. doi:10.1111/j.1476-5381.2008.00085.x.
116. Wagner FF, Bishop JA, Gale JP, et al. Inhibitors of Glycogen Synthase Kinase 3 with Exquisite Kinome-Wide Selectivity and Their Functional Effects. *ACS Chem. Biol.* 2016;11(7):1952-1963. doi:10.1021/acschembio.6b00306.
117. Cohen P, Goedert M. GSK3 inhibitors: development and therapeutic potential. *Nat. Rev. Drug Discov.* 2004;3(6):479-487. doi:10.1038/nrd1415.
118. Woodgett JR. Judging a Protein by More Than Its Name: GSK-3. *Sci. Signal.* 2001;2001(100):re12-re12. doi:10.1126/stke.2001.100.re12.
119. Cohen P, Frame S. The renaissance of GSK3. *Nat. Rev. Mol. Cell Biol.* 2001;2(10):769-776. doi:10.1038/35096075.
120. Ng SS, Mahmoudi T, Danenberg E, et al. Phosphatidylinositol 3-kinase signaling does not activate the Wnt cascade. *J. Biol. Chem.* 2009;284(51):35308-35313. doi:10.1074/jbc.M109.078261.
121. Ding VW, Chen RH, McCormick F. Differential regulation of glycogen synthase kinase 3β by insulin and Wnt signaling. *J. Biol. Chem.* 2000;275(42):32475-81. doi:10.1074/jbc.M005342200.
122. Doble BW, Patel S, Wood GA, Kockeritz LK, Woodgett JR. Functional Redundancy of GSK-3α and GSK-3β in Wnt/β-Catenin Signaling Shown by Using an Allelic Series of Embryonic Stem Cell Lines. *Dev. Cell* 2007;12(6):957-971. doi:10.1016/j.devcel.2007.04.001.
123. Sato N, Meijer L, Skaltsounis L, Greengard P, Brivanlou AH. Maintenance of pluripotency in human and mouse embryonic stem cells through activation of Wnt signaling by a pharmacological GSK-3-specific inhibitor. *Nat. Med.* 2004;10(1):55-63. doi:10.1038/nm979.
124. Dravid G, Ye Z, Hammond H, et al. Defining the role of Wnt/beta-catenin signaling in the survival, proliferation, and self-renewal of human embryonic stem cells. *Stem Cells* 2005;23(10):1489-501. doi:10.1634/stemcells.2005-0034.
125. Lyashenko N, Winter M, Migliorini D, Biechele T, Moon RT, Hartmann C. Differential requirement for the dual functions of β-catenin in embryonic stem cell self-renewal and germ layer formation. *Nat. Cell Biol.* 2011;13(7):753-61. doi:10.1038/ncb2260.
126. Siller R, Greenhough S, Naumovska E, Sullivan GJ. Small-molecule-driven hepatocyte differentiation of human pluripotent stem cells. *Stem Cell Reports* 2015;4(5):939-952. doi:10.1016/j.stemcr.2015.04.001.
127. Tahamtani Y, Azarnia M, Farrokhi A, Sharifi-Zarchi A, Aghdami N, Baharvand H. Treatment of human embryonic stem cells with different combinations of priming and inducing factors toward definitive endoderm. *Stem Cells Dev.* 2013;22(9):1419-1432.
128. Ying Q-L, Wray J, Nichols J, et al. The ground state of embryonic stem cell self-renewal. *Nature* 2008;453(7194):519-523. doi:10.1038/nature06968.

129. Voskas D, Ling LS, Woodgett JR. Does GSK-3 provide a shortcut for PI3K activation of Wnt signalling? *F1000 Biol. Rep.* 2010;2(November):82. doi:10.3410/B2-82.
130. Wu D, Pan W. GSK3: a multifaceted kinase in Wnt signaling. *Trends Biochem. Sci.* 2010;35(3):161-168. doi:10.1016/j.tibs.2009.10.002.
131. Zeng X, Tamai K, Doble B, et al. A dual-kinase mechanism for Wnt co-receptor phosphorylation and activation. *Nature* 2005;438(7069):873-877. doi:10.1038/nature04185.
132. Zeng X, Huang H, Tamai K, et al. Initiation of Wnt signaling: control of Wnt coreceptor LRP6 phosphorylation/activation via Frizzled, Dishevelled and Axin functions. *Development* 2008;135(2):367-375. doi:10.1242/dev.013540.
133. Metcalfe C, Bienz M. Inhibition of GSK3 by Wnt signalling - two contrasting models. *J. Cell Sci.* 2011;124(21):3537-3544. doi:10.1242/jcs.091991.
134. Vinyoles M, DelValle-Pérez B, Curto J, et al. Multivesicular GSK3 Sequestration upon Wnt Signaling Is Controlled by p120-Catenin/Cadherin Interaction with LRP5/6. *Mol. Cell* 2014;53(3):444-457. doi:10.1016/j.molcel.2013.12.010.
135. Taelman VF, Dobrowolski R, Plouhinec JL, et al. Wnt signaling requires sequestration of Glycogen Synthase Kinase 3 inside multivesicular endosomes. *Cell* 2010;143(7):1136-1148. doi:10.1016/j.cell.2010.11.034.
136. Haikarainen T, Lehtio SK and L. Tankyrases: Structure, Function and Therapeutic Implications in Cancer. *Curr. Pharm. Des.* 2014;20(41):6472-6488. doi:http://dx.doi.org/10.2174/1381612820666140630101525.
137. Lee E, Salic A, Krüger R, Heinrich R, Kirschner MW. The roles of APC and axin derived from experimental and theoretical analysis of the Wnt pathway. *PLoS Biol.* 2003;1(1). doi:10.1371/journal.pbio.0000010.
138. Salic a, Lee E, Mayer L, Kirschner MW. Control of β-catenin stability: reconstitution of the cytoplasmic steps of the Wnt pathway in Xenopus egg extracts. *Mol. Cell* 2000;5(3):523-532. doi:10.1016/S1097-2765(00)80446-3.
139. Nakamura T, Hamada F, Ishidate T, et al. Axin, an inhibitor of the Wnt signalling pathway, interacts with β-catenin, GSK-3β and APC and reduces the β-catenin level. *Genes Cells* 1998;3(6):395-403. doi:10.1046/j.1365-2443.1998.00198.x.
140. Voronkov A, Krauss S. Wnt/β-catenin signaling and small molecule inhibitors. *Curr. Pharm. Des.* 2013;19(4):634-64. doi:10.2174/138161213804581837.
141. Chia I V, Costantini F. Mouse Axin and Axin2 / Conductin Proteins Are Functionally Equivalent In Vivo Mouse Axin and Axin2 / Conductin Proteins Are Functionally Equivalent In Vivo. *Mol. Cell. Biol.* 2005;25(11). doi:10.1128/MCB.25.11.4371–4376.2005.
142. Salahshor S, Woodgett JR. The links between axin and carcinogenesis. *J. Clin. Pathol.* 2005;58(3):225-36. doi:10.1136/jcp.2003.009506.
143. Figeac N, Zammit PS. Coordinated action of Axin1 and Axin2 suppresses β-catenin to regulate muscle stem cell function. *Cell. Signal.* 2015;27(8):1652-1665. doi:10.1016/j.cellsig.2015.03.025.
144. Liu W, Dong X, Mai M, et al. Mutations in AXIN2 cause colorectal cancer with defective mismatch repair by activating β-catenin/TCF signalling. *Nat. Genet.* 2000;26(2):146-147. doi:10.1038/79859.
145. Xie R, Jiang R, Chen D. Generation of Axin1 conditional mutant mice. *Genesis* 2011;49(2):98-102. doi:10.1002/dvg.20703.
146. Yu H-MI, Jerchow B, Sheu T-J, et al. The role of Axin2 in calvarial morphogenesis and craniosynostosis. *Development* 2005;132(8):1995-2005. doi:10.1242/dev.01786.
147. Qian L, Mahaffey JP, Alcorn HL, Anderson K V. Tissue-specific roles of Axin2 in the inhibition and activation of Wnt signaling in the mouse embryo. *Proc. Natl. Acad. Sci. U. S. A.* 2011;108(21):8692-7. doi:10.1073/pnas.1100328108.

148. Lustig B, Jerchow B, Sachs M, et al. Negative Feedback Loop of Wnt Signaling through Upregulation of Conductin/Axin2 in Colorectal and Liver Tumors. *Mol. Cell. Biol.* 2002;22(4):1184-1193. doi:10.1128/MCB.22.4.1184-1193.2002.
149. Bernkopf DB, Hadjihannas M V, Behrens J. Negative-feedback regulation of the Wnt pathway by conductin/axin2 involves insensitivity to upstream signalling. *J. Cell Sci.* 2015;128(1):33-9. doi:10.1242/jcs.159145.
150. Huang S-M a, Mishina YM, Liu S, et al. Tankyrase inhibition stabilizes axin and antagonizes Wnt signalling. *Nature* 2009;461(7264):614-620. doi:10.1038/nature08356.
151. Smith S, Giriat I, Schmitt A, de Lange T. Tankyrase, a poly(ADP-ribose) polymerase at human telomeres. *Science* 1998;282(5393):1484-7. doi:10.1126/science.282.5393.1484.
152. Hottiger MO, Hassa PO, Lüscher B, Schüler H, Koch-Nolte F. Toward a unified nomenclature for mammalian ADP-ribosyltransferases. *Trends Biochem. Sci.* 2010;35(4):208-219. doi:10.1016/j.tibs.2009.12.003.
153. Chiang YJ, Hsiao SJ, Yver D, et al. Tankyrase 1 and tankyrase 2 are essential but redundant for mouse embryonic development. *PLoS One* 2008;3(7). doi:10.1371/journal.pone.0002639.
154. Waaler J, Machon O, Tumova L, et al. A novel tankyrase inhibitor decreases canonical Wnt signaling in colon carcinoma cells and reduces tumor growth in conditional APC mutant mice. *Cancer Res.* 2012;72(11):2822-2832. doi:10.1158/0008-5472.CAN-11-3336.
155. Fearon ER. PARsing the Phrase “All in for Axin”- Wnt Pathway Targets in Cancer. *Cancer Cell* 2009;16(5):366-368. doi:10.1016/j.ccr.2009.10.007.
156. Zhang Y, Liu S, Mickanin C, et al. RNF146 is a poly(ADP-ribose)-directed E3 ligase that regulates axin degradation and Wnt signalling. *Nat. Cell Biol.* 2011;13(5):623-9. doi:10.1038/ncb2222.
157. Callow MG, Tran H, Phu L, et al. Ubiquitin ligase RNF146 regulates tankyrase and Axin to promote Wnt signaling. *PLoS One* 2011;6(7). doi:10.1371/journal.pone.0022595.
158. Bao R, Christova T, Song S, Angers S, Yan X, Attisano L. Inhibition of Tankyrases Induces Axin Stabilization and Blocks Wnt Signalling in Breast Cancer Cells. *PLoS One* 2012;7(11). doi:10.1371/journal.pone.0048670.
159. Waaler J, Machon O, von Kries JP, et al. Novel Synthetic Antagonists of Canonical Wnt Signaling Inhibit Colorectal Cancer Cell Growth. *Cancer Res.* 2011;71(1):197-205. doi:10.1158/0008-5472.Can-10-1282.
160. Waaler J (Faculty of medicine/University of O. Development of specific Tankyrase inhibitors for attenuating canonical WNT/β-catenin signaling. 2013.
161. Okada-Iwasaki R, Takahashi Y, Watanabe Y, et al. The Discovery and Characterization of K-756, a Novel Wnt/β-Catenin Pathway Inhibitor Targeting Tankyrase. *Mol. Cancer Ther.* 2016;15(7):1525 LP-1534.
162. Yang E, Tacchelly-Benites O, Wang Z, et al. Wnt pathway activation by ADP-ribosylation. *Nat. Commun.* 2016;7:11430. doi:10.1038/ncomms11430.
163. Song X, Wang S, Li L. New insights into the regulation of Axin function in canonical Wnt signaling pathway. *Protein Cell* 2014;5(3):186-93. doi:10.1007/s13238-014-0019-2.
164. Kahn BB, Alquier T, Carling D, Hardie DG. AMP-activated protein kinase: Ancient energy gauge provides clues to modern understanding of metabolism. *Cell Metab.* 2005;1(1):15-25. doi:10.1016/j.cmet.2004.12.003.
165. Hardie DG, Ross F a., Hawley S a. AMPK: a nutrient and energy sensor that maintains energy homeostasis. *Nat. Rev. Mol. Cell Biol.* 2012;13(4):251-262. doi:10.1038/nrm3311.
166. Carling D, Thornton C, Woods A, Sanders MJ. AMP-activated protein kinase: new regulation, new roles? *Biochem. J.* 2012;445(1):11-27.

doi:10.1042/BJ20120546.
167. Inoki K, Ouyang H, Zhu T, et al. TSC2 Integrates Wnt and Energy Signals via a Coordinated Phosphorylation by AMPK and GSK3 to Regulate Cell Growth. *Cell* 2006;126(5):955-968. doi:10.1016/j.cell.2006.06.055.
168. Ochocki JD, Simon MC. Nutrient-sensing pathways and metabolic regulation in stem cells. *J. Cell Biol.* 2013;203(1):23-33. doi:10.1083/jcb.201303110.
169. Teslaa T, Teitell MA. Pluripotent stem cell energy metabolism: an update. *EMBO J.* 2015;34(2):138-53. doi:10.15252/embj.201490446.
170. Zhang YL, Guo H, Zhang CS, et al. AMP as a low-energy charge signal autonomously initiates assembly of axin- AMPK-LKB1 complex for AMPK activation. *Cell Metab.* 2013;18(4):546-555. doi:10.1016/j.cmet.2013.09.005.
171. Shimobayashi M, Hall MN. Making new contacts: the mTOR network in metabolism and signalling crosstalk. *Nat. Rev. Mol. Cell Biol.* 2014;15(3):155-62. doi:10.1038/nrm3757.
172. Inoki K, Li Y, Zhu T, Wu J, Guan K-L. TSC2 is phosphorylated and inhibited by Akt and suppresses mTOR signalling. *Nat. Cell Biol.* 2002;4(9):648-57. doi:10.1038/ncb839.
173. Zhao J, Yue W, Zhu MJ, Sreejayan N, Du M. AMP-activated protein kinase (AMPK) cross-talks with canonical Wnt signaling via phosphorylation of β-catenin at Ser 552. *Biochem. Biophys. Res. Commun.* 2010;395(1):146-151. doi:10.1016/j.bbrc.2010.03.161.
174. Faubert B, Boily G, Izreig S, et al. AMPK Is a Negative Regulator of the Warburg Effect and Suppresses Tumor Growth In Vivo. *Cell Metab.* 2012;17(1):113-124. doi:10.1016/j.cmet.2012.12.001.
175. Reznick RM, Shulman GI. The role of AMP-activated protein kinase in mitochondrial biogenesis. *J. Physiol.* 2006;574(Pt 1):33-9. doi:10.1113/jphysiol.2006.109512.
176. Ito K, Suda T. Metabolic requirements for the maintenance of self-renewing stem cells. *Nat. Rev. Mol. Cell Biol.* 2014;15(4):243-56. doi:10.1038/nrm3772.
177. Vazquez-Martin A, Vellon L, Quirós PM, et al. Activation of AMP-activated protein kinase (AMPK) provides a metabolic barrier to reprogramming somatic cells into stem cells. *Cell Cycle* 2012;11(5):974-89. doi:10.4161/cc.11.5.19450.
178. Mizushima N, Levine B. Autophagy in mammalian development and differentiation. *Nat Cell Biol* 2010;12(9):823-830. doi:10.1038/ncb0910-823.
179. Kim J, Kundu M, Viollet B, Guan K-L. AMPK and mTOR regulate autophagy through direct phosphorylation of ULK1. *Nat. Cell Biol.* 2011;13(2):132-41. doi:10.1038/ncb2152.
180. Zhou J, Su P, Wang L, et al. mTOR supports long-term self-renewal and suppresses mesoderm and endoderm activities of human embryonic stem cells. *Proc. Natl. Acad. Sci. U. S. A.* 2009;106(19):7840-7845. doi:10.1073/pnas.0901854106.
181. Yu JSL, Cui W. Proliferation, survival and metabolism: the role of PI3K/AKT/mTOR signalling in pluripotency and cell fate determination. *Development* 2016;143(17):3050 LP-3060.
182. Yu JSL, Ramasamy TS, Murphy N, et al. PI3K/mTORC2 regulates TGF-β/Activin signalling by modulating Smad2/3 activity via linker phosphorylation. *Nat. Commun.* 2015;6:7212. doi:10.1038/ncomms8212.
183. Mathapati S, Siller R, Impellizzeri AAR, et al. Small-Molecule-Directed Hepatocyte-Like Cell Differentiation of Human Pluripotent Stem Cells. *Curr. Protoc. Stem Cell Biol.* 2016. doi:10.1002/cpsc.13.
184. Watanabe K, Ueno M, Kamiya D, et al. A ROCK inhibitor permits survival of dissociated human embryonic stem cells. *Nat. Biotechnol.* 2007;25(6):681-6. doi:10.1038/nbt1310.
185. Technologies L. TRIzol® Reagent. *Prod. Man.* 2010. Available at: https://tools.thermofisher.com/content/sfs/manuals/trizol_reagent.pdf.

186. Pfaffl MW. Relative quantification. *Real-time PCR* 2004:63-82. doi:10.1186/1756-6614-3-5.
187. Livak KJ, Schmittgen TD. Analysis of relative gene expression data using real-time quantitative PCR and the 2(-Delta Delta C(T)) Method. *Methods* 2001;25(4):402-8. doi:10.1006/meth.2001.1262.
188. Ström S, Holm F, Bergström R, Strömberg AM, Hovatta O. Derivation of 30 human embryonic stem cell lines-improving the quality. *Vitr. Cell. Dev. Biol. - Anim.* 2010;46(3-4):337-344. doi:10.1007/s11626-010-9308-0.
189. Engert S, Burtscher I, Liao WP, Dulev S, Schotta G, Lickert H. Wnt/β-catenin signalling regulates Sox17 expression and is essential for organizer and endoderm formation in the mouse. *Development* 2013;140(15):3128 LP-3138. Available at: http://dev.biologists.org/content/140/15/3128.abstract.
190. Viotti M, Nowotschin S, Hadjantonakis A-K. SOX17 links gut endoderm morphogenesis and germ layer segregation. *Nat. Cell Biol.* 2014;16(12):1146-1156. doi:10.1038/ncb3070.
191. Shi Y, Paluch BE, Wang X, Jiang X. PTEN at a Glance. *J. Cell Sci.* 2012;125(20):4687 LP-4692.
192. Copps KD, White MF. Regulation of insulin sensitivity by serine/threonine phosphorylation of insulin receptor substrate proteins IRS1 and IRS2. *Diabetologia* 2012;55(10):2565-2582. doi:10.1007/s00125-012-2644-8.
193. Pruett W, Yuan Y, Rose E, Batzer a G, Harada N, Skolnik EY. Association between GRB2/Sos and insulin receptor substrate 1 is not sufficient for activation of extracellular signal-regulated kinases by interleukin-4: implications for Ras activation by insulin. *Mol. Cell. Biol.* 1995;15(3):1778-1785.
194. Huang T-S, Li L, Moalim-Nour a L, et al. A Regulatory Network Involving b-Catenin, E-Cadherin, PI3K/Akt, and Slug Balances Self-Renewal and Differentiation of Human Pluripotent Stem Cells in Response to Wnt Signaling. *Stem Cells* 2015;33:1419–1433. doi:10.1002/stem.1334.
195. Adams MM, Ainslie GR, Ambrósio AF, et al. *List of Contributors BT - Molecules to Medicine with mTOR*. Boston: Academic Press; 2016. doi:http://dx.doi.org/10.1016/B978-0-12-802733-2.00035-9.
196. Gu L, Xie L, Zuo C, et al. Targeting mTOR/p70S6K/glycolysis signaling pathway restores glucocorticoid sensitivity to 4E-BP1 null Burkitt Lymphoma. *BMC Cancer* 2015;15:529. doi:10.1186/s12885-015-1535-z.
197. Demagny H, Araki T, De Robertis EM. The Tumor Suppressor Smad4/DPC4 Is Regulated by Phosphorylations that Integrate FGF, Wnt, and TGF-β; Signaling. *Cell Rep.* 2014;9(2):688-700. doi:10.1016/j.celrep.2014.09.020.
198. Ding Q, Xia W, Liu JC, et al. Erk associates with and primes GSK-3β for its inactivation resulting in upregulation of β-catenin. *Mol. Cell* 2005;19(2):159-170. doi:10.1016/j.molcel.2005.06.009.
199. Aslaksen S. Investigation of the WNT and AKT/mTOR signaling pathways in early differentiation in embryonic stem cells . 2016.
200. Willert K, Jones KA. Wnt signaling: Is the party in the nucleus? *Genes Dev.* 2006;20(11):1394-1404. doi:10.1101/gad.1424006.
201. Schmitz Y, Rateitschak K, Wolkenhauer O. Analysing the impact of nucleo-cytoplasmic shuttling of β-catenin and its antagonists APC, Axin and GSK3 on Wnt/β-catenin signalling. *Cell. Signal.* 2013;25(11):2210-2221. doi:10.1016/j.cellsig.2013.07.005.
202. Rennoll SA, Konsavage WM, Yochum GS. Nuclear AXIN2 represses MYC gene expression. *Biochem. Biophys. Res. Commun.* 2014;443(1):217-222. doi:10.1016/j.bbrc.2013.11.089.
203. Smith K, Dalton S. Myc transcription factors: key regulators behind establishment and maintenance of pluripotency. *Regen. Med.* 2010;5(6):947-59. doi:10.2217/rme.10.79.
204. Bouchard C, Staller P, Eilers M. Control of cell proliferation by Myc. *Trends*

Cell Biol. 1998;8(5):202-206.
205. Schmidt E V. The role of c-myc in cellular growth control. *Oncogene* 1999;18(19):2988-2996. doi:10.1038/sj.onc.1202751.
206. Hofmann JW, Zhao X, De Cecco M, et al. Reduced expression of MYC increases longevity and enhances healthspan. *Cell* 2015;160(3):477-488. doi:10.1016/j.cell.2014.12.016.
207. Turner D a, Rué P, Mackenzie JP, Davies E, Martinez Arias A. Brachyury cooperates with Wnt/β-catenin signalling to elicit primitive-streak-like behaviour in differentiating mouse embryonic stem cells. *BMC Biol.* 2014;12:63. doi:10.1186/s12915-014-0063-7.
208. Lim J, Thiery JP. Epithelial-mesenchymal transitions: insights from development. *Development* 2012;139(19):3471-3486. doi:10.1242/dev.071209.
209. Voiculescu O, Bodenstein L, Jun IL, Stern CD. Local cell interactions and self-amplifying individual cell ingression drive amniote gastrulation. *Elife* 2014;2014(3). doi:10.7554/eLife.01817.
210. Kim Y-S, Yi B-R, Kim N-H, Choi K-C. Role of the epithelial-mesenchymal transition and its effects on embryonic stem cells. *Exp. Mol. Med.* 2014;46(April):1-5. doi:10.1038/emm.2014.44.
211. Maccario H, Perera NM, Davidson L, Downes CP, Leslie NR. PTEN is destabilized by phosphorylation on Thr366. *Biochem. J.* 2007;405(3):439-44. doi:10.1042/BJ20061837.
212. Al-Khouri AM, Ma Y, Togo SH, Williams S, Mustelin T. Cooperative phosphorylation of the tumor suppressor phosphatase and tensin homologue (PTEN) by casein kinases and glycogen synthase kinase 3β. *J. Biol. Chem.* 2005;280(42):35195-35202. doi:10.1074/jbc.M503045200.
213. Rahdar M, Inoue T, Meyer T, Zhang J, Vazquez F, Devreotes PN. A phosphorylation-dependent intramolecular interaction regulates the membrane association and activity of the tumor suppressor PTEN. *Proc. Natl. Acad. Sci. U. S. A.* 2009;106:480-485. doi:10.1073/pnas.0811212106.
214. Nahuel Villegas S, Rothová M, Barrios-Llerena ME, et al. PI3K/Akt1 signalling specifies foregut precursors by generating regionalized extra-cellular matrix. *Elife* 2013;2013(2). doi:10.7554/eLife.00806.
215. Waraky A, Aleem E, Larsson O. Downregulation of IGF-1 receptor occurs after hepatic linage commitment during hepatocyte differentiation from human embryonic stem cells. *Biochem. Biophys. Res. Commun.* 2016;478(4):1575-1581. doi:http://dx.doi.org/10.1016/j.bbrc.2016.08.157.
216. Georgopoulos NT, Kirkwood L a, Southgate J. A novel bidirectional positive-feedback loop between Wnt-β-catenin and EGFR-ERK plays a role in context-specific modulation of epithelial tissue regeneration. *J. Cell Sci.* 2014;127(Pt 13):2967-82. doi:10.1242/jcs.150888.
217. Zinzalla V, Stracka D, Oppliger W, Hall MN. Activation of mTORC2 by association with the ribosome. *Cell* 2011;144(5):757-768. doi:10.1016/j.cell.2011.02.014.
218. Demagny H, Araki T, De Robertis EM. The Tumor Suppressor Smad4/DPC4 Is Regulated by Phosphorylations that Integrate FGF, Wnt, and TGF-β Signaling. *Cell Rep.* 2016;9(2):688-700. doi:10.1016/j.celrep.2014.09.020.
219. Gross JC, Chaudhary V, Bartscherer K, Boutros M. Active Wnt proteins are secreted on exosomes. *Nat. Cell Biol.* 2012;14(10):1036-1045. doi:10.1038/ncb2574.
220. Ross A, Gericke A. Phosphorylation keeps PTEN phosphatase closed for business. *Proc. Natl. Acad. Sci. U. S. A.* 2009;106(5):1297-8. doi:10.1073/pnas.0812473106.
221. Yanes O, Clark J, Wong DM, et al. Metabolic oxidation regulates embryonic stem cell differentiation. *Nat. Chem. Biol.* 2010;6(6):411-7. doi:10.1038/nchembio.364.

222. Shyh-Chang N, Daley GQ. Metabolic switches linked to pluripotency and embryonic stem cell differentiation. *Cell Metab.* 2015;21(3):349-350. doi:10.1016/j.cmet.2015.02.011.
223. Toren, P. Zoubeidi A. Targeting the PI3K/Akt pathway in prostate cancer: Challenges and opportunities. *Int. J. Oncol.* 2014;45:1793-1801.
224. Mihaylova MM, Shaw RJ. The AMPK signalling pathway coordinates cell growth, autophagy and metabolism. *Nat. Cell Biol.* 2011;13(9):1016-23. doi:10.1038/ncb2329.
225. Shackelford DB, Shaw RJ. The LKB1-AMPK pathway: metabolism and growth control in tumour suppression. *Nat. Rev. Cancer* 2009;9(8):563-575. doi:10.1038/nrc2676.
226. Cell Signaling Technology. AMPK Signaling Pathway. Available at: https://www.cellsignal.com/contents/science-pathway-research-cellular-metabolism/ampk-signaling-pathway/pathways-ampk.

7 APPENDIX

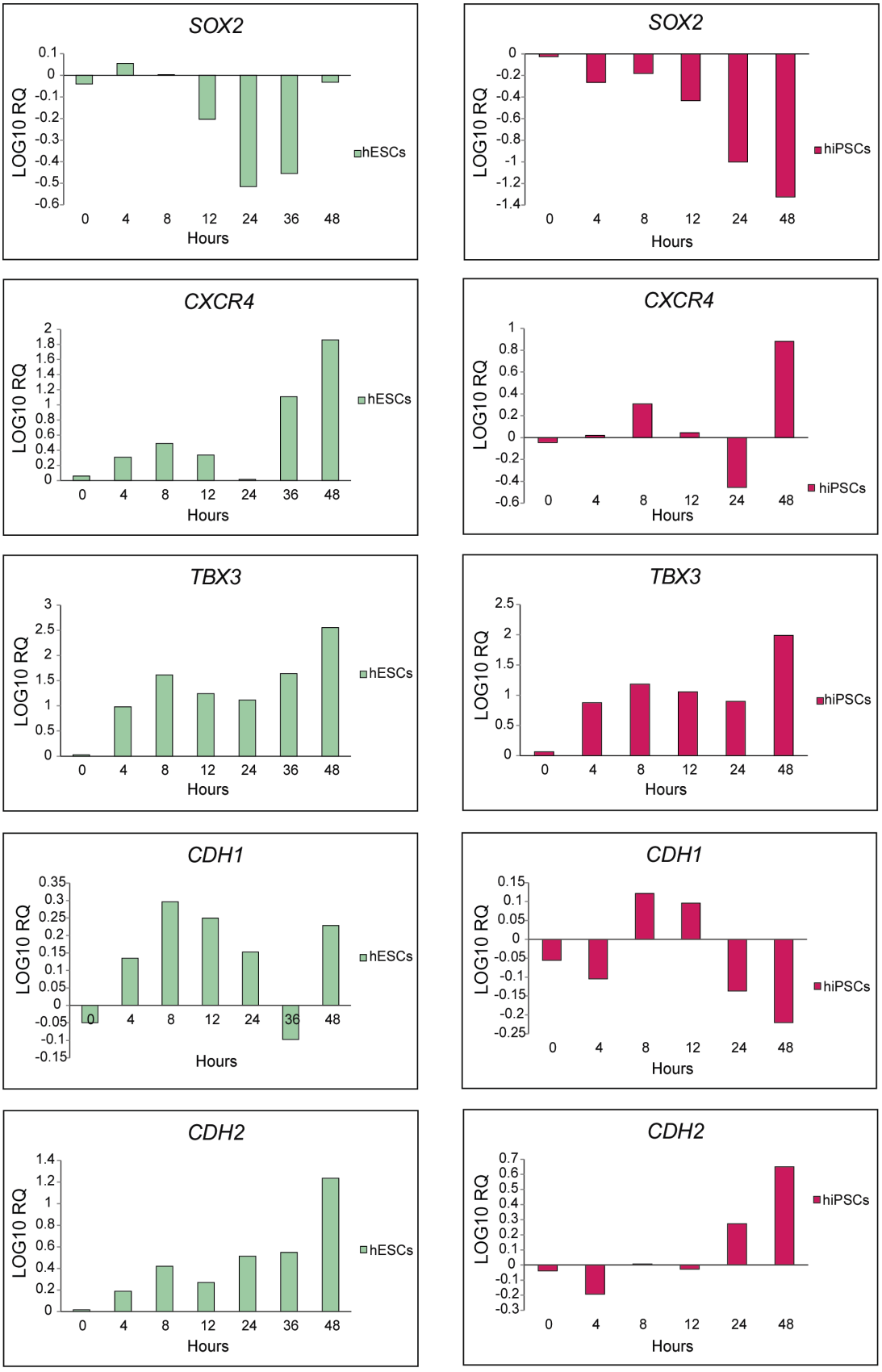

Figure S1. qRT-PCR gene expression analysis. These graphs show gene expression levels for additional gene markers that were analysed in only one biological replicate, (the third time course) for each cell line. The 36 hour time points are included for the H1 cell line. In all of the graphs, gene expression levels are normalized to β-actin expression in undifferentiated hPSCs (0 hours)

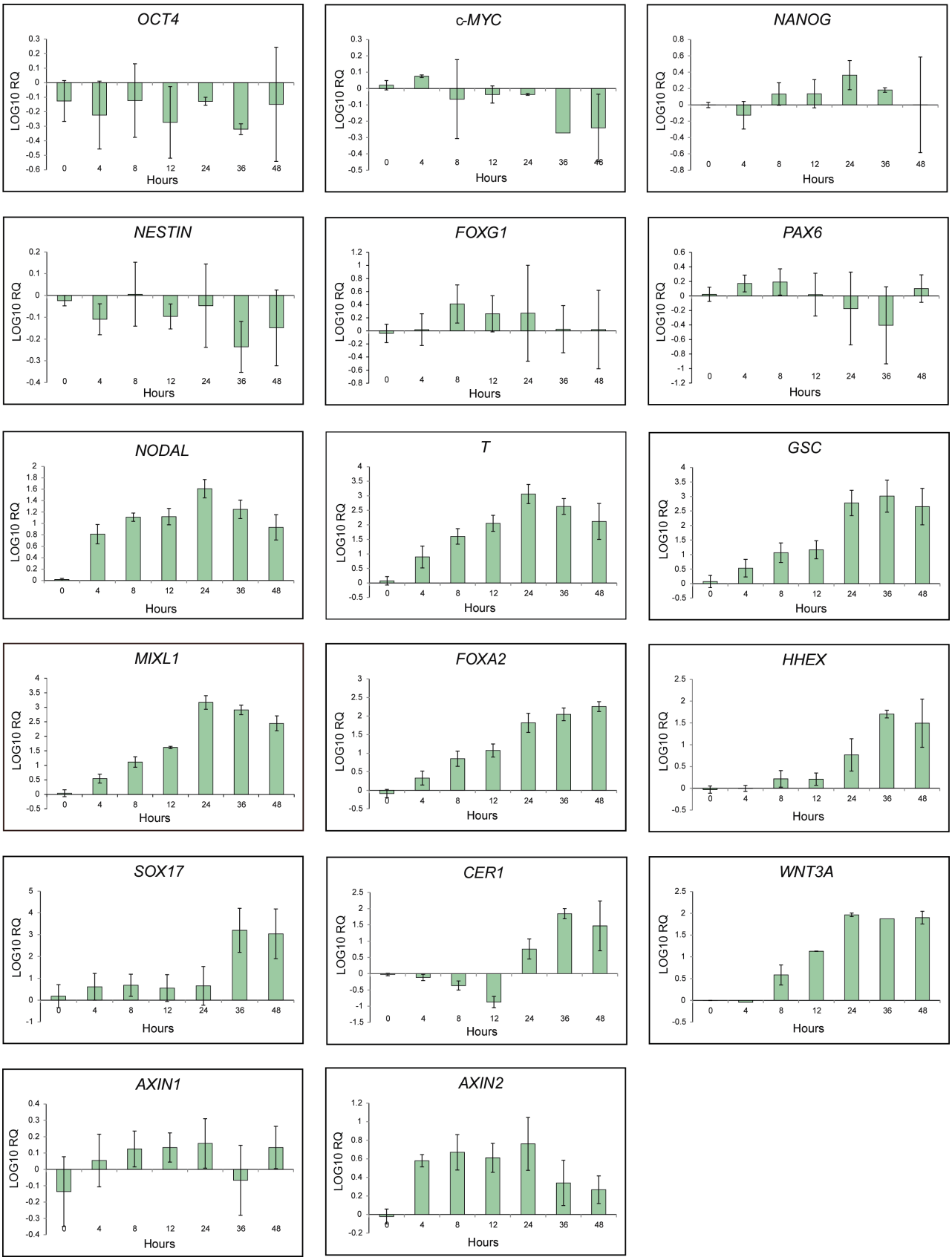

Figure S2. H1 qRT-PCR gene expression analysis with 36 hour time-point: For the last two time course repeats of the H1 (hESC) line we included a 36 hour time point, which was removed from the figures in the main body of the thesis to facilitate comparisons between the two cell lines. The 36 hour time points for *MYC* and *WNT3A* do not have error bars as these genes were only analysed in two time course repeats, one of which (TC-1) lacked a 36H time point. In all of the graphs, gene expression levels are normalized to β-actin expression in undifferentiated

H1 - Wnt/B-Catenin Proteins

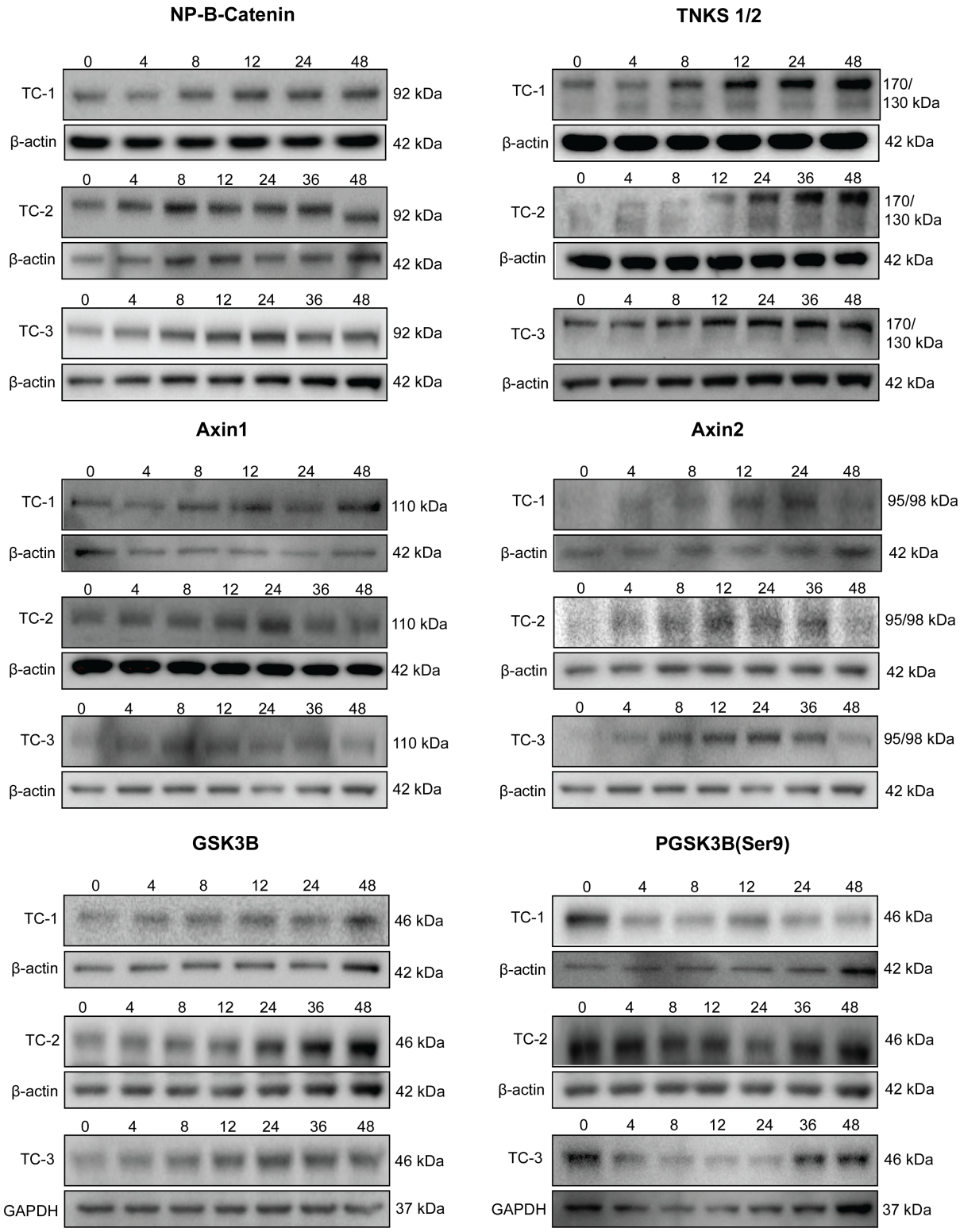

Figure S3. Wnt Pathway protein expression for H1 cell line: The figure shows all western blotting results for NP β-catenin, TNKS1/2, Axin1, Axin2, GSK3β, and p-GSK3β (Ser9) in each biological replicate (time course) of the H1 Cell line. The time course for DE differentiation was repeated in triplicate. For H1 cells, a 36 hour time point was also collected for TC-2 and 3. The abbreviations TC-1, 2, and 3 are used to designate the different time courses. β-actin was used as a loading control

AG Wnt/B-Catenin Proteins

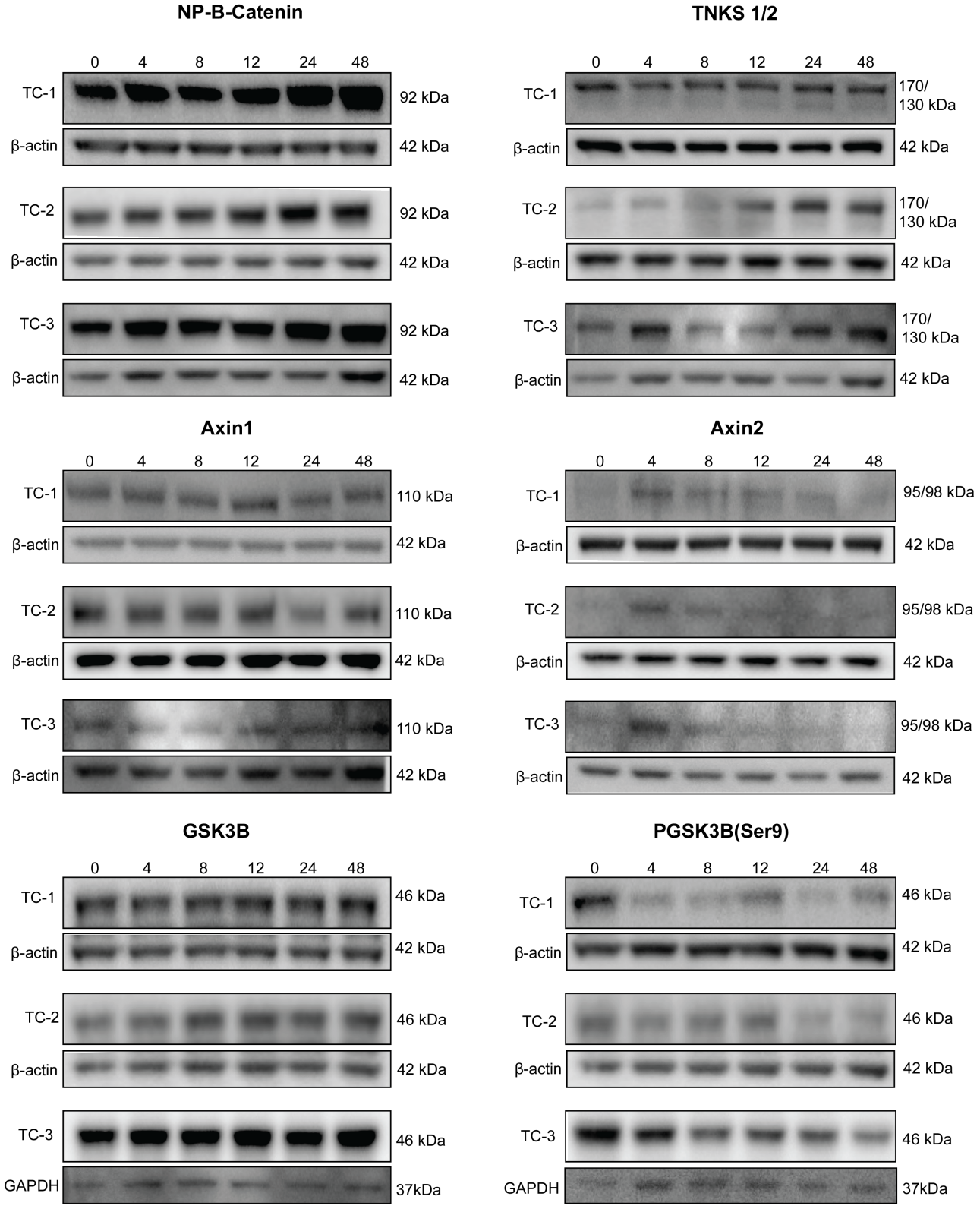

Figure S4. Wnt Pathway Protein Expression for AG-27 Cell Line: The figure shows all western blotting results for NP-β-catenin, TNKS1/2, Axin1, Axin2, GSK3β, and p-GSK3β (Ser9) in each biological replicate (time course) of the AG-27 Cell line. The time course for DE differentiation was repeated in triplicate. The abbreviations TC-1, 2, and 3 are used to designate the different time courses. β-actin or GAPDH were used as loading controls.

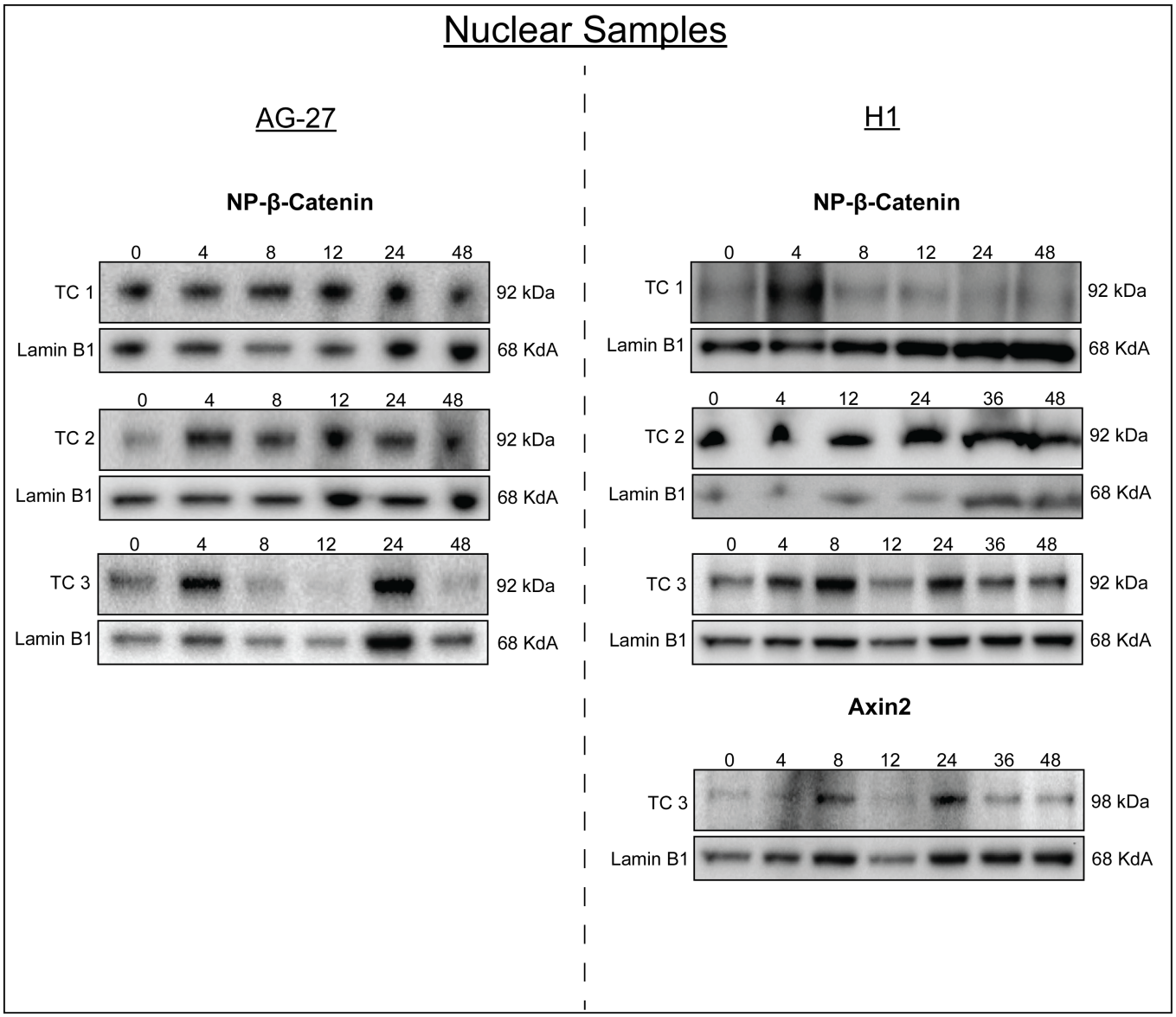

Figure S5. Protein levels of β-catenin and Axin2 in the nuclear fractions: We analysed protein levels of NP-β-catenin and Axin2 in the nuclear lysates for the hiPSC cell line (left) and the hESC cell line (right). Analysis of NP-β-catenin was performed in triplicate (for each time course), Axin2 was however only repeated once, due to time constraints. The low level of Axin2 protein expression at 12 hours is due to loading error, as seen in the Lamin B1 control band.

H1 - mTOR Pathway

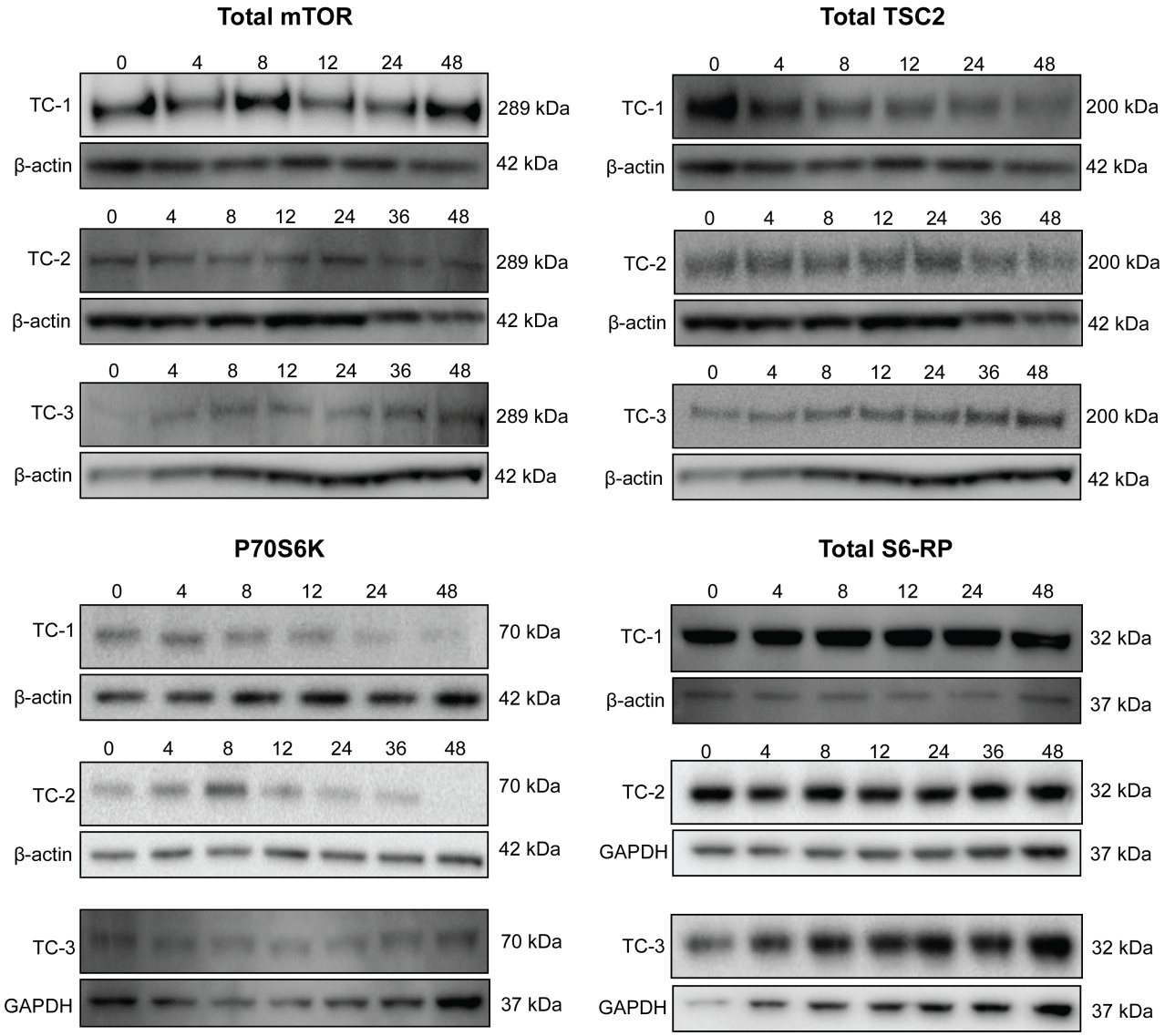

Figure S6. mTOR pathway protein expression for H1 cell line: The figure shows all western blotting results for mTORC, TSC2, p70S6K, and S6-RP in each biological replicate (time course) of the H1 cell line. The time course for DE differentiation was repeated in triplicate. The abbreviations TC-1, 2, and 3 are used to designate the different time courses. For H1 cells, a 36 hour time point was also collected for TC-2 and 3. β-actin and GAPDH were used as loading controls.

AG - mTOR Pathway

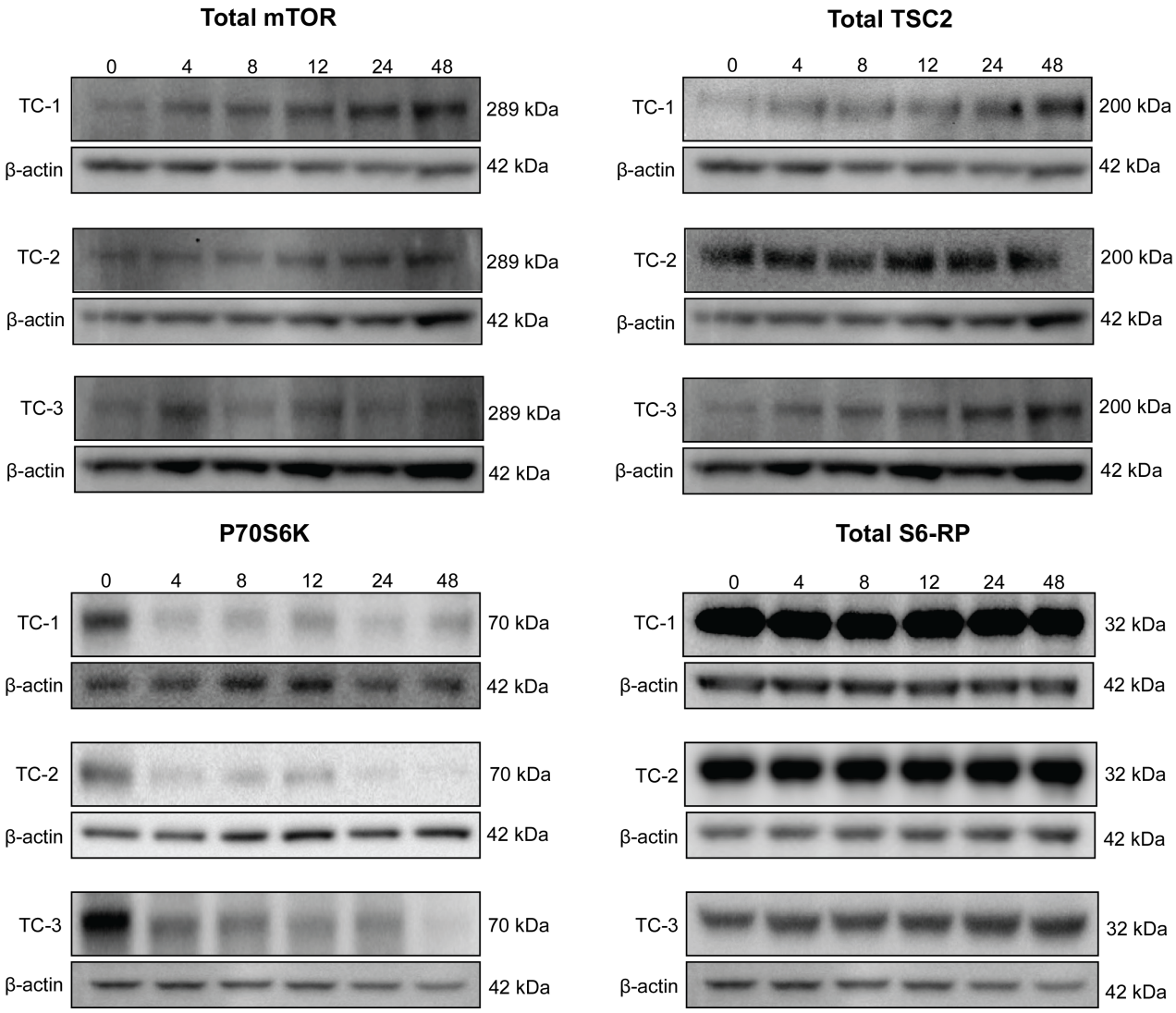

Figure S7. mTOR pathway protein expression for AG-27 cell line: The figure shows all western blotting results for mTORC, TSC2, p70S6K, and S6-RP in each biological replicate (time course) of the AG-27 cell line. The time course for DE differentiation was repeated in triplicate. The abbreviations TC-1, 2, and 3 are used to designate the different time courses. β-actin was used as a loading control.

H1 Akt/AMPK Pathway

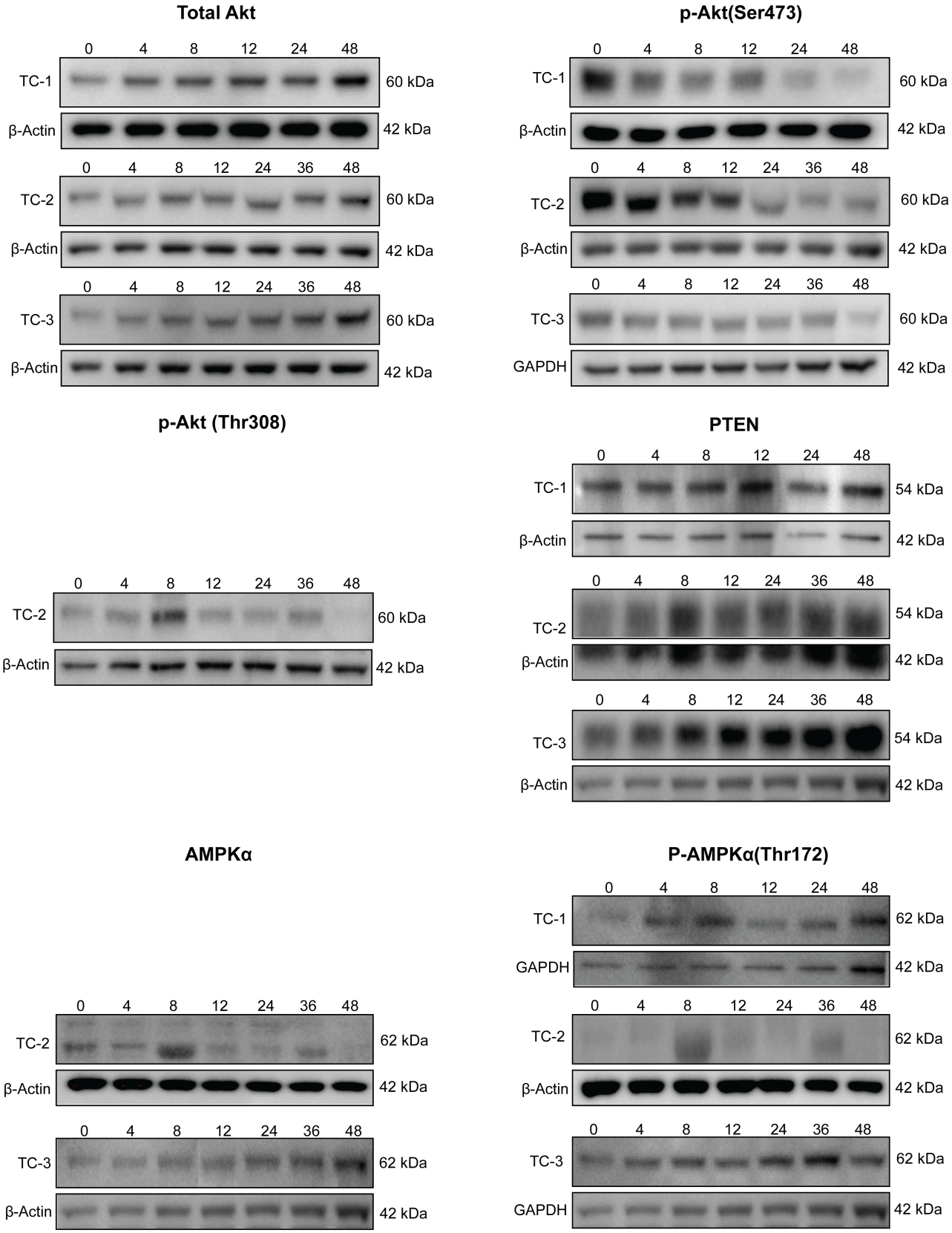

Figure S8. Akt and AMPK pathway protein expression for H1 cell line: The figure shows all western blotting results for for Akt, p-Akt (Ser473), p-Akt (Thr308), PTEN, AMPKa, pAMPKa (Thr172) in each biological replicate (time course) of the H1 cell line. The time course for DE differentiation was repeated in triplicate for each cell line. The abbreviations TC-1, 2, and 3 are used to designate the time courses. For H1 cells, a 36 hour time point was also collected for TC-2 and 3. Western analysis of p-Akt (Thr308) levels could not be completed in time for TC-2 and 3. Nor could AMPKα for TC-1. β-actin and GAPDH were used as loading controls.

AG Akt/AMPK

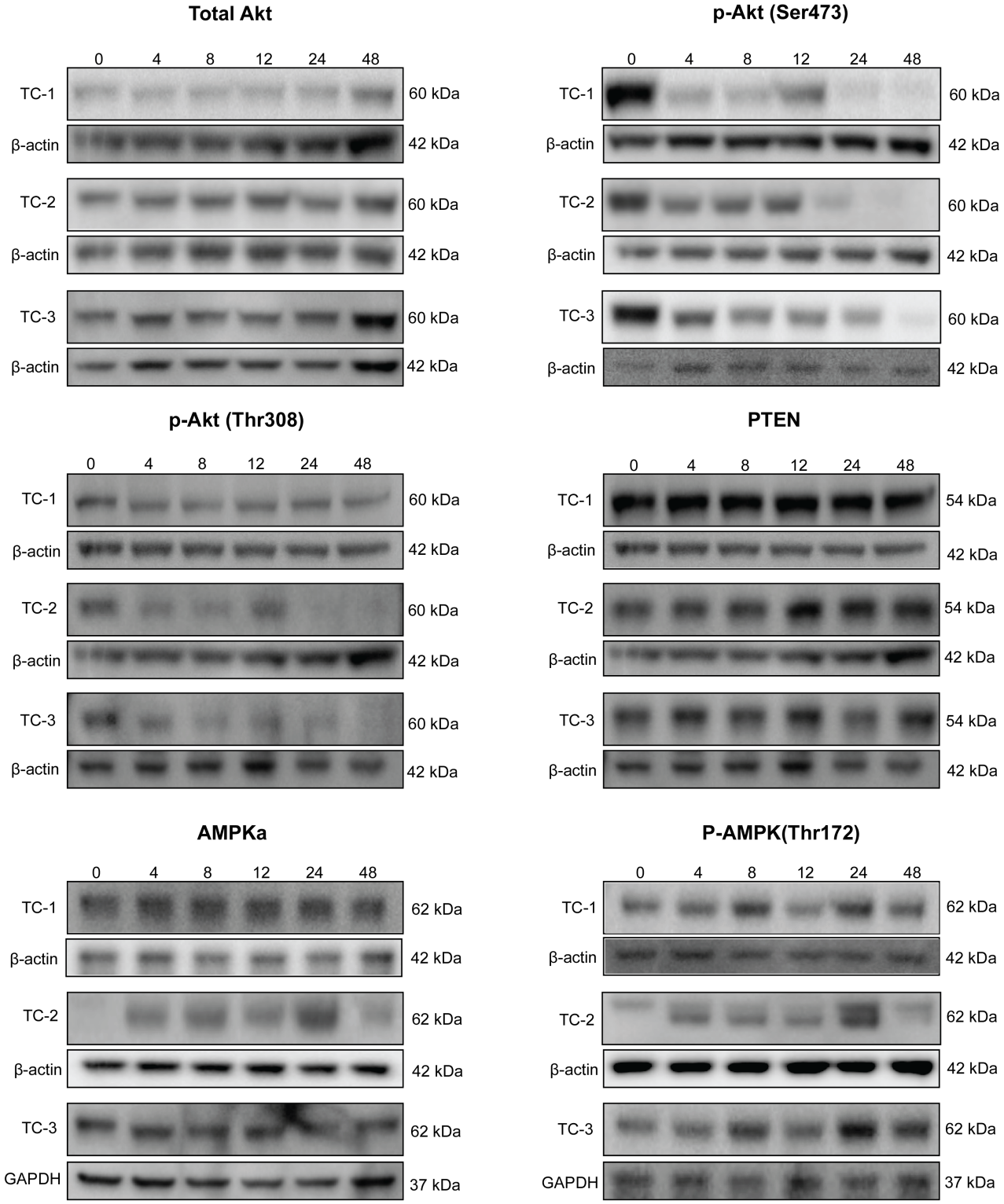

Figure S9. Akt and AMPK pathway protein expression for AG-27 cell line: The figure shows all western blotting results for Akt, p-Akt (Ser473), p-Akt (Thr308), PTEN, AMPKa, pAMPKa (Thr172) in each biological replicate (time course) of the AG-27 cell line. The time course for DE differentiation was repeated in triplicate for each cell line. The abbreviations TC-1, 2, and 3 are used to designate the different time courses. β-actin and GAPDH were used as loading controls.

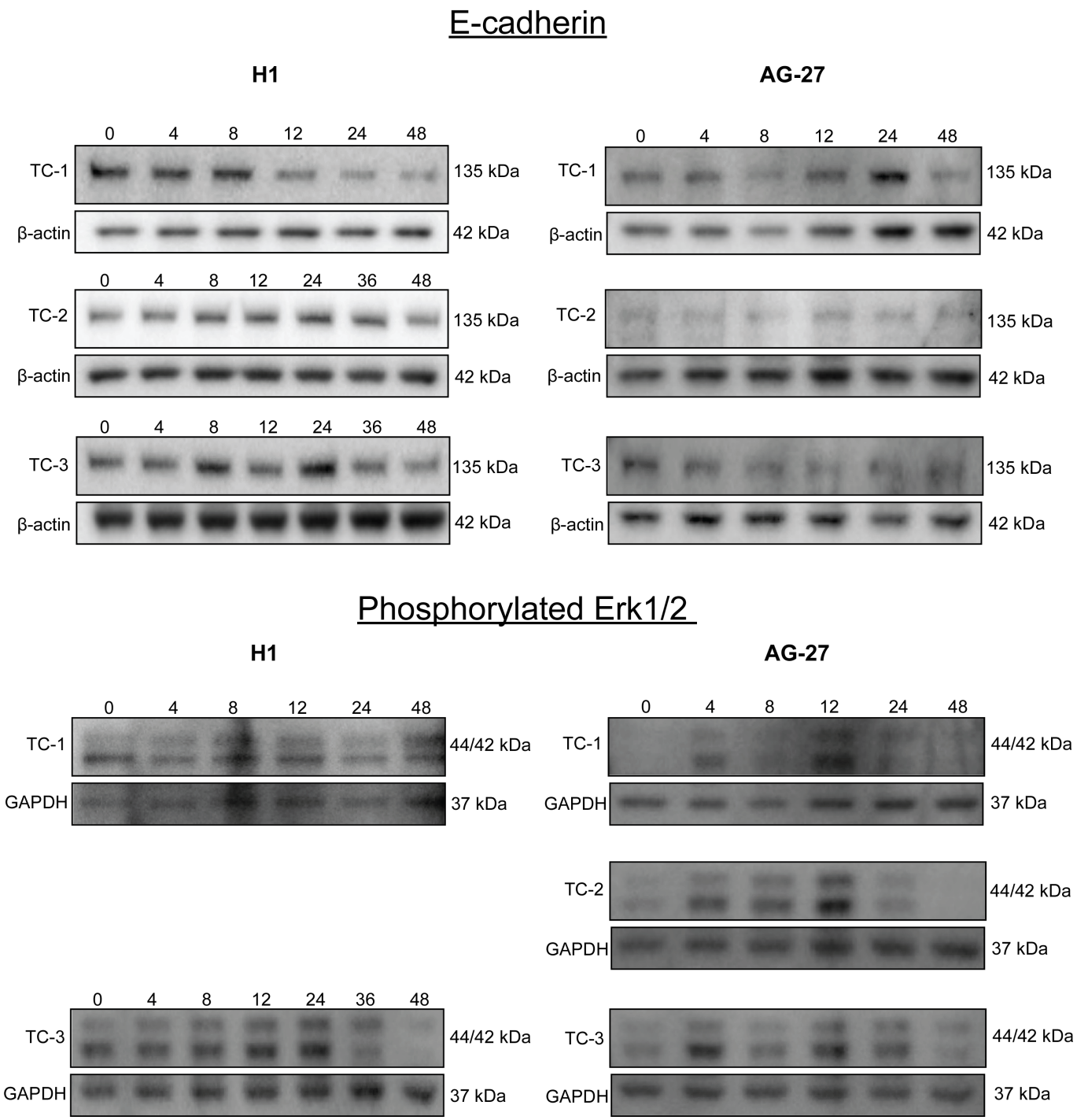

Figure S10. E-cadherin and p-ERK1/2 protein expression: The figure shows all western blotting results for E-cadherin and p-ERK1/2 expression in the H1 and the AG-27 cell lines. The time course for DE differentiation was repeated in triplicate for each cell line. The abbreviations TC-1, 2, and 3 are used to designate the different time courses. For H1 cells, a 36H time point was also collected for TC-2 and 3. Western analysis of p-ERK1/2 levels in could not be completed for second time course (TC-2) of the H1 cell line. β-actin was used as loading control for the E-cadherin blots, and GAPDH was used as loading control for the p-Erk1/2 blots.